3.15.1 Recommended Mix Design

Based on extensive testing of trial mixes and analysis of the results as given in Task 3, the following mixture proportions were recommended for the high strength HPC for prestressed girders and HPC mix for the bridge deck using silica fume.

3.15.1.1 Recommended Mixture Proportions for Bridge Deck Concrete: (for Quartzite Aggregates)

Cement Type 1/11	303 kg/m^3 (511 lb/cu.yd.)	0.073 m^3 (2.58 cu.ft.)
Fine Aggregate	652 kg/m^3 (1100 lb/cu.yd.)	0.190 m^3 (6.70 cu.ft.)
Coarse Aggregate	1023 kg/m^3 (1725 lb/cu.yd.)	0.297 m^3 (10.51cu.ft.)
Water	157 kg/m^3 (264 lb/cu.yd.)	0.120 m^3 (4.23 cu.ft.)
Fly Ash	70 kg/m^3 (118 lb/cu.yd.)	0.022 m^3 (0.76 cu.ft.)
Silica Fume	33 kg/m^3 (55 lb/cu.yd.)	0.012 m^3 (0.42 cu.ft.)
Air	6.5% $\pm$ 1.0%	0.050 m^3 (1.76 cu. ft.)
		0.764 m^3 (26.96 cu.ft.)

Note:
A mid range water reducer (Polyheed-997 Master Builders) was used at 8 oz/cwt of cement. The Air-entraining agent MB-VR Standard (Master Builders) shall be used. An appropriate amount of air-entraining agent should be used to obtain an air content of 6.5 + 1%.
The recommended slump is 127 to 178 mm (5 to 7 inches). An appropriate amount of approved superplasticizer (High Range water reducer) can be used if needed to obtain the specified slump.
The following properties were obtained from the trial mixes done at the SDSM&T Laboratory:

Plastic Properties:

Slump:	190 mm (7.5 in.)
Air Content:	5.40%
Unit Weight:	2258.85 kg/m^3 (141.2 Ib/ft^3)

Hardened Properties:

	14-day	**28-day**
Compressive Strength:	35.41 Mpa (5135 psi)	42 Mpa (6140 psi)
Static Modulus:	2.92x10^4 Mpa (4.24x10^6 psi)	3.24x10^4 Mpa (4. 7x10^6 psi)
Modulus of Rupture:	4.55 Mpa (660 psi)	5.5 Mpa (800 psi)
Chloride Permeability: (at 90 days)	1207 Coulombs (Category: Low)	

3.15.1.2 Recommended Mixture Proportions for High Strength Concrete for Prestressed Girders:

Cement Type I/II	374 kg/ m^3 (630 lb/cu.yd.)	0.089 m^3 (3.18 cu.ft.)
Fine Aggregate	712 kg/ m^3 (1200 lb/cu.yd.)	0.204 m^3 (7.31 cu.ft.)

Coarse Aggregate	1082 kg/ m^3 (1825 lb/cu.yd.)	0.311 m^3 (11.12 cu.ft.)
Water	112 kg/ m^3 (189 lb/cu.yd.)	0.085 m^3 (3.03 cu.ft.)
Silica Fume	42 kg/ m^3 (70 lb/cu.yd.)	0.015 m^3 (0.53 cu.ft.)
Air	4.0% $\pm$ 1.5%	0.050 m^3 (1.76 cu.ft.)
		0.754 m^3 (26.93 cu.ft.)

Note:
A High Range Water Reducer (RHEOBUILD 1000 Master Builders) was used at 26.7 oz/cwt of cementitious material (1739 ml/100 kg). The Air-entraining agent MB-VR Standard (Master Builders) shall be used. Appropriate amount of air-entraining agent should be used to obtain an air content of 6.5 ± 1.5 %.
The recommended slump is 127 to 178 mm (5 to 7 inches). An appropriate amount of approved superplasticizer (High Range water reducer) should be used to obtain the specified slump.
The following properties were obtained from the trial mixes done at the SDSM&T Laboratory:

Plastic Properties:

Slump:	146 mm (5.75 in.)
Air Content:	6.20%
Unit Weight:	2300.04 kg/m^3 (143.6 lb/ft^3)

Hardened Properties:

	7 -day	**28-day**
Compressive Strength:	85 Mpa (12280 psi)	97 Mpa (14065 psi)
Static Modulus:	4.28x10^4 Mpa	4.97x10^4 Mpa
	(6.2x10^6 psi)	(7 .2x10^6 psi)
Chloride Permeability:	158 Coulombs (Category:Very Low)	
(at 2 days after accelerated curing)		

Note:
1. Required fc' = 68.95 MPa (10,000 psi)
According to ACI 214, the target strength for the mixture should be fc' x1.2=82.74 MPa (12,000 psi). We used 101.6x203.2 mm (4"x8") cylinders for the compression tests. We can assume that the compressive strength indicated by the smaller cylinders 101.6x203.2 mm (4"x8") will be slightly higher than that indicated by standard cylinders 152.4x304.8 mm (6"xI2"). This may be approximately about 8 to 10%. Therefore the target strength should be slightly higher than 82.74 MPa (12,000 psi).
2. The trial mix for which the properties are given below contained 49.8 kg/m^3 (84 lbs./cu.yd of silica fume, which is 12% replacement of cement by weight. The suggested mixture proportions which has 10% replacement of cement by weight will have very similar properties as the trial mix H8F0S10W0.30. We have used Rheobuild 1000 as the superplasticizer but any equivalent, approved superplasticizer can be used.

The silica fume used should satisfy ASTM C1240, which covers both densified silica fume and liquid form. Class F fly ash was recommended. The same aggregates (both fine and coarse) currently used in the SDDOT projects in the Sioux Falls area, without any change in the aggregate gradation could be used. The recommended slump of 127 to 177.8 mm (5 to 7 inches) was based on the experience of other states (particularly Virginia). They did not have any problems when the finishing machine was used. Because of the inclusion of silica fume and fly ash, no segregation was anticipated. The reason for recommending high slump was to ensure proper distribution of silica fume and good consolidation. With this slump, the rate of

development of heat of hydration would be reduced and the potential for microcracking in the concrete would be reduced, which would be essential for reduced permeability. No change in the setting time compared the standard concrete in the summer time was anticipated based on the laboratory trial mixes and in discussions with others who have used similar mixes. Of course, the set properties might vary, within reasonable limits, with a change in the ambient temperature and humidity conditions. No special finishing requirements were recommended. It was strongly recommend that, whenever silica fume was used, a proper 100% humid curing 5 to 7 days was essential. This could be achieved with continuous water sprays or misting and/or fogging devices.

In the laboratory trial mixes dry densified silica fume was used. However, the concrete supplier on the project had requested to use the slurry form of silica fume in the HPC mixes, eventhough the specifications for this project did not allow slurry. After considerable discussions and research, the concrete supplier was allowed to use the slurry form of silica fume. However certain conditions were specified, such as sampling of the slurry before and during addition of the slurry to the mix. Because the silica fume is suspended in water (not dissolved), there is an inevitable tendency for the silicafume to settle to the bottom. To avoid this, a continuous agitation of the liquid with proper instruments was recommended. The standard vibration used for plain concrete was suggested because from our experience and experience of others (Virginia, Texas and other states) the entrapped air in silica fume concrete was not a problem. Therefore excessive vibration was not necessary and the standard air test was recommended to measure the air content in fresh concrete.

Trial mixes were done at the Concrete Materials Plant (concrete supplier) and transported to the prestressing plant (Gage Brothers). The slump, air, and unit weight tests were conducted. The compressive strength tests indicated the specified early strength (prestress release strength) was not obtained eventhough the 28 day design strength was satisfactory. This might have been due to the addition of silica fume in the slurry form instead of the condensed silica fume powder used in the laboratory trial mixes. Therefore, to obtain the required early strength, the cement quantity was increased by 29.65 kg/m^3 (50lbs.cu.yd) with the approval of SDDOT engineers and the admixture water was considered. However the water to cement ratio was kept the same at 0.28. Two mixes of 4.59 m^3 (6 cubic yards) of concrete were mixed at the concrete materials plant and transported to the casting yard (Gage Brothers) by transit mixer. 652 milliliters of

superplasticizer per 100 kgs (10 ounces per 100 lbs.) of cement was added during the mixing at Concrete Materials and a slump of 101.6 mm (4 inch) was obtained. Another 652 milliliters of superplasticizer per 100 kgs (10 ounces per 100 lbs.) of cement was added at the prestressing yard and a slump of 215.9 mm (8.5 inches) was obtained. The air was found to be 4.1 percent. Inspection of the fresh concrete had shown that the materials had mixed well with no segregation. The compressive strength tests indicated that the specified early strengths were obtained. Because of the satisfactory performance of this mix both at the fresh and hardened states this mix was recommended for all further girder fabrication. However the air content specification was changed to 4±1% because the HPC concrete for the girders will be more dense and less permeable than normal girder concretes, less entrained air can be tolerated without affecting the durability of the concrete girders. The reduced air content also helped to increase the strength slightly. The following was the final mix design recommended for high strength HPC mix for prestressed girders.

Mix Proportions	**for 1 Cubic Meter**	**for 1 Cubic Yard**
Cement (Type II)	403.24 kg	680 lbs.
Water included from silica fume slurry and HRWR	112.67 kg	190 lbs.
Coarse aggregate (3/4" quartzite)	1082.23 kg	1825 lbs.
Fine aggregate (S.S.D)	683.16 kg	1200 lbs.
Silica fume	49.81 kg	84 lbs.
Air Content	4.0±1.0%	4.0±1.0%
Water to Cement ratio	0.28	0.28
Water/C+S.F. ratio	0.25	0.25

Note: The recommended slump was 127 to 178 mm (5 to 7 inches). The dosage of High Range Water Reducer (HRWR) and/or water reducer should be adjusted according to the field conditions to achieve the specified slump. The 19mm (3/4 inch) quartzite aggregate used in this project conformed to the standard specifications for Roads and Bridges, Section 820 for Size No. 1 (SDDOT).

The approximate admixture dosages used in this project are given below:

Air entraining agent - Master Builders/ Pavair 232 milliliter/m^3 (6 oz per cubic yard)

HRWR- W.R.Grace/ Daracem 19-	2217 milliliters/100 kgs (34 oz per 100 lbs.) of cementitious material.
Water Reducer-	
Master Builders/ MB 997 -	391 milliliters/100 kg (6 oz per 100 lbs.) of cementitious material.
Silica fume slurry -	
W.R.Grace / Force 10,000-	69.15 liters/m^3 (13.97 gallons per cubic yard).

The cement used was produced at the South Dakota Cement Plant.

3.15.2 Recommended mix proportions for Bridge Deck

For bridge no 1, the recommended HPC mix with silica fume based on the laboratory trial mixes performed satisfactorily in the field in both fresh and hardened states. However highly controlled curing was required to eliminate plastic shrinkage cracking. These were a number of cracks at bottom surfaces of the deck due to the high restraint caused by the deck reinforcement. It seemed that silica fume addition caused higher shrinkage cracking. Therefore, for the second bridge, silica fume was omitted and only fly ash was included as a cement replacement. This mix performed well both in fresh and hardened states. There was also less cracking at the bottom surface of the slab. Therefore this mix is recommended for all future bridge deck construction. The recommended mix proportions are given in Task 6.

3.15.3 Recommended Quality Control Testing

When silica fume is used in the slurry form, it is recommended that the slurry must be sampled and tested before use and at specified intervals during concrete production. The amount of silica fume in the slurry can be determined by a hydrometer test. It is suggested that a curve can be generated by taking a sample and running the hydrometer testing on the slurry. For a given sample hydrometer tests could be run with different water contents to generate a curve. Also, from a sample, the slurry could be carefully dried to determine the amount of silica fume in the sample. Based on this information and the curve, the silica fume content could be easily and quickly determined when the slurry consists of water and silica fume only.

When HPC mixes are used, it is recommended that the following quality control tests should be conducted in the field using ASTM test procedures for the fresh concrete: slump, unit

weight, air content, and the concrete temperature. The ambient temperature, humidity, and the wind velocity be recorded during placing of the concrete in the bridge deck or fabricating the prestressed girders. The following hardened concrete control tests should be conducted on the field samples collected and cured according to the ASTM standard procedures at 28 days: compressive strength and static modulus. When HPC is used for fabricating prestressed girders, it is recommended that companion cylinders (preferably 102 mm × 204 mm (4" × 8")) be placed near the girder and cured under identical conditions as the girders, to determine when the prestress can be released as per specifications.

The specifications for bridge deck concrete and also for the high strength concrete used for prestressed girders should include a required Chloride Permeability value as measured by the ASTM C 1202. When chloride permeability is specified, the hardened concrete samples made from the actual concrete placed should be tested for rapid chloride permeability as per ASTM C 1202.

The standard ASTM test procedures to be followed are given in Chapter 2.

3.15.4 Construction Guidelines

When silica fume concrete is used for the bridge deck, the curing specifications (as mentioned earlier) should be strictly followed. The same construction procedures for mixing, transporting, placing, consolidating, finishing and tinning used for construction with standard concrete, be followed. The same construction techniques and equipment without major modification could be used for the construction of HPC bridge decks.

3.16 Task 16: Submit a final report summarizing relevant literature, research methodology, test results, specifications, design standards, conclusions, and recommendations.

With the acceptance of this draft final report the revised final report will be submitted before December 30, 2001.

3.17 Task 17: Make an executive presentation to the SDDOT Research Board summarizing the findings and conclusions.

A presentation to the SDDOT Research Board will be given on November 28, 2001.

CHAPTER 4.0

FINDINGS AND CONCLUSIONS

4.1 Compressive strength results:

Summaries of the extensive tests that were conducted in order to assess the strength and strength development with time are provided in Tables 4.1 through 4.6. Tables 4.1 through 4.4 provide information on the concrete used in the prestressed girders while Tables 4.5 and 4.6 provide strength information for the deck concretes. Note that a single result in a table is the average of three separate cylinder tests. The exception to this is trial mix one where more cylinders were tested. In some instances, both companion cured cylinders as well as moist cured cylinders were used. Companion cured cylinders were cured with the girder for which they were representative up until the cylinders were retrieved for testing. Table 4.1 contains the information

Table 4.1: Trial Mixes, Bridge no. 1 (B1), Compressive strength results.

Concrete Age Days	Trial Mix no. 1 Cast: April 28, 1999		Trial Mix no. 2 Cast: May 4, 1999		Deck Trial Mix Cast: July 9, 1999
	Moist cure		Moist cure	Companion cure	Moist cure
	No. of cylinders	f_c' (psi)	f_c' (psi)	f_c' (psi)	f_c' (psi)
1	6	3,430	5,500[2]	5,500[2]	-
3	9	6,400[3]	7,290	7,090	5,840
7	8	7,590	8,550	9,220	7,230
14	6	9,670	9,820[4]	9,450	8,070
28	6	10,720	11,660	11,840[5]	8,910
56	6	11,520	12,760	13,170[5]	9,020
180	3	11,880	-	-	-

Unit Conversions: 1 psi = 0.006895 MPa

Note 1: All compressive strength results are the average of three cylinders except as specified for Trial mix no. 1.

Note 2: No difference between the companion cure and the moist cure at one day. Only three cylinders were tested.

Note 3: Tests were conducted at four days instead of three days.

Note 4: Tests were conducted at thirteen days instead of fourteen days.

Note 5: Companion cured the first fourteen days, moist cured thereafter.

Table 4.2 Bridge no. 1 (B1) Girder Fabrications, Compressive strength results[1].

Conc. Age Days	Fabrication 1 May 21, 1999		Fabrication 2 May 24, 1999		Fabrication 4 June 4, 1999		Fabrication 5 June 11, 1999		Fabrication 6 June 14, 1999	
	Girder no. 1 f_c' (psi)	Girder no. 2 f_c' (psi)	Girder no. 1 f_c' (psi)	Girder no. 2 f_c' (psi)	Girder no. 1 f_c' (psi)	Girder no. 2 f_c' (psi)	Girder no. 1 f_c' (psi)	Girder no. 2 f_c' (psi)	Girder no. 1 f_c' (psi)	Girder no. 2 f_c' (psi)
1	7,200	-	6,120	-	-	-	-	-	-	-
3	9,830	-	8,670	8,950	-	-	-	-	-	-
7	11,880	12,140	10,740	11,350	12,630	13,170	11,710	11,720	12,410	11,900
14	13,800	14,200	12,960	13,300	15,560	15,930	14,070	14,810	16,500	15,950
28	15,350	15,950	14,100	14,860	15,740	16,540	14,480	15,360	16,690	17,300
56	16,180	16,780	14,700	15,400	-	-	-	-	-	-
180	-	18,100[2]	-	-	-	-	-	-	-	-

Unit Conversions: 1 psi = 0.006895 MPa
Note 1: All compressive strength results are the average of three cylinders.
Note 2: One cylinder broke significantly higher than the other two. The test cylinder results were as follows: 17,600, 17,330 and 19,100.

for the various trial mixes that were conducted. They do not provide information on the specific mixes that were employed but they are included here for completeness. Trial mixes no. 1 and 2, were conducted on April 28, and May 4, 1999. The specified strength for the girder mix was 68.26 MPa (9,900 psi) at 28 days. The stress at prestress transfer was required to be 58.6 MPa (8,520 psi). Upon reflection, it is clear that the governing requirement is the stress at transfer. In order to meet the production schedule the prestress supplier wanted to transfer prestress at three days or less. By inspecting the trial mix results, it is seen that neither of these mixes met this requirement.

The deck trial mix employing silica fume was conducted on the interstate near the bridge site and was conducted on June 14, 1999. This mix employed silica fume and the trial mix was conducted to provide experience with handling the production mix and to test the fogging equipment that the contractor was required to use with this concrete. Strength was not the main concern for the deck concrete. The major emphasis was to produce concrete of very low permeability so that the decks would have superior resistance to the migration of chlorides to the

level of the reinforcing steel. As stated, the trial mix results are simply reproduced here for completeness.

The results from the production girder mixes are presented in Tables 4.2 through 4.4. Table 4.2 contains the compressive strength results for the five girder fabrication sequences for bridge B1. Initially, the plan was to test cylinders from the concrete from the instrumented girders only. A change was made and during the first year all girder fabrications were attended with cylinders being prepared and tested from each sequence. The time series for these girders employed tests at 7, 14 and 28 days. The second year, only half the girder fabrications were attended but a more complete time history was developed. These results appear in Table 4.3. In general these concretes achieved sufficient strength at three days 58.7 MPa (8,520 psi) in order to permit the transfer of prestress to the girders.

Table 4.3: Bridge no. 2 (B2) Girder Fabrications, Compressive strength results[1].

Conc. Age Days	Fabrication 2 April 28, 2000		Fabrication 3 May 9, 2000	
	Girder no. 1 $f_c^{'}$ (psi)	Girder no. 2 $f_c^{'}$ (psi)	Girder no. 1 $f_c^{'}$ (psi)	Girder no. 2 $f_c^{'}$ (psi)
3	6,770	7,310	8,000	8,380
7	9,050	10,020	10,200	10,140
14	11,050	12,670	12,350	11,650
28	12,340	13,880	13,780	14,080
90	13,190	15,190	15,010	14,950
180	13,410	15,190	14,810	15,350
1 year	14,090	15,690	15,470	16,150

Unit Conversions: 1 psi = 0.006895 MPa
Note 1: Each compressive strength is the average of three cylinders.

When reviewing these results it should be noted that the ready-mix supplier was trying to produce the same mix with the expectation that the strengths would be the same. By perusing the row an estimate of the variation from mix to mix can be noted. Two separate trucks were used to produce each girder. An interesting phenomenon that was noted throughout the project was that the cylinder strengths from the second truck were always higher than the strengths from the first truck.

In each year, two girders were selected to receive instrumentation. The instrumentation permitted the measurement of strain and temperature at mid-span of each girder. In addition, reference points were established on the girder to permit the measurement of deflections. These two girders were always the two girders that were to be placed in the end span at the north end of the bridge. These girders occupied the west exterior and the next adjacent interior girder positions. The first year these two girders were fabricated third in the sequence. The second year the instrumented girders were fabricated fifth in the sequence. The compressive strength results for these four instrumented girders are listed in Table 4.4.

The instrumented girders exhibited a 28-day compressive strength ranging from a low of 91.0 MPa (13,200 psi) to a high of 108.2 MPa (15,690 psi). If one computes the statistics on the 28-day compressive strengths, the results yield a mean of 99.3 MPa (14,400 psi) and a standard deviation of 6.82 MPa (990 psi). The ratio of the standard deviation to the mean defines the coefficient of variation and this is 6.9 percent. This indicates a well-controlled process. It appears that these strength results can be achieved with reasonable expectation.

Assuming the acceptance tests were, as is the case in this report, made up of three cylinders averaged to produce a single result. Then— if one expects 95 percent of these results to be above the specified design strength at 28 days, the design strength of this mix could be set at 88.2 MPa (12,800 psi), or conservatively at 82.7 MPa (12,000 psi). This assumes that the test results are normally distributed. An instrumented girder time series begin at one day and was defined as ages of 3, 7, 14, 28, 56 or 90, and 180 days with the final test being conducted at one year. Note that in the second year the 56-day test of the first year was not carried out, but that a 90-day test was substituted. This, it is believed, permits a better plot.

These time series are presented graphically in Figure 4.1. Also presented in this figure is a line that represents the results from the standard equation that is used to predict strength vs. time for a moist cured Type I cement concrete. In this figure, the line for each bridge is the average of the results from the two instrumented girders for that bridge. Though difficult to discern in the figure, the maximum early period difference between these two curves (The first 28 days) is about 11.0 percent. At later ages, they are essentially identical.

The deck compressive strength results are provided in Tables 4.5 and 4.6. For each deck five time series were developed. The time histories in the tables were defined by testing three cylinders at each age. The concrete for each series was taken at one time and the time selected

depended upon where in the deck placement the contractor was. Concrete was sampled at the center of the first span, at the first bent, at the middle of the center span, at the second bent and at the middle of the last span. In the case of bridge one, the deck placement proceeded from north to south. Therefore, series one is representative of the concrete at the middle of the north span and at the location of the deck instrumentation.

Table 4.4: Instrumented Girders, Bridges 1 and 2, Compressive strength results[1].

Conc. Age Days	Bridge no 1 Casting date: June 3, 1999				Bridge no. 2 Casting date: May 18, 2000			
	Girder no. 1 (G3B)		Girder no. 2 (G3A)		Girder no. 1 (G5A)		Girder no. 2 (G5B)	
	Moist Cure	Comp. Cure	Moist Cure	Comp. Cure	Moist Cure	Comp. Cure	Moist Cure	Comp. Cure
	f_c' (psi))	f_c' (psi)	f_c' (psi)	f_c' (psi)	f_c' (psi)	f_c' (psi)	f_c' (psi)	f_c' (psi)
1	6,430	6,430	6,060	6,060	5,240	5,408	6,103	6,198
4	9,510	10,600	10,400	11,330	7,810	8,790	9,540	10,030
7	11,020	12,140	11,770	13,000	9,520	10,690	11,470	12,110
14	12,800	12,940	13,790	14,070	10,880	12,020	13,310	13,605
28	13,200	13,840	14,630	15,320	13,230	13,950	15,410	15,690
56	14,200	14,230	15,660	14,990	-	-	-	-
90	-	-	-	-	14,180	14,270	16,540	15,940
180	14,300	15,140	16,530	16,240	14,860	13,900	16,820	16,270
1 year	15,680	15,100	17,200	16,450	15,390	15,000	16,900	16,650

Unit Conversions: 1 psi = 0.006895 MPa
Note 1: Each compressive strength is the average of three cylinders.

Series two was taken from concrete placed at the first bent and coincided with a location at which instrumentation is located. Table 4.6 presents the parallel information for bridge 2. In this case, the placement was from south to north so series four and five represent the concrete at the locations of the instrumentation in the second bridge. The two deck concretes were not the same. In bridge 1, a silica fume mix was used while in bridge 2 a fly ash mix was employed. Figure 4.2 provides a time history plot of the average strength from all series for each bridge.

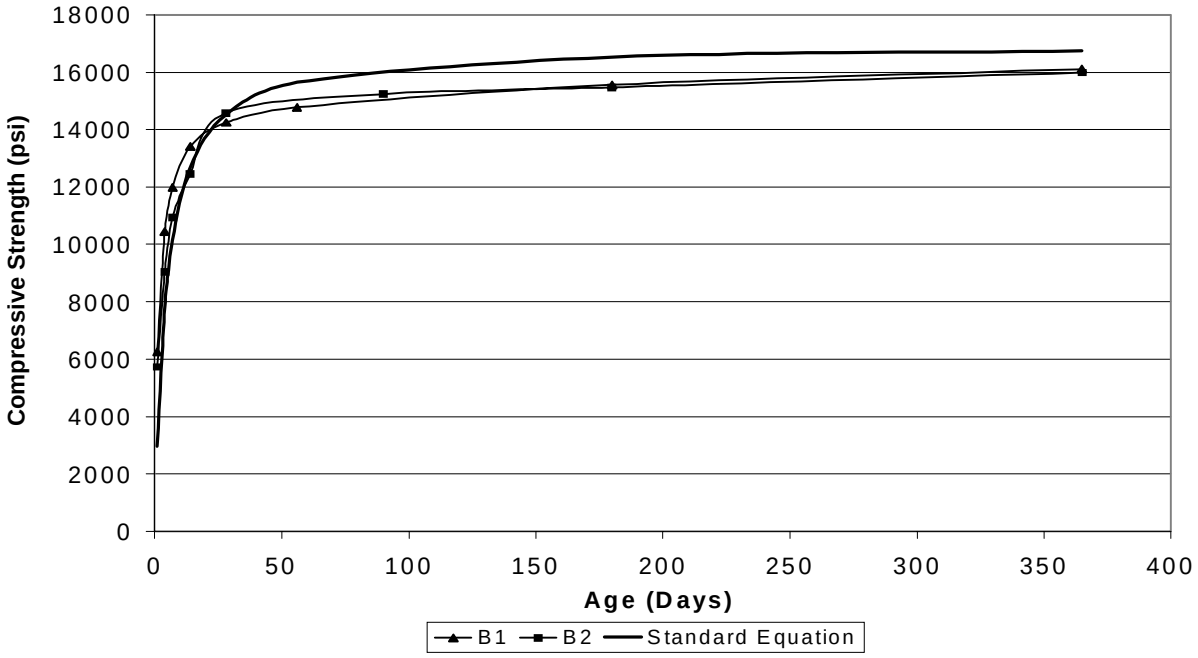

Figure 4.1: Compressive strength history for the instrumented girders of Bridges 1 and 2.

Table 4.5: Bridge 1, Deck placement (August 16, 1999) compressive strength summary.

Concrete Age	Series (All entries lbs/in^2, value listed, result from 3 cylinders)					Row Average
	No. 1	No. 2	No. 3	No. 4	No. 5	
3	4030	3740	3720	3640	3990	3830
7	5300	5020	5040	4960	5290	5120
14	6730	6100	5960	5970	6490	6250
28	7530	6830	6960	6750	7290	7070
90	8260	7560	7520	7430	8000	7750
191	8140	7820	7900	7890	8410	8030
1 year	8510	8080	8290	8280	8570	8350

Unit Conversions: 1 psi = 0.006895 MPa

Table 4.6: Bridge 2, Deck placement (July 20, 2000) compressive strength summary.

Concrete Age	Series (All entries lbs/in^2, value listed, result from 3 cylinders)					Row Average
	No. 1	No. 2	No. 3	No. 4	No. 5	
3	4450	3990	4420	4270	4420	4310
7	5030	4440	5000	4970	5150	4920
14	5840	5400	5870	5610	6070	5760
28	6860	6330	6950	6530	7110	6760
90	8120	7030	7930	7520	8360	7770
180	9090	7690	8110	8100	8720	8340
1 year	9590	8655	8705	8850	9420	9040

Unit Conversions: 1 psi = 0.006895 MPa

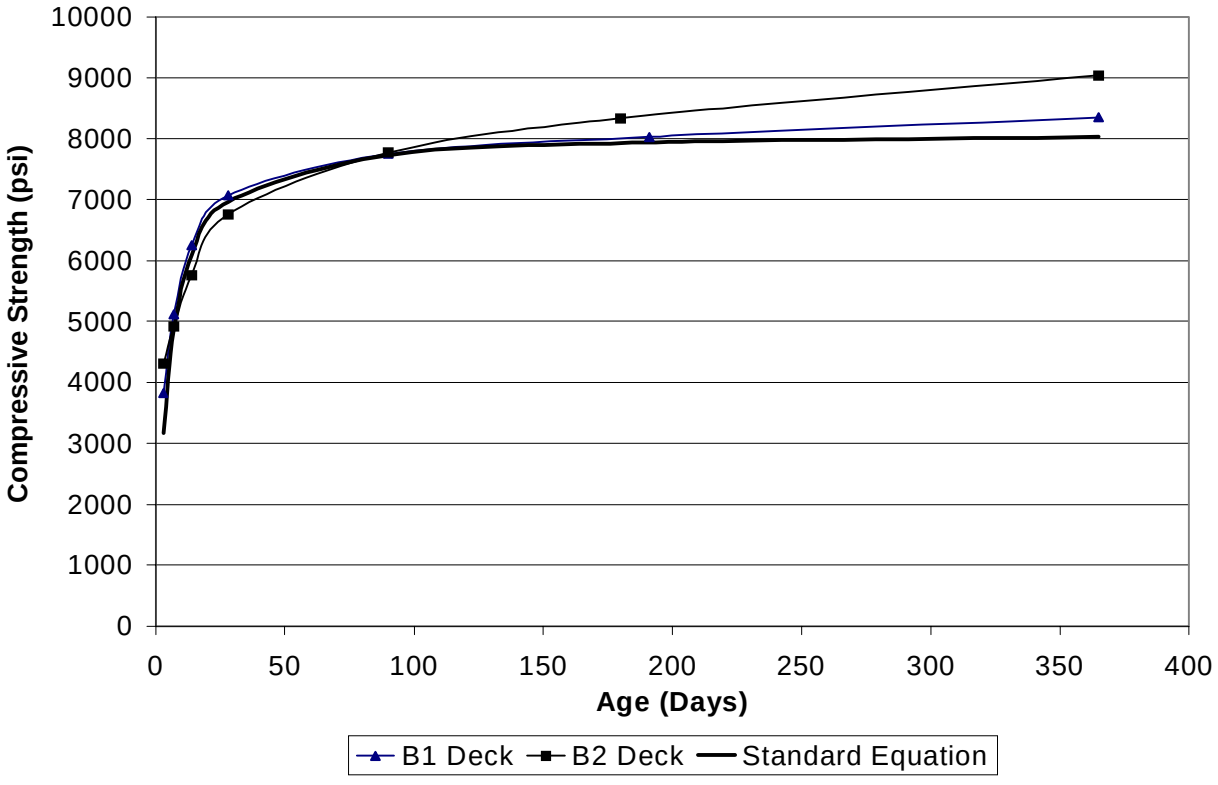

Figure 4.2: Compressive strength history of the deck concrete of Bridges 1 and 2.

The compressive strength results from these two mixes are rather comparable. One notes from Figure 4.2 that the fly ash mix produced slightly higher long term strength than the silica fume mix. It is well established that fly ash tends to hydrate slower than silica fume, and thus contributes more significantly to later strength gain. The previously mentioned standard equation is also presented in Figure 4.2. This standard curve is calibrated to the average of the two mixes at 28 days. It provides relatively good strength prediction with time for both of the mixes.

4.2 Modulus of Elasticity Results:

In order to design prestressed structures or even regular concrete structures utilizing HPC or HSC one needs an equation that is capable of providing a reasonably accurate estimate of the modulus of elasticity of the concrete at various ages. As has been noted earlier in this report, several equations have been used for this purpose. Equation 4-1 given below is the long-standing equation used in both the AASHTO and ACI 318 design specifications. The ACI 363 equation is the one currently recommended for high strength concrete.

AASHTO and ACI 318 equation:

$$E_c = 33 w_c^{1.5} \sqrt{f_c'} \qquad \text{eq. 4-1}$$

ACI equation 363:

$$E_c = \left(40{,}000\sqrt{f_c'} + 1{,}000{,}000 \right) \left(\frac{w_c}{145} \right)^{1.5} \qquad \text{eq. 4-2}$$

E_c = Modulus of Elasticity (psi units).

w_c = Unit weight of the concrete (lbs/ft^3).

f_c' = Compressive strength of the concrete (psi units.)

The equation 4-1 is the one that has long been used to estimate the modulus of elasticity of normal strength concrete. It is considered to yield results that are too high for HSC. The ACI 363 equation is recommended for HSC concrete, i.e. concrete with a 28-day compressive strength greater than 6,000 psi. This equation was based on concrete utilizing limestone aggregates.

The results from all the modulus of elasticity tests conducted on the concrete from the instrumented girders are presented in Table 4.7. The table includes data from both bridges. In

Table 4.7: Bridges 1 and 2, Modulus of Elasticity results for the instrumented girders[1].

Conc. Age Days	Bridge 1				Bridge 2			
	f_c'		Mod of Elast.		f_c'		Mod of Elast.	
	Av. (psi)	st. dev. (psi)	Av. ($x10^{-6}$) (psi)	st. dev. ($x10^{-6}$) (psi)	Av. (psi)	st. dev. (psi)	Av. ($x10^{-6}$) (psi)	st. dev. ($x10^{-6}$) (psi)
1	-	-	-	-	5,740	462	4.98	0.213
4	10,460	1,120	6.27	0.289	9,010	951	5.62	0.351
7	12,090	775	6.60	0.269	11,090	1260	6.26	0.363
14	13,390	882	6.89	0.261	12,450	1290	6.82	0.340
28	14,320	984	7.28	0.148	14,460	1080	7.13	0.332
56	14,750	671	7.18	0.387	-	-	-	-
90	-	-	-	-	15,450	1410	7.03	0.366
180	15,600	1060	7.01	0.387	15,600	1124	7.06	0.268
1 year	16,230	589	7.02	0.230	15,920	863	7.20	0.318

Unit Conversions: 1 psi = 0.006895 MPa
Note 1: The results at each age are from four individual cylinders.

total, this data represents 60 tests. These tests were conducted according to the procedure outlined in ASTM C-469, "Standard test method for static modulus of elasticity and poisson' s ratio of concrete in compression". The unit weight of the test concrete was obtained from the individual cylinders used in the test. These results are plotted in Figure 4.3. The square symbols in Figure 4.3 represent all of the data from the instrumented girders. The data from the two sets of girders from the two bridges were tested statistically with the conclusion that the two sets of modulus data were not significantly different. Proceeding from the left side of the figure, the regression line on the experimental data is the upper line. Two thirds of the way along its length it passes under the line that represents the long-standing equation that has been in the ACI code for many years, the ACI 318 equation. Included in this figure is the ACI 363 equation and the equation by Iravani. The regression results on the data yielded a line essentially parallel to the

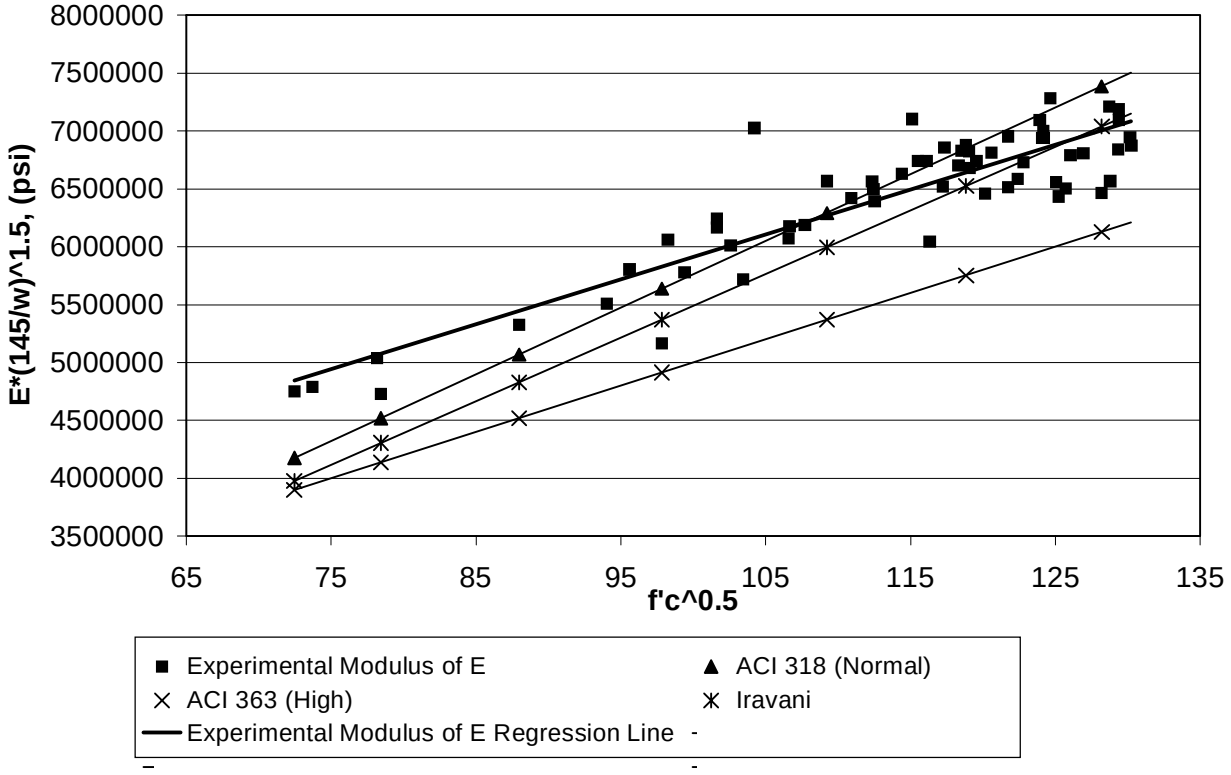

Figure 4.3 Modulus of elasticity regression analysis, all instrumented girders and both bridges.

ACI 363 equation. The specific form is –

$$E_c = \left(38{,}900\sqrt{f_c'} + 2{,}000{,}000\right)\left(\frac{w_c}{145}\right)^{1.5} \qquad \text{eq. 4-3 .}$$

The terms in this equation are as previously defined. The constant multiplying the $\sqrt{f_c'}$ term in the ACI 363 equation was determined to be 38,900 in the present work. This is not viewed as significantly different than the value, 40,000 in the ACI 363 equation. The constant of 1,000,000 psi in the ACI 363 equation was determined from the project data to be 2,000,000 psi. This is viewed as a significant difference.

This difference can be partially explained by noting that the work that was done to develop the ACI 363 equation was conducted on concrete that utilized limestone aggregates. As is known, the quartzite aggregate which was used in the mixes developed in this project, is a

much harder rock and expected to exhibit a higher modulus. It is interesting to note that the standard equation that is considered to yield results that are too high for HSC, produces

Table 4.8: Bridges 1 and 2, Modulus of Elasticity results for the deck concrete[1].

Conc. Age Days	Bridge no. 1				Bridge no. 2			
	f_c'		Mod. of Elast.		f_c'		Mod. of Elast.	
	Av. (psi)	st. dev. (psi)	Av. ($x10^{-6}$) (psi)	st. dev. ($x10^{-6}$) (psi)	Av. (psi)	st. dev. (psi)	Av. ($x10^{-6}$) (psi)	st. dev. ($x10^{-6}$) (psi)
3	3,750	202	3.84	0.028	4,230	271	4.40	0.211
7	5,170	240	4.51	0.243	4,800	267	4.55	0.152
14	6,090	303	4.90	0.163	5,840	220	5.23	0.338
28	7,120	465	5.22	0.231	6,640	421	5.62	0.217
90	7,840	262	5.14	0.276	7,480	817	5.67	0.079
180[2]	7,820	67	5.34	0.182	8,400	472	5.96	0.133
1 year	8,150	278	5.37	0.079	9,280	464	6.19	0.372

Unit Conversions: 1 psi = 0.006895 MPa
Note 1: The results at each age are from three individual cylinders.
Note 2: The cylinders for bridge no. 1 were tested at 191 days instead of 180 days.

reasonable results for the mixes used in this project. Iravani' s equation is also seen to produce acceptable results. He includes a factor in his equation for the type of aggregate used in the mix. underside of the girders.

Forty-two modulus of elasticity tests were conducted on the deck concrete from the two bridges. The basic test results are summarized in Table 4.8 and presented in graphical form in Figure 4.4. In Figure 4.4 two regression lines are presented, one for each bridge. These data sets have not been tested statistically in order to determine if they are significantly different, but it is believed that they will test as one set of data. Included in this figure as was done in the previous figure, are the ACI 318 and 363 equations. By inspection it is observed that the two regression lines for bridges 1 and 2 are reasonably parallel to the ACI 363 equation. The offset between these two is also about the same. The conclusion is that the previous equation 4.3 obtained from the girder tests will yield reasonable results for this data as well.

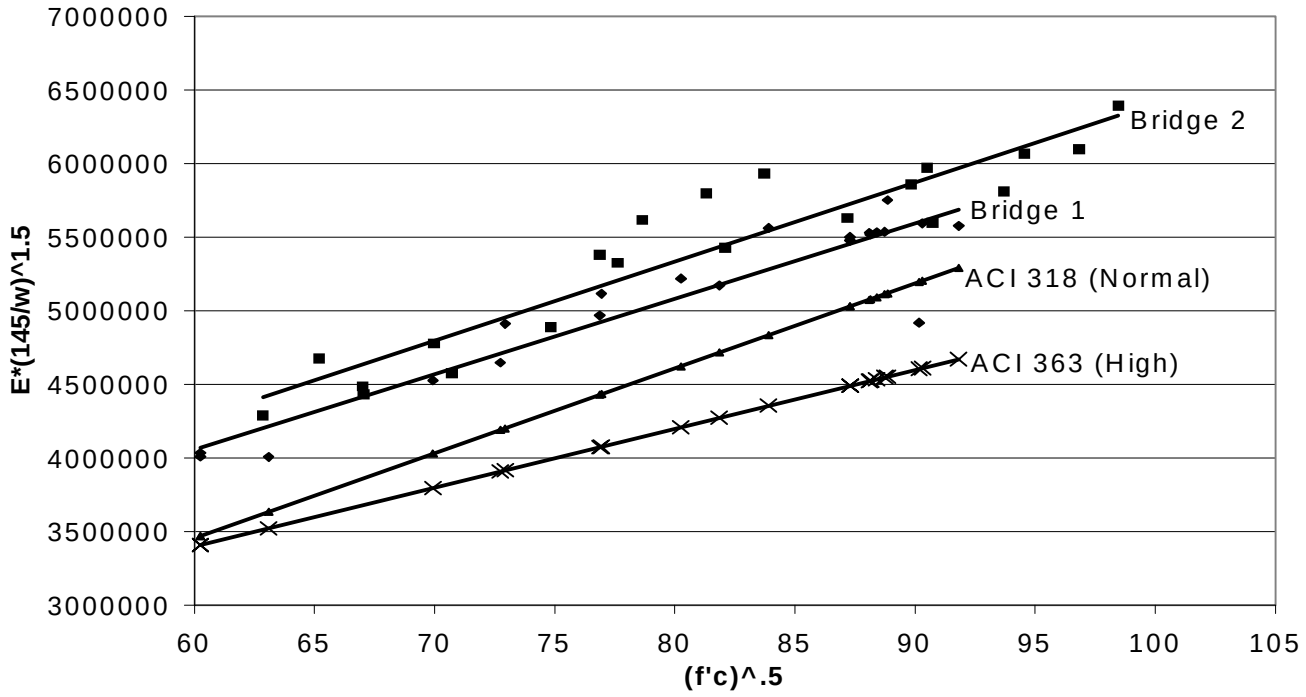

Figure 4.4: Modulus of elasticity regression analysis of the deck concrete, both bridges.

4.3 Girder and Bridge Deflections.

Initial girder deflections were taken immediately after the transfer of prestress. Observations continued to be taken at close, but increasing time intervals out to one month, thereafter readings were taken approximately monthly. After the concrete decks was placed readings had to be taken from the underside of the girders. The three wire leveling technique employed is expected to yield results within ±0.46 mm (± 0.0015 ft)

Deflection summaries are provided in Table 4.9. Note that the girders from bridge 2 exhibited more early camber, more deflection due to the deck loading, and maintained a greater camber under long term loading. In both cases, prestress was transferred over the period of about a half-day, and the girders were removed from the bed the next day. Deflection readings were taken just at the conclusion of prestress transfer, on the bed the next day prior to removing the girders from the bed, and immediately after the beams were removed from the prestressing bed.

The girders from bridge number two increased their camber about 0.4064 mm (0.016 inches) during the time they were lifted from the bed. Both girders exhibited the same deflection increase. This increase did not occur with the girders from bridge 1.

Table 4.9 Mid-span deflection data, both bridges.

	Bridge 1		Bridge 2	
	G3-A (in.)	G3-B (in.)	G5-A (in.)	G5-B (in.)
Instantaneous Camber	0.74	0.67	0.72	0.60
Maximum Camber	1.00	0.93	1.25	1.18
Deck Placement Deflection	-0.33	-0.36	-0.45	-0.42
Average deflections:				
Winter 1999	0.25	0.21	-	-
Summer 2000	0.29	0.25	-	-
Winter 2000	0.23	0.20	0.48	0.44
Summer 2001	0.29	0.24	0.54	0.49

Unit Conversions: 1 psi = 0.006895 MPa
Note 1: Positive values indicate an upward deflection.
Note 2: The deflections have not been corrected for temperature.
Note 3: Girders G3-A and G5-A are inside girders while Girders G3-B and G5-B are exterior girders.

The averages for the winters and summers indicate that the girder deflections have not changed very much over the monitoring period. The graph of the deflection history for the instrumented girders in bridge 1, specifically, G3A and G3B, is provided in Figure 4.5. A parallel graph for the girders G5A and G5B in bridge 2 is provided in Figure 4.6.

The change in camber that was previously noted as the G5A and G5B girders were removed from the bed is easily seen in Figure 4.6. The two graphs clearly show the development of camber with time. This camber being due to the creep and shrinkage occurring in the girders. Careful inspection notes the onset of the downward deflection due to the placement of the deck formwork. Clearly visible is the instantaneous deflection due to the placement of the deck. In both bridges, the outside girder tends to deflect more than the inside girder. The slight tendency for the deflections to decrease during the winter months and increase slightly during the summer months can be observed. In general, the girder deflections are not changing significantly. The separate deflections of the two instrumented girder for each bridge were averaged and plotted on

a time scale having zero as the time at which prestress was transferred to the girder, these results are provided in Figure 4.7.

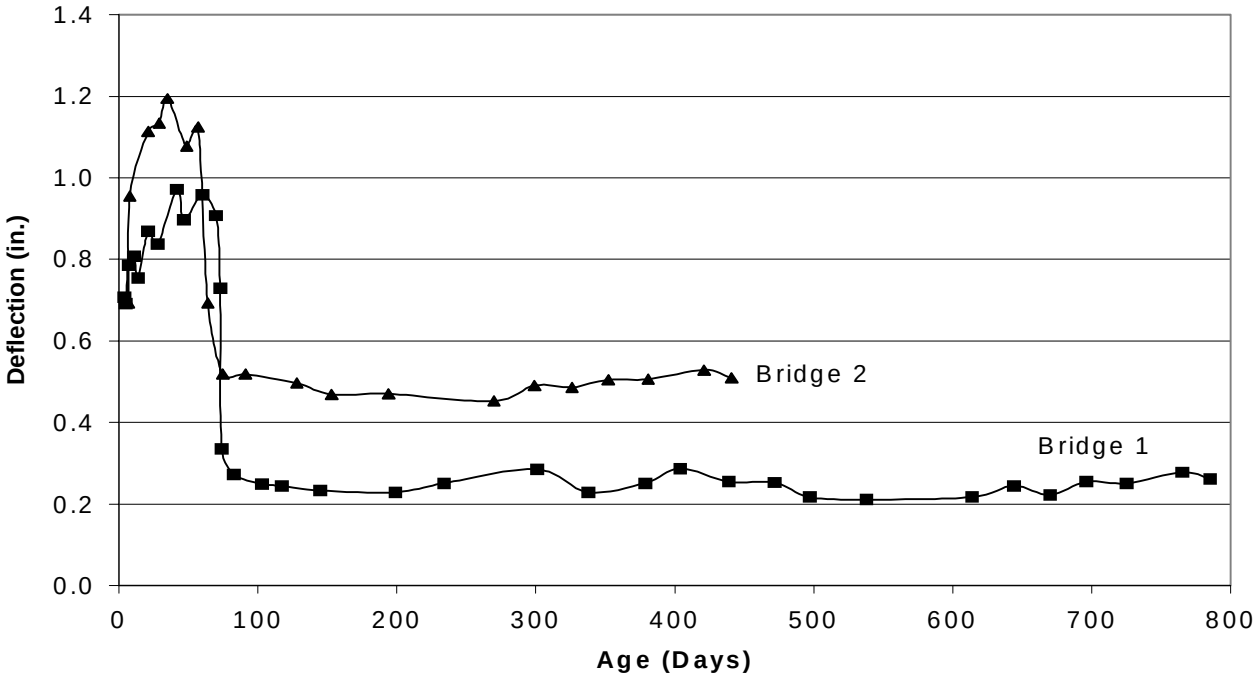

Figure 4.5: Bridge no. 1, mid-span deflection history of both instrumented girders.

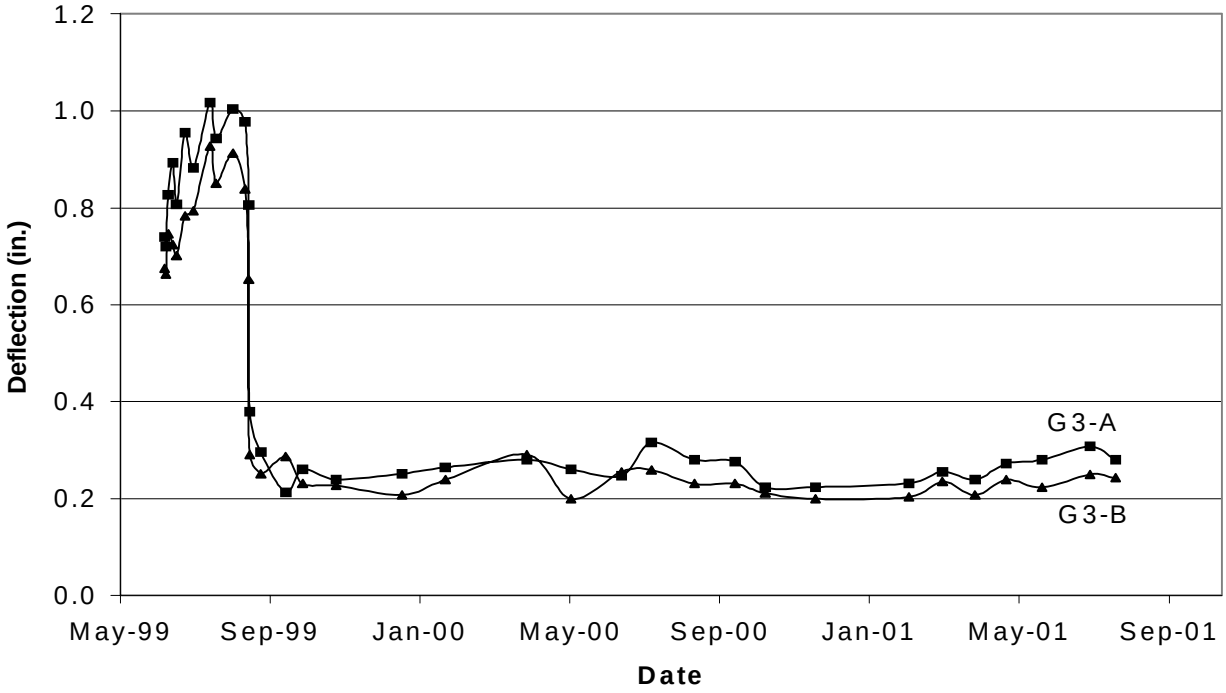

Figure 4.6: Bridge no. 2, mid-span deflection history of both instrumented girders.

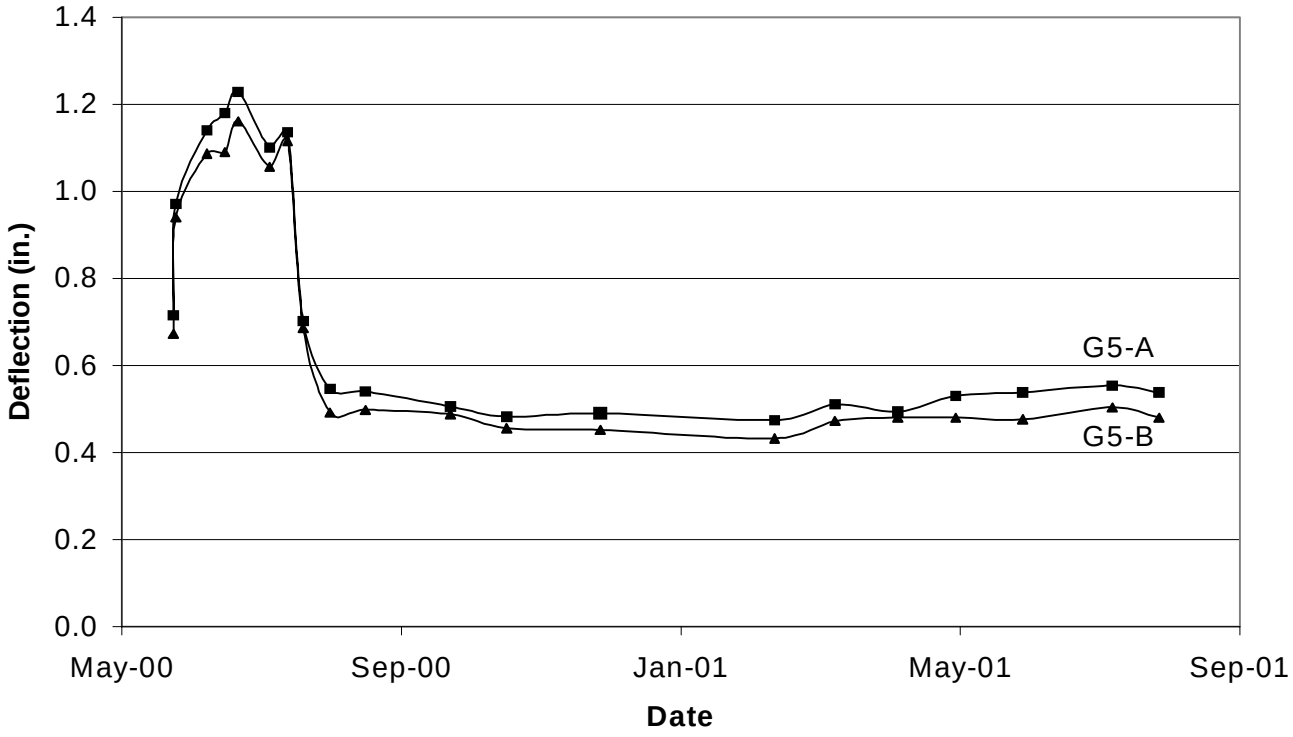

Figure 4.7: Bridges 1 and 2, average mid-span deflection for each bridge.

The elapsed time in this case represents concrete age. By placing both sets of girders on this scale one can inspect what is happening in each bridge relative to the age of the concrete. The camber differences are easily observed as well as the greater long-term deflection differences in the two bridges.

4.4 Impedance Measurements:

As was detailed in chapter 3, six devices were embedded in the deck concrete of each bridge that permitted the measurement of the electrical resistance in the concrete. The electrical resistance of the concrete was measured using these parallel plate devices. There is some belief that high values of electrical resistance are indicative of relatively impermeable concrete. Also, a sudden change in resistance may indicate the presence of chloride ions and thus the potential for corrosion to be initiated in the steel.

The deck on bridge 1 was placed on August 16, 1999. Due to the slow pace at which the formwork was removed, the first electrical resistance measurements were not made until

September 23, 1999. Since that time, measurements have been taken at approximately monthly intervals. The deck for the second bridge was placed on July 20, 2000. The first readings from this deck were recorded on September 18, 2000. This was only about one month after the deck was placed.

The measurements from the silica fume concrete of the first bridge have tended to exhibit a great deal of variability. While the measurements from the fly ash concrete in the second deck have not shown nearly as much variability. The detailed readings are not presented in this report (They are given in the quarterly reports.) but a summary of the measurements is presented in Figure 4.8. Each point that is plotted in the figure is the average of the six readings from the individual devices embedded in the deck. A great deal of variability is evident in the silica fume concrete over a one-year period. In general, the winter period results are much higher readings than the summer. It was noted that a transducer could give very different readings from month to month.

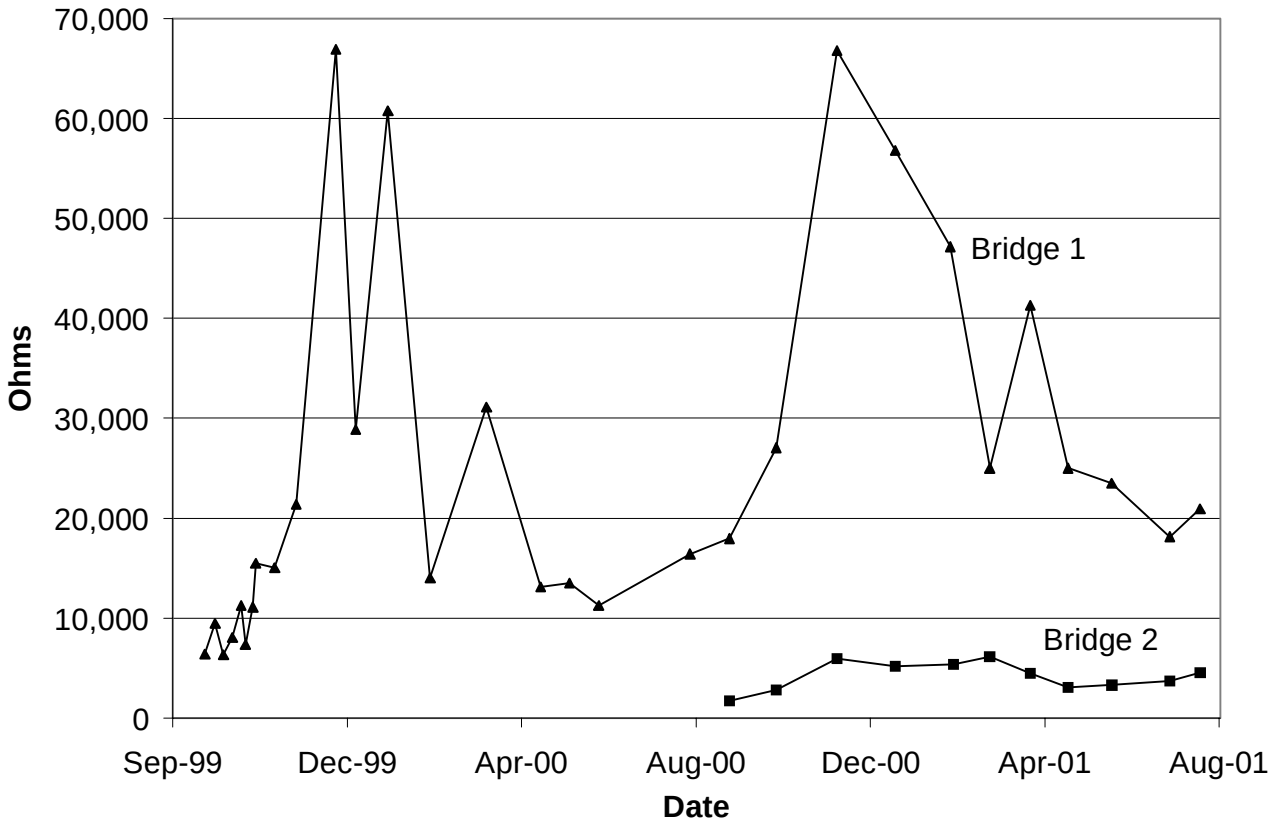

Figure 4.8: Deck impedance readings.

To provide a partial diagnosis of the reason for these readings, the instrument was checked by measuring the resistance of a high precision known resistance. This indicated that the instrument was working correctly. The next diagnostic test that was conducted involved taking multiple readings from the array of devices by disconnecting and reconnecting the leads to the instrument. This procedure of disconnecting and reconnecting the device was followed if the device being read yielded greatly different readings, either from the time before, or quite different from the others in the array. This procedure was followed to determine the change in resistance that could be attributed to simply making the connection to the measuring instrument. This provided no explanation as to the variability of the readings. The only remaining conclusion is that the readings in the silica fume concrete have a high degree of variability and border on being erratic.

This tendency is not observed in the fly-ash concrete deck. These readings have been relatively stable. As with the silica-fume concrete, the fly-ash concrete also tends to exhibit higher values in the cold months and lower values in the warmer months.

4.5 Thermal Strains:

Shrinkage and temperature related strains were evaluated with the use of shrinkage blocks. These blocks were fabricated along with the bridge girders and decks and subjected to the same environmental conditions. The shrinkage blocks have dimensions 152.4×152.4×304.8 mm (6×6×12 in) and contain vibrating wire gages that are embedded in the approximate center of each block. In total, eight blocks were cast, a companion block for each instrumented girder and two companion blocks for each deck.

The blocks experience both temperature and shrinkage strains. In order to be able to evaluate the shrinkage strains, one must first filter out the thermal strains. To accomplish this, the coefficient of thermal expansion for the concrete must be determined.

Early in the history of the shrinkage blocks, the shrinkage strains and the thermal strains are approximately of the same order of magnitude. For this reason, a significant time must elapse so that the shrinkage strains that occur during a half diurnal cycle are small with respect to the thermal strains. After analysis of the time variation of shrinkage strains, it was determined that this condition would be met approximately 90 days after the concrete was cast.

The equation for evaluating the coefficient of thermal expansion is

$$\alpha_c = \frac{(\varepsilon_1 - \varepsilon_0)B}{(T_1 - T_0)} + \alpha_g \qquad \text{Eq. 4.4}$$

α_c = Coefficient of thermal expansion for the concrete.
α_g = Coefficient of thermal expansion for the vibrating wire gage. (6.78×10^{-6} 1/°F)
ε_0, ε_1 = Strains measured at times t_0 and t_1 respectively.
T_0, T_1 = Temperatures measured at times t_0 and t_1 respectively.
B = Calibration factor for the gage (0.980).

Each day's cycle gives an opportunity to calculate two estimates of the coefficient of thermal expansion. After inspecting the daily temperature effects, it was determined the best results correlated with cycles showing reasonably large temperature changes. Therefore, the calculation of the estimate of the coefficients of thermal expansion was restricted to time-periods with temperature changes greater than 10.0 °C (18 °F). The original plan was to group the data into months and evaluate the results for the entire data logging time-frame. A curious problem developed during the analysis. It appeared that during the cold months the coefficient of thermal expansion was significantly less than during the summer months. It seemed that the blocks were frozen, or, perhaps, frozen to the supports and were not responding without restraint to the temperature change. Therefore, data was analyzed for the summer months only, this included May, June, July, and August of 2000 and 2001.

The means and variances for each month were computed. These means were tested to see if they were significantly different statistically. For this analysis it was determined that the monthly means of the coefficient of thermal expansion were statistically different. The difference in the coefficient of thermal expansion from month to month could be attributed to seasonal thermohygrometric cycles. In previous research it has been hypothesized that the coefficient of thermal expansion in concrete is not constant, where hygrometric exchanges with the atmosphere causes fluctuations in the value. The next step was to compare the average values from block to block to determine if they differed significantly from each other. From this analysis it was determined that there is a small but statistically significant difference among the means for the coefficient of thermal expansion for the blocks. Because the difference is small, it was decided

to ignore this difference and use a single average value for the coefficient of thermal expansion. Results on the average values for each block during each month are shown in Tables 4.10 for bridge 1 and 4.11 for bridge 2.

It is noted that analysis of coefficients of thermal expansion during year 2001 produced a slightly larger value than in year 2000. This could be due to the improved field support conditions of the shrinkage blocks for the year 2001. In year 2000 the blocks were simply set on a flat piece of wood. In 2001 the blocks were set on a frame and supported by rollers. This set up was better suited for the analysis of temperature effects because air was allowed to circulate underneath the blocks and the rollers provided less friction against movement.

Table 4.10 Bridge no. 1, coefficient of thermal expansion, summary results.

Month Year 2000	Girder G3-A Shrinkage block		Girder G3-B Shrinkage Block		Deck Shrinkage Block no. 1		Deck Shrinkage Block no. 2	
	Average $1/^oF$	n^1	Average $1/^oF$	n^1	Average $1/^oF$	n^1	Average $1/^oF$	n^1
May, 2000	7.283	39	7.172	43	7.333	33	7.289	37
June, 2000	7.406	37	7.183	44	7.400	32	7.417	37
July, 2000	7.761	48	7.761	44	7.628	43	7.661	45
Aug., 2000	7.606	38	7.506	38	7.567	41	7.478	38
Summary Preceding Four Months	7.528	162	7.406	169	7.500	149	7.472	157
May, 2001	7.761	45	7.350	47	7.656	40	7.472	34
June, 2001	7.561	38	7.517	40	7.756	49	7.628	44
July, 2001	7.628	49	7.600	53	7.611	55	7.633	54
Summary Preceding Three Months	7.556	132	7.494	140	7.678	144	7.589	132

Note 1: The 'n ' v alue in the table indicates how many separate coefficients were in the sample for which the average is quoted in the table.
Note 2: All coefficients of thermal expansion in the table have been multiplied by 10^6.

Table 4.11 Bridge no. 2, coefficient of thermal expansion, summary results.

Month Year 2001	Girder G5-A Shrinkage Block		Girder G5-B Shrinkage Block		Deck Shrinkage Block no. 1		Deck Shrinkage Block no. 2	
	Average $1/^oF$	n^1	Average $1/^oF$	n^1	Average $1/^oF$	n^1	Average $1/^oF$	n^1
May, 2001	7.628	43	7.611	37	7.450	41	7.455	42
June, 2001	7.817	51	7.850	46	7.639	47	7.555	47
July, 2001	7.739	55	7.744	55	7.717	55	7.628	556
Summary Preceding Three Months	7.739	149	7.744	138	7.644	143	7.578	145

Note 1: The 'n ' v alue in the table indicates how many separate coefficients were in the sample for which the average is quoted in the table.
Note 2: All coefficients of thermal expansion in the table have been multiplied by 10^6.

It had been decided, based on some of the year 2000 results and before all of the data was available, that a coefficient of thermal expansion equal to 7.50 x $10^{-6}/^oF$ would be used for the project. As it turned out this value may have been a little low, but, in any case, it was used. The strain analysis is not that sensitive to the exact value of the coefficient of thermal expansion. The value selected for use does fit within the range of values that are quoted for quartzite aggregate concrete in ACI Publication 209R-92, 11.76 x 10^{-6} / ^oC to 14.6 x 10^{-6} / ^oC (6.50 x 10^{-6} / ^oF – 8.11 x 10^{-6} / ^oF).

4.6 Shrinkage strains.

Having a value for the coefficient of thermal expansion, the thermal strains were filtered from the shrinkage block strain histories. This isolates the shrinkage strain and permits the analysis of the time variation of the shrinkage strains. The resulting strain histories for all eight blocks are provided in Figures 4.9 through 4.12. All four figures illustrate the classical increase in shrinkage strain with time during the early age of the concrete. After this more rapid development of shrinkage strains the development of shrinkage strains levels off and, in theory, asymptotically approaches a limiting maximum value.

In the results from all eight blocks there appears to be a significant seasonal effect after the initial shrinkage occurs. The shrinkage decreases over the winter months and then rises to a maximum value during the summer months. The reason for this phenomenon is not fully

understood. It is likely that the concrete actually gains back a portion of the initial shrinkage when water from rain or melted snow permeates into the blocks. A further complicating factor in the behavior of the blocks is the effect of freezing and subsequent thawing, or the occurrence of several freeze-thaw cycles. In addition, the support conditions may have been an issue. It will be interesting to see if the seasonal effects continue.

Further monitoring of the bridges is needed in order to determine whether it is a seasonal phenomenon due to the interaction of the blocks with the environment, or something different. The daily and weekly undulations of the plots represent the influence of seasonal and daily variations in relative atmospheric humidity and the fact that the temperature related strains may not be completely removed.

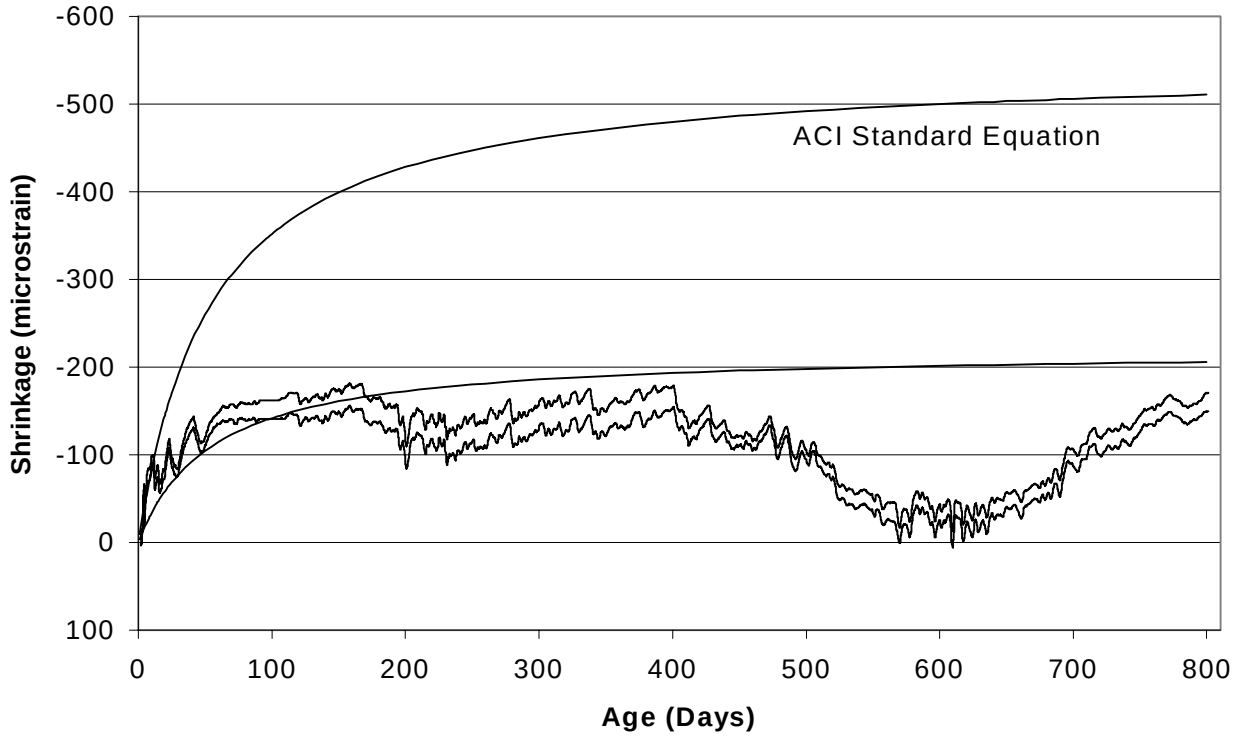

Figure 4.9: Bridge 1, girder shrinkage strains, both blocks.

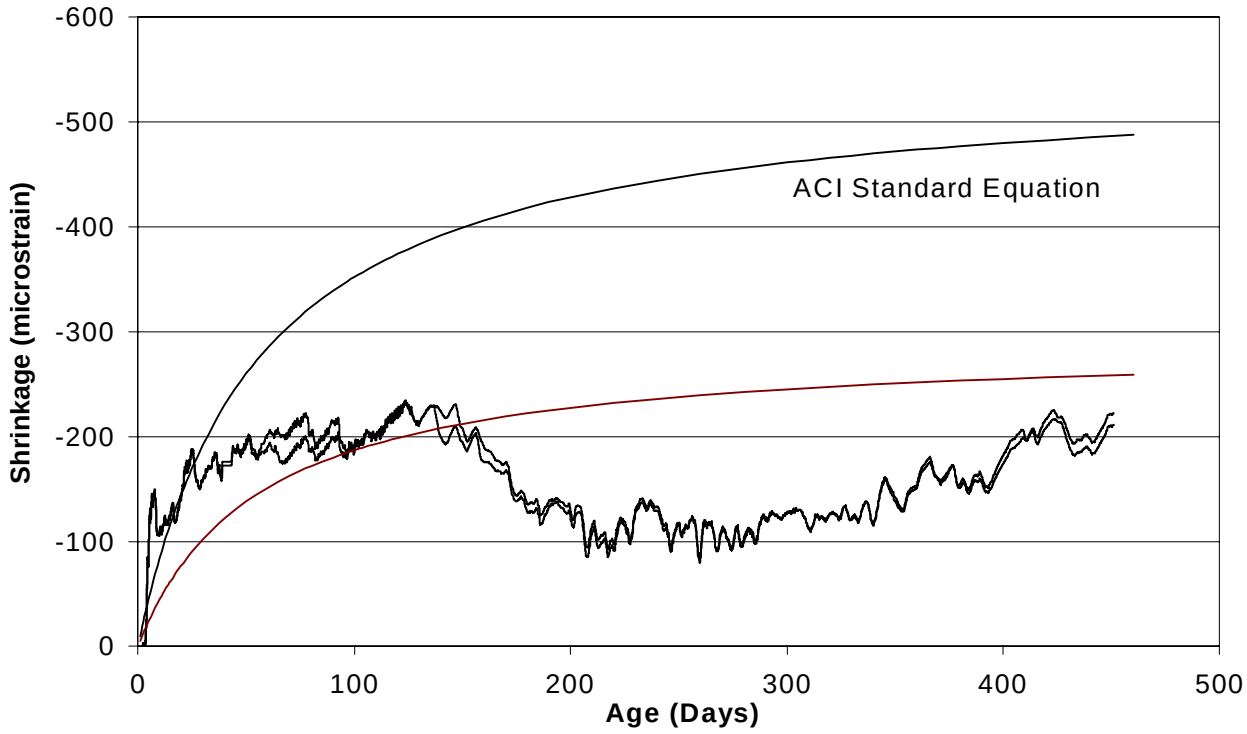

Figure 4.10: Bridge 2, girder shrinkage strains, both blocks.

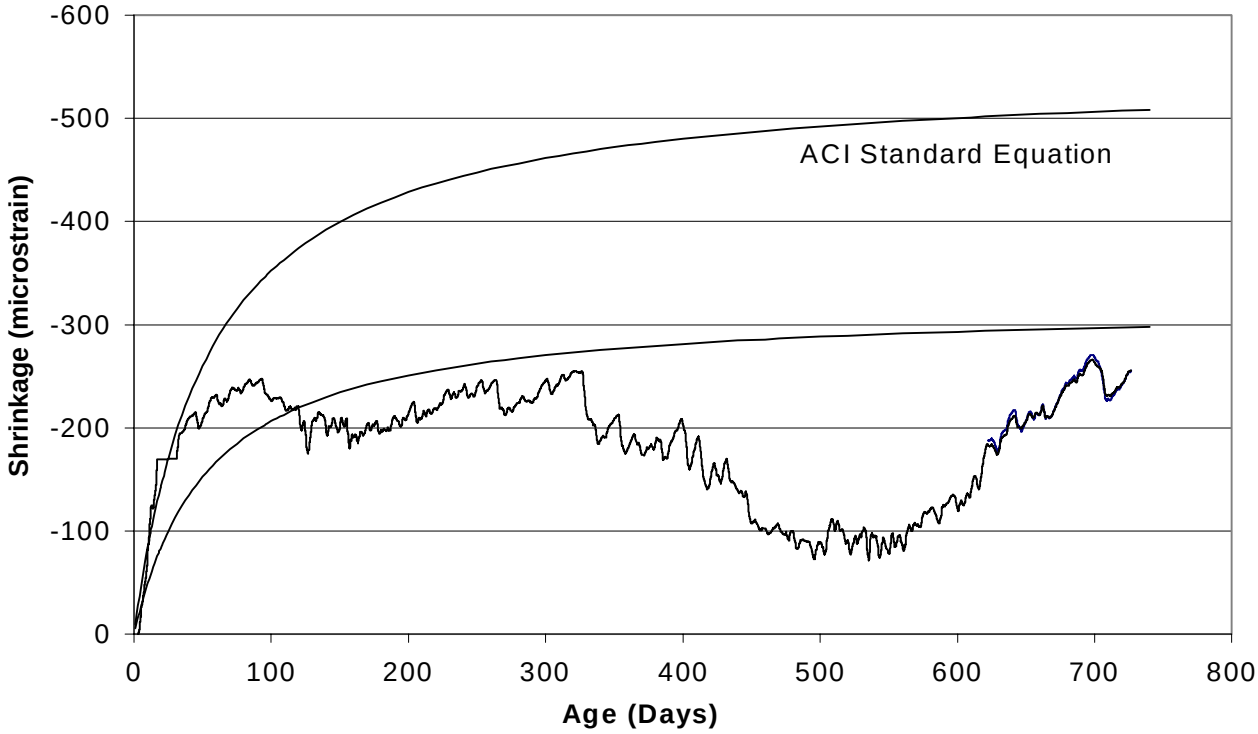

Figure 4.11: Bridge 1, deck shrinkage strains (silica fume), both blocks.

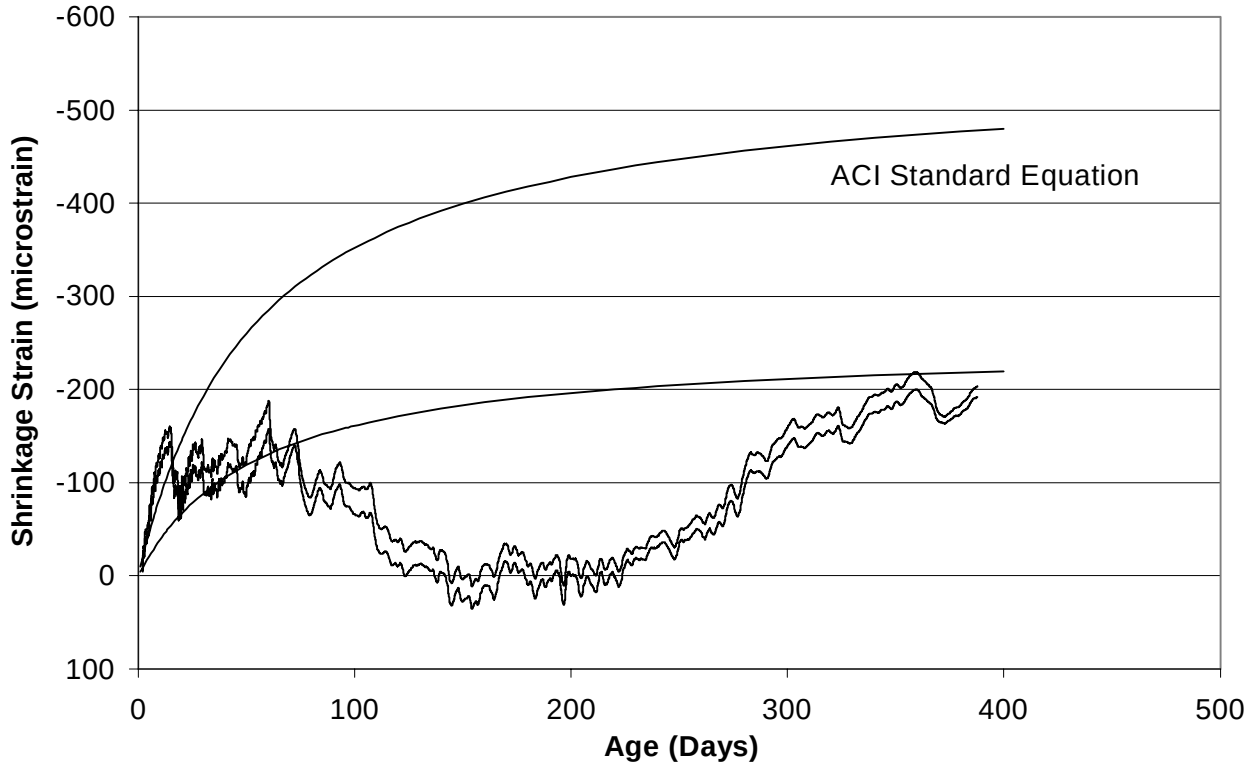

Figure 4.12: Bridge 2, deck shrinkage strains (fly ash), both blocks.

A logarithmic trend-line has been fitted for each set of data to show the general development of shrinkage strain. Another trend-line is shown on the plots illustrating the predicted value for shrinkage using the standard shrinkage equation listed in ACI Publication 209R-92. The form of this equation is (moist cured concrete)-

$$\varepsilon_{sh,t} = \frac{t}{35+t}\varepsilon_{sh,u} \qquad \text{equ. 4.5}$$

$\xi_{sh,t}$ = Shrinkage strain at age t, days.
t = Age of the concrete in days
$\xi_{sh,u}$ = Ultimate shrinkage strain as t goes to infinity.

If no better information is available, this publication recommends an ultimate shrinkage strain value of 780 με. The symbol 'μ' , represents a multiplier equal to 10^{-6}. The term 'ε' stands for strain. To this ultimate shrinkage value, a correction for humidity is recommended. Eastern South Dakota has an annual average relative humidity of 70 percent. The coefficient for this humidity is 0.70. With this modification the ultimate shrinkage strain estimate is 550 με.

The AASHTO specification does not have an equation of this exact form. The approach in the AASHTO specification is to predict the stress loss due to ultimate shrinkage directly in one calculation. In addition, the correction for humidity is incorporated in the equation. The AASHTO equation can be put in a strain form by dividing the referenced equation by the modulus of elasticity of prestressing strand, which is 186.1 MPa (27,000,000 psi). The resulting equation is given below-

$$\xi_{sh,u} = (630 - 5.56\ H)\ 10^{-6} \qquad \text{equ. 4.6}$$

$\xi_{sh,u}$ = Ultimate shrinkage strain.

H = Relative humidity in percent

Substituting the average relative humidity of 70 percent for Eastern South Dakota one obtains an estimate of the ultimate shrinkage of 240 με.

If one considers the early shrinkage to be that that occurs within the first 100 days, the following observations can be made. The girder concrete for bridge 1 demonstrated a maximum early age shrinkage of about 150 με the corresponding value for the girders in bridge 2 is 200 με. This difference is about 25 to 30 percent depending on how one elects to express the difference. The average of these two strains is about 180 με. What is interesting is that there is not nearly this variation between the respective shrinkage blocks from the same bridge. It may be indicative of the variation inherent in dealing with a silica fume mix. This difference in shrinkage is a factor in the increased camber that developed in the girders for bridge 2.

Turning to the point of predicting ultimate shrinkage and computing the ratio of the 180 με average to the ultimate shrinkage as recommended by the ACI 209 Committee (590 με) the results is 0.30. In general one could use a conservative estimate of about half of 590 με to estimate the ultimate shrinkage for the concrete used in the girders in these bridges. If one next compares this value to the ultimate shrinkage as predicted from the current AASHTO equation, one must note that a modifying coefficient is required that reflects the surface area to volume ratio of the element for which the ultimate shrinkage is being estimated. This coefficient is about 0.76 for the girders used in these bridges. Applying this coefficient to the 590 με one ends up with an estimated ultimate shrinkage strain for the girders of about 450 με. Applying this coefficient to the average of the maximum 100-day shrinkage strain from the blocks one obtains approximately, 135 με. This is less than the value predicted from the current AASHTO

equation, 240 με. The conclusion is that the shrinkage strains in the silica fume girder mix appear to be less than what one would predict for normal concrete. One must be careful about generalizing this result.

The deck concretes present a little different picture. The early period shrinkage for the silica fume concrete making up the deck is about 240 to 250 με. The corresponding fly ash concrete early period (first 100 days) shrinkage is about 150 με. This difference is significant. The silica fume concrete exhibited about 1.6 times as much early period shrinkage as the fly ash concrete. This difference holds true for the late shrinkage as well.

4.7 Development of the strain time series and selection of the initial time (t_0):

The data from the vibrating wire strain transducers is initially converted to raw strains. These strains are subsequently converted to a base temperature so that the series can be analyzed without the temperature effects. The base temperature that was selected was 22.2 ^{o}C (72.0 ^{o}F). The conversion of the strain to the base temperature requires a correction for expansion of the gage as well as a correction for the thermal expansion of the concrete. This produced a series that can be considered to have been taken at a common temperature. The next step was to define a zero time so that the difference in strain relative to this time-zero could be determined.

This equation is given as

$$\Delta\varepsilon_{t_i} = \varepsilon_{t_i} - \varepsilon_{t_0} \qquad \text{equ. 4.7}$$

$\Delta\varepsilon_{t_i}$ = Change in strain since t_0

ε_{t_i} = Strain at time t_i

ε_{t_0} = Strain at time t_0

These differences in strain are the values that are of interest in the time history analysis of strain. Time zero was selected by inspecting the data over the first few days after the concrete was placed. One seeks a time close to the time that the concrete has set, yet at a time at which the temperature has settled down a little bit. In all four cases, the two girder placements and the two deck placements, a time zero was selected about 2 days after the concrete was initially placed in the forms. The selection of time zero does influence the subsequent time histories, but a half day one way or the other will not have a large influence on the strain time histories that are calculated.

Once the time histories were generated, the shrinkage block time histories were used to remove the shrinkage strains. This was done according to the following equation-

$$\Delta\varepsilon'_{t_i} = \Delta\varepsilon_{t_i} - \Delta\varepsilon_{sh,ti} \qquad \text{equ. 4.8}$$

$\Delta\varepsilon'_{t_i}$ = Strain increment at time t_i, with the shrinkage strain removed.
$\Delta\varepsilon_{t_i}$ = Strain at time t_i.
$\Delta_{sh,ti}$ = Shrinkage strain at time t_i.

The strain time series that result from the application of equation 4.6 are then subjected to further analysis.

4.8 Analysis of the girder strain time histories:

As has been noted earlier in this report, each prestressed girder had four vibrating wire strain transducers located at mid-span. These transducers were distributed uniformly through the depth of the girder. A program was developed that permitted the linear regression analysis on these four readings. After the regression analysis was performed, the resulting regression results were used to compute strains on the top, bottom and at the centroid of the AASHTO Type II girders. This exercise was repeated at each 30-minute interval throughout a 24-hour period.

After this was completed, the readings were averaged through the day. This averaging tends to remove the remaining cyclical daily variations in the data. Once this was completed on all of the data, the results for each girder were plotted. These two separate plots are similar to each other. The next step was to average the results from the two separate girders. The result of this operation is provided in Figure 4.13 for the instrumented girders from bridge 1, and in Figure 4.14 for the girders from bridge 2. Inspection of these two graphs provides interesting insights into the behavior of these girders.

By inspecting Figures 4.13 and 4.14, the strains introduced into the prestressed girders due to transferring prestress is readily observed. The average compressive strain at the centroid of the girders from bridge 1 is about 425 με. Since this strain is at the centroid of the section it is an indicator of the initial prestress force, P_i. Inspecting the graph for bridge 2, it is observed that the initial compressive strain at the centroid is about 525 με. The difference between these two values is about 19 percent. This difference seems a little large considering the agreement in

the initial deflections. (Table 4.9). The changes in strain associated with the early camber development are noted in the figures.

The change in strains associated with the placing of the decks is clearly observed in the figures by focusing on the lines that represent the strains at the top and bottom fibers of the beam. The plot of the strain at the centroid should not show any effect from the placement of the deck. The fact that it does show a small increment of strain indicates that the actual centroid is not located exactly as predicted.

The change in the strain with time at the centroid of the cross section is indicative of the effect of creep. It would include shrinkage strains but these have been removed. It does include the effect of relaxation in the steel, but low-relaxation strand was specified, so the relaxation effect is not very large. The time variation change in the strain due to creep from the time the girder was cast until the deck was placed is about 25 με in bridge 1 and about 75 με in bridge 2. These values represent a change of about 5.9 percent in the initial prestress in the girders for bridge 1 and about a 14.0 percent change in the initial prestress for bridge 2. This change in strain occurs over an approximate two-month period

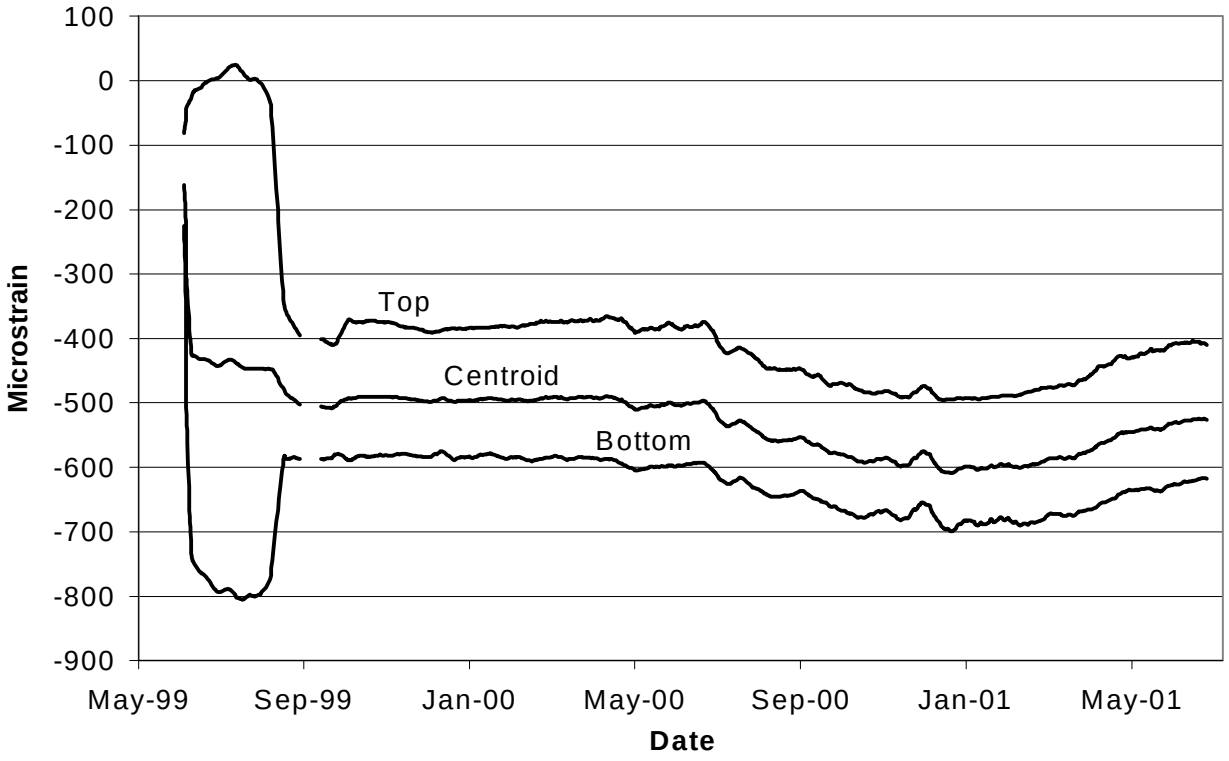

Figure 4.13: Bridge no. 1, girder daily average strain histories.

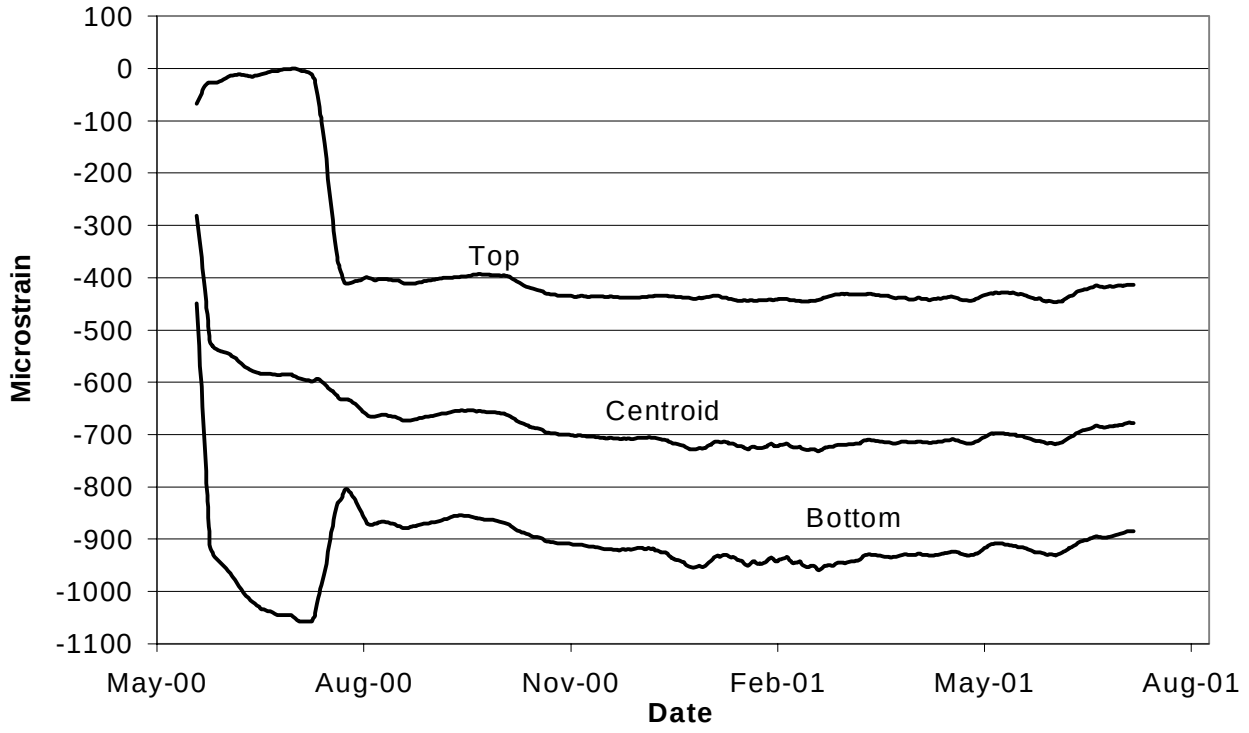

Figure 4.14: Bridge 2, Girder daily average strain histories.

After the deck is in place, the neutral axis shifts upward to a location near the top fiber of the girder. The top line in the figure can be traced to determine the time dependent changes that take place after the deck is placed. There is no significant long-term change in the graph for Bridge 1 from August 1999, through March 2000. After March 2000, it appears that a seasonal effect begins. If it is not seasonal, it is at least a long period change. It will be interesting to see if these trends are indeed long period seasonal changes, or simply a nonrecurring change. Note, that all three lines remain separated by an equal amount. This indicates the system is responding in a linear manner. Since the strains moved in a compressive direction, it indicates the beams are coming under a uniform compressive force. This behavior is interesting.

Inspecting Figure 4.14 (bridge 2 data) for this same long-term change, it is noted that the strains at the top edge of the girder do indicate a long-term change. It is noted to be about 20 to 30 με. This strain developing over an 11-month period. This indicates a further 4 to 5 percent loss in the initial prestress force. It appears that this trend tends to reverse at the end of this 11-month period. More data is needed to see if this continues; if it continues, it is the same behavior as observed in bridge 1.

There is one curious event in the strain history of bridge 1. Note the gap in the data during September 1999. A little to the right of this gap is a small but noticeable inflection in the strain registered by all three transducers. The gap itself is due to the failure of the computer sometime after Labor Day in September 1999. The computer was put back on-line in late September. The location in time of this inflection corresponds approximately to the time that the traffic was routed over the bridge. The inflection takes place over several days, perhaps ten days. The change on the top fiber of the beam is tensile which corresponds to a small increase in camber (upward deflection). In any case, it is interesting. In later analysis, it will be noted that this inflection only occurred in the outer girder.

4.9 Girder curvature analysis:

The curvature of a beam is an indicator of the radius to which the beam is bent. Specifically the curvature is the reciprocal of the radius to which the beam is flexed. In general, it changes in a continuous manner along the beam. It is defined by the following equations-

$$\phi = \frac{1}{\rho} = \frac{(\varepsilon_2 - \varepsilon_1)}{h} \qquad \text{Equ. 4.9}$$

ϕ = curvature

ρ = radius to which the beam is bent

ε_1, ε_2 = strain at the top and bottom fiber of the beam respectively.

h = the depth of the beam.

From the strain measurements, the strains at the top and bottom fiber of the beam are known. These equations are simply equations of kinematics and do not require elastic behavior of the material. A program was developed that computed the curvature in the girders from the transducer readings. There are four transducers at the center of the girder, and, as has been stated, a regression line was computed from these four readings. From this regression line the strain was computed on the top and bottom fibers of the beam. From these two values of strain, the curvatures are computed. The curvatures for the two girders (G3-A and G3-B) in bridge 1 are provided in Figure 4.15. The curvatures for the instrumented girders (G5-A and G5-B) in Bridge 2 are provided in Figure 4.16. Larger positive values of curvature indicate a tendency for

the beam to exhibit upward camber (upward deflection). A decrease in positive curvature indicates the beam is tending to exhibit downward deflection.

This positive change in curvature is noted in all four girders over the period that they were stored in the prestressing yard. In addition, the instantaneous and maximum camber are in general agreement with the deflections that were measured on these girders. From Table 4.9 it is noted that girder G3-A exhibited a maximum camber of 25.4 mm (1.00 inches) and girder G3-B exhibited a maximum camber of 23.62 mm (0.93 inches). The difference in these two values is about 3 percent. The curvature for these two girders is about 22.0 and 24.0 respectively. This is a difference of about 8 percent. This is relatively good agreement. The maximum camber noted in girders G5-A and G5-B was 31.8 mm (1.25 in.) and 30.0 mm (1.18 inches) respectively. Their two curvatures are nearly identical, as are the deflections. In both figures, the effect of the deck placement is noted by a sharp drop in curvature. The deck placement occurring in August 1999 for bridge 1 and in July 2000 for Bridge 2.

There is a sharp positive curvature change in Girder G5-B (Bridge 2) immediately after the deck was placed. This change is not mirrored in Girder G5-A. This is puzzling. If it were an elastic change, it would reflect a change of about 4.8 mm (0.19 inches) in deflection. This is not noted on the graph of deflections. This could indicate that the response was inelastic. Thereafter the two girders exhibit nearly identical curvatures.

Creep should show up as a positive or negative drift in the curvature with time. The trends in these figures reflect the observations made on the strain at the centroid of the girders. The difficulty is that it is not as easy to observe small changes in this figure due to the scale employed. For example if the curvature were about 6, then a 10 percent change would change this value by 0.6. This change not being obvious due to the scale of the graph.

The inflection that was previously noted on Figure 4.13 on Bridge 1 can be observed as a change in the curvature of Girder G3B in Figure 4.15. There may be a small corresponding change on the graph of Girder G3A, but it is very slight. This inflection results in an increase in the camber of the beam.

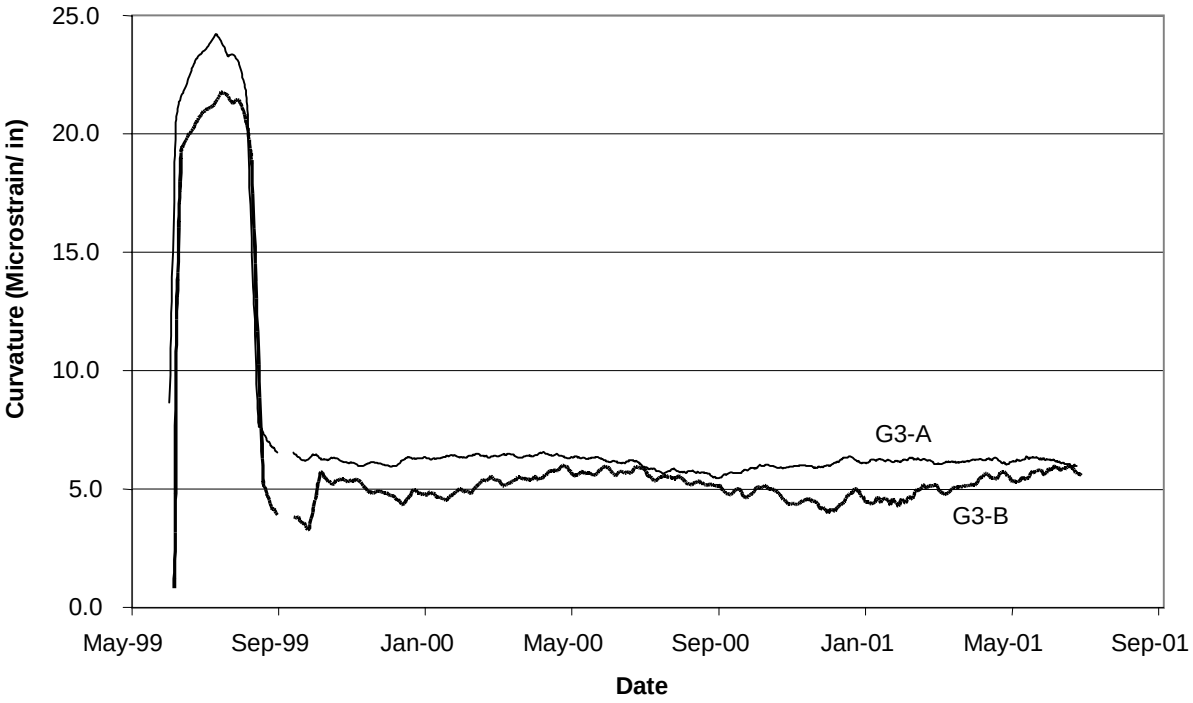

Figure 4.15: Bridge no. 1, individual girder curvature at mid-span.

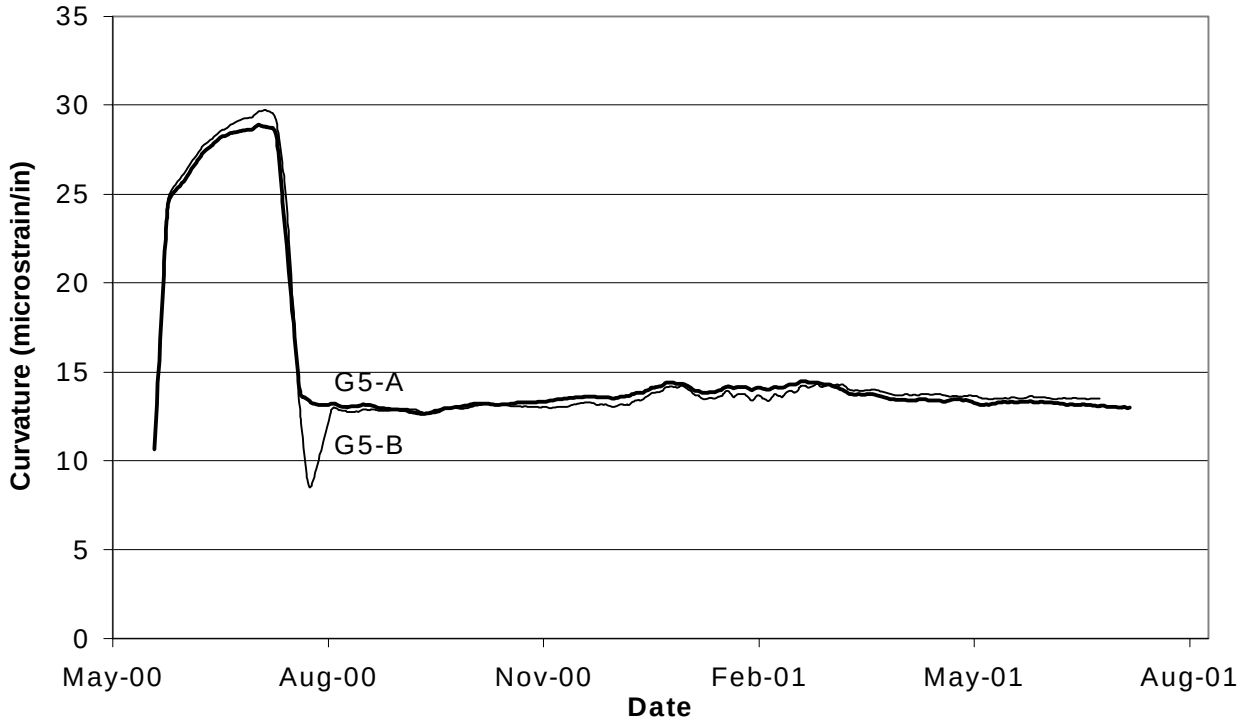

Figure 4.16: Bridge no. 2, individual girder curvature at mid-span.

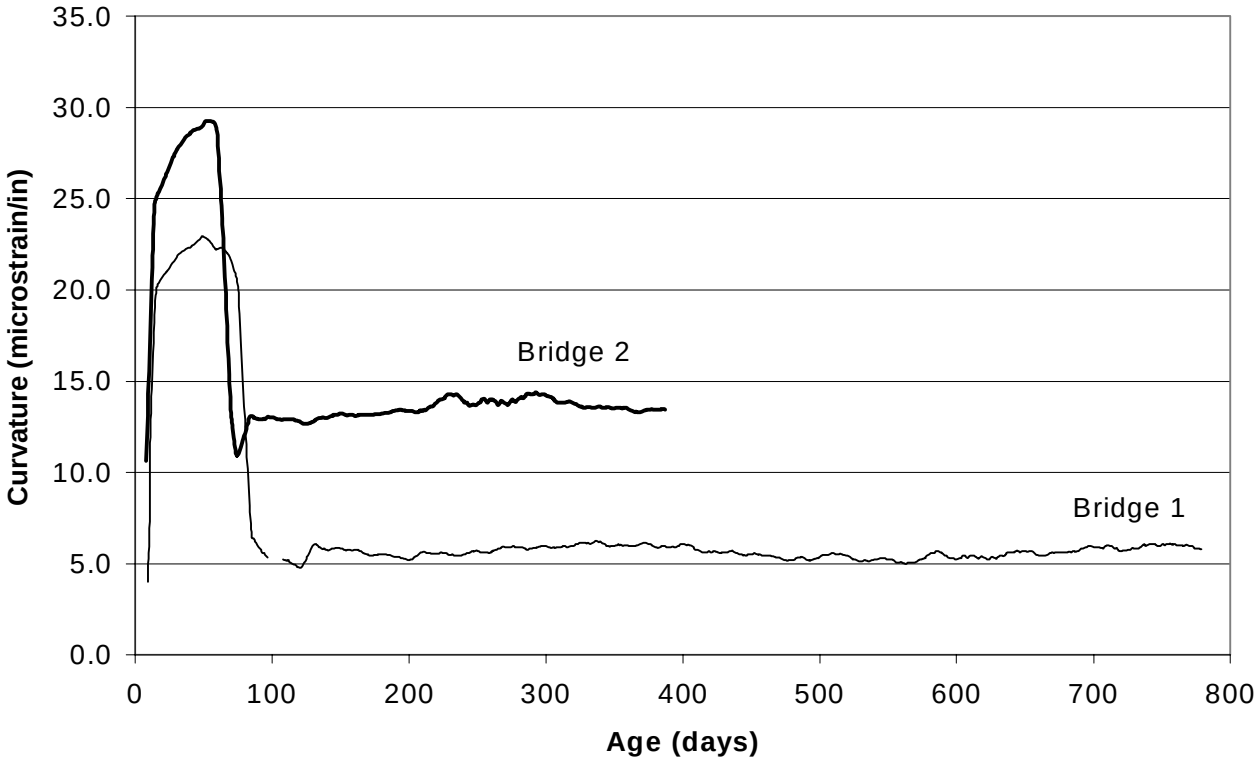

Figure 4.17: Bridges 1 and 2, average girder mid-span curvature.

The curvatures for the two separate girders in each bridge were averaged. The results of this exercise are presented in Figure 4.17. In this figure, the time scale is just days from time zero, time zero being the time of the casting of the girders. The difference between the two girder averages is easier to view in this figure. As noted previously, the camber and thus the prestress, was greater in the girders cast for bridge 2. Not only this, but the long term curvature is about double in this second set of girders as compared to the girders from bridge 1. These trends can be verified by inspecting the change in the deflections back in Figure 4.7. These also are in the same ratio.

4.10 Bent curvature analysis:

A uniformly spaced stacked set of three vibrating wire transducers was placed at the bent in the gap between the prestressed girders. As the deck is placed this region between the girders is filled with fresh concrete. This forms an integral bent diaphragm. In each bridge two sets of transducers were placed at the bent. One set was placed in the gap between the two girders located on the outside girder line. The second set was placed in the gap between the girders at

the adjacent interior girder line. The bent transducers in bridge 1 are all providing, what appears to be useable readings. In bridge 2 one of the bottom bent transducers was apparently ruined during the placement of the deck. This reduced the set of three to two transducers. The remaining two do not appear to be giving good readings. Because of these apparent poor readings, this group was not used to develop the information for the following discussion. The second set in bridge 2 is believed to be providing useable results and has been employed to develop the following results.

The bent curvatures were computed employing the same method that was used for the girder curvatures. The results are provided in Figure 4.18. The plot for bridge 1 is the most interesting. It is observed that the curvature has steadily decreased over the two years that the bridge has been monitored. This graph is the average of two locations, but both locations show this same general trend. It is possible that this curvature change is due to the higher deck shrinkage that has been noted in bridge 1. The girders are tending to come together at their tops and tending to separate at their bottom fibers. This same trend may be showing up in the second bridge, but there has not been sufficient data gathered to indicate that it is definitely taking place.

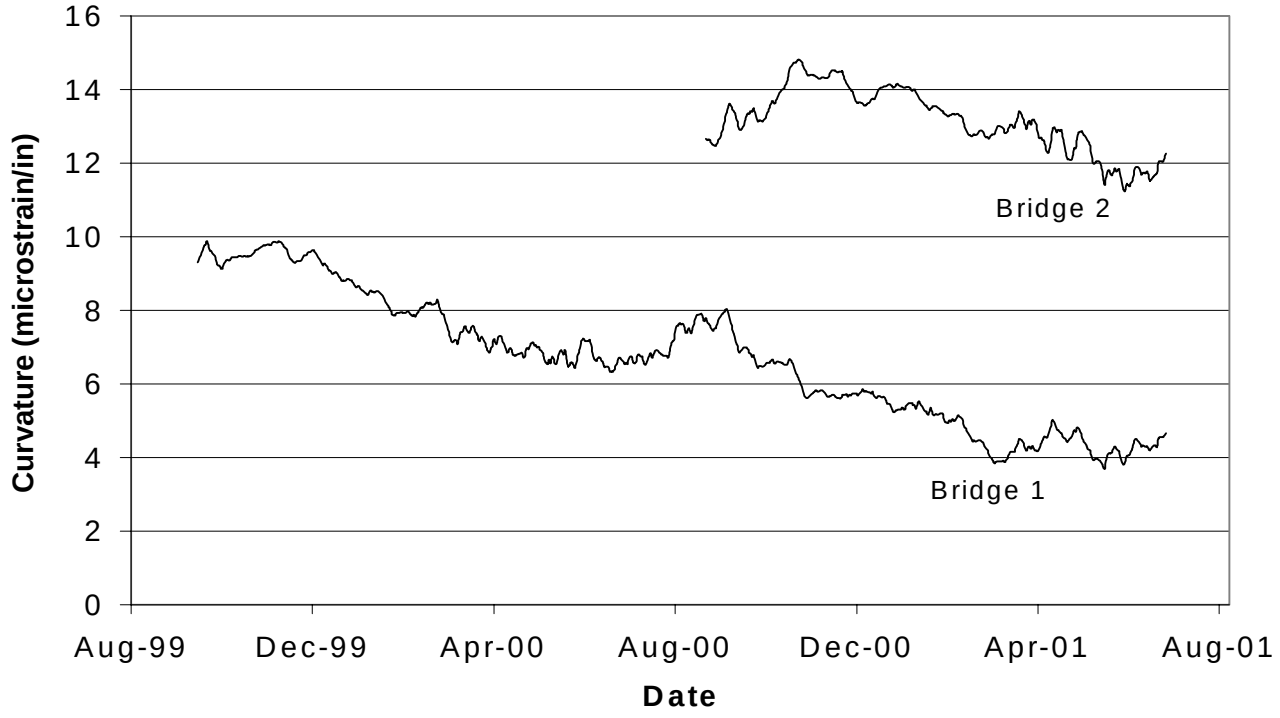

Figure 4.18: Bridges 1 and 2, curvature between the girders at the bent.

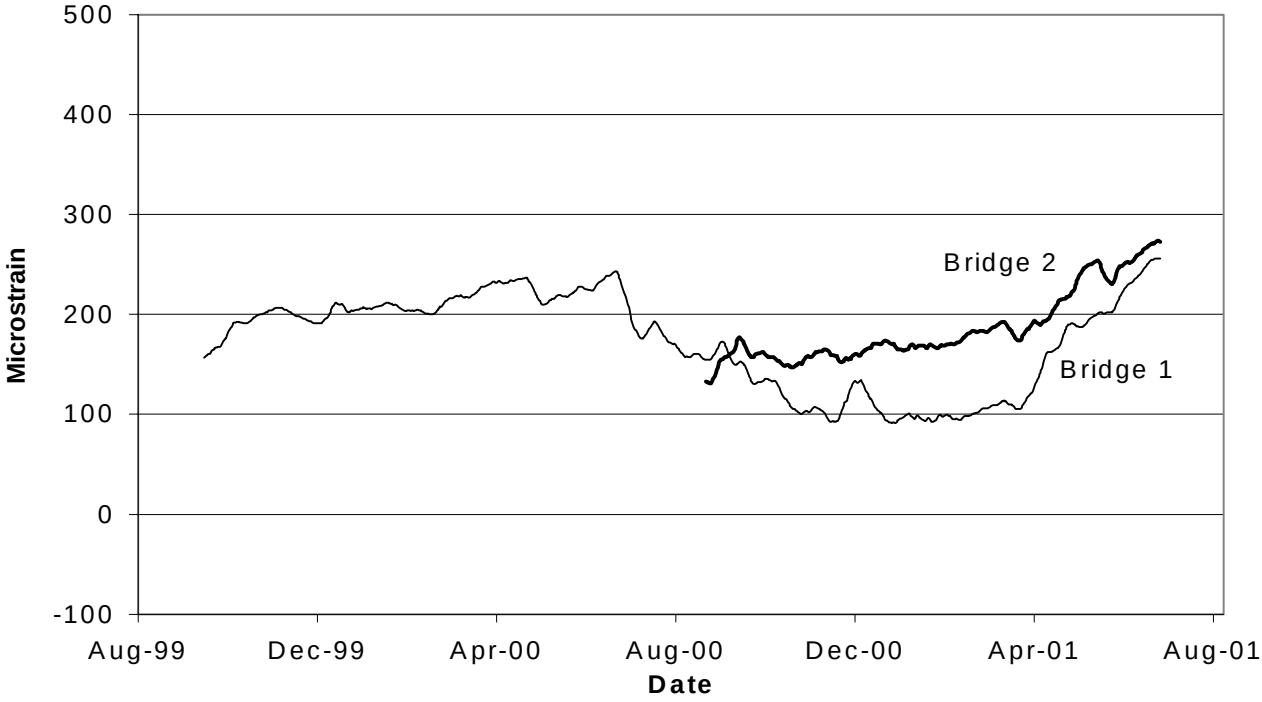

Figure 4.19: Bridges 1 and 2, centroidal strains between the girders at the bent.

One could argue that during the first year the change in curvature was about 2. Over the first year in bridge1, this change was about 2.5. More data is needed to see if this trend continues. Strain between the girders at the level of the girder centroids is plotted in Figure 4.19. This strain is relatively insensitive to the curvature. These strains demonstrate that tensile strains are developing between the girder ends at the level of the girder centroids. In this case, the two bridges are comparable. As stated, the strains between the girder ends are tensile, and vary cyclically about a value of about 175 με. More data records and further analysis are needed before one can make further comments on the behavior of the bridge at the bent locations

4.11 Deck Strains:

There are four sets of two strain transducers positioned at mid-span with a second similar array over the bent. Utilizing the two transducers that are stacked vertically in the deck, regression analysis was employed to compute the constants for an equation that would permit the computation of strain through the thickness of the deck. The strain was then computed at the

mid-depth of the deck. After the separate values were computed they were then averaged. Figure 4.20 presents the results from both bridges for the mid-span location. Figure 4.21 provides similar results over the bent.

The results before the shrinkage strains are removed are presented along with the results after the shrinkage strains are subtracted. Since the shrinkage strains are negative, subtracting them from the record results in a shift in the tensile, or positive, direction. Here as in other results, there is a long period cyclical change indicated. This cyclical change is demonstrated in both figures and is occurring in both bridges. Focusing on the net strains, after subtracting out the shrinkage strains, it is observed that overall the tensile strains are significantly higher in bridge 1 as compare to bridge 2. Bridge one has an average tensile strain of about 160 με at mid-span. The corresponding value over the bent is about 420 με. Similar results for Bridge 2 are 60 με at mid-span and 250 με over the bent. If one ratios the numbers for each bridge, the results are 2.6 for Bridge no. one and 4.2 for bridge 2. The ratios are not comparable.

The strains in the deck are interesting, but difficult to explain. They are consistent with the developing data that indicates that the silica fume deck exhibited a greater tendency to shrink and thus develop tensile stresses. On the other hand, as will be seen, there are about twice as many transverse cracks in the silica fume deck as compared to the fly ash deck, thus with cracking the tensile stresses should be reduced.

The data is consistent with a highly restrained element, which the deck seems to be. Not much is known about the creep of concrete in tension except that it certainly takes place. Additional data and further detailed analysis is needed before additional comments can be made.

4.12 Underside deck crack surveys:

Significant transverse deck cracking was noted in bridge 1 during the first winter (Early January 2000) after it was constructed. Transverse deck cracking was also noted in bridge 2 during this bridge' s first winter. In August of 2001, underside deck surveys were conducted on these two bridges. These surveys were conducted from the ground. The number of cracks was counted between each girder and along the overhangs. In some cases, a significant distance occurred between the end of the span and the first crack. When this was observed the distance to the first crack was estimated and this dimension to the first crack was taken into consideration when computing the crack spacing in that span. In general, within a span the spacing between

cracks was relatively uniform. Reasonable estimates of dimensions could be made due to the imprint of the 4x8 plywood form-sheets on the underside of the deck concrete. Nearly all of these cracks are exhibiting calcium carbonate precipitate and under appropriate winter conditions exhibit moisture seepage. This was readily observed during the winter months and was the reason that the cracks were first noted in January 2000. The results of the surveys on the two bridges are summarized in Table 4.12.

A couple of points must be noted. Consider the first bridge. The crack spacing in the end spans is about double the spacing in the center span. This same relative spacing is true as well for bridge 2. This indicates, which makes sense, that there is more restraint in the center span which contributes to greater cracking. Overall, the average crack spacing in bridge 1 is about 1.37 m (4.5 feet). The corresponding value for bridge 2 is about 2.32 m (7.6 feet). The ratio of the crack spacing in bridge 2 to the crack spacing in bridge 1 is 1.7. This is in general agreement with the shrinkage data from the two bridges. This ratio, as previously cited, is 1.6. The basic point is that there is significantly more cracking in the silica fume deck as compared to the fly ash deck and this is supported by the data that has been taken.

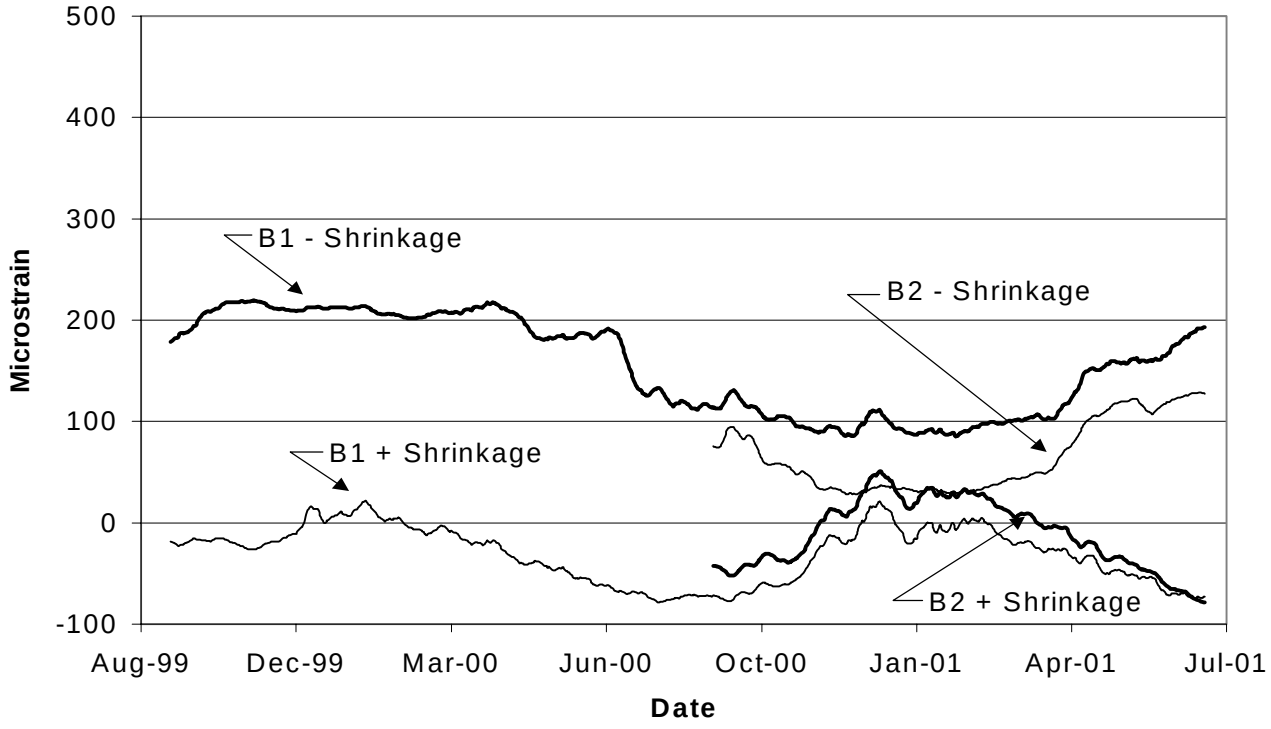

Figure 4.20: Bridges 1 and 2, mid-thickness deck strain at mid-span.

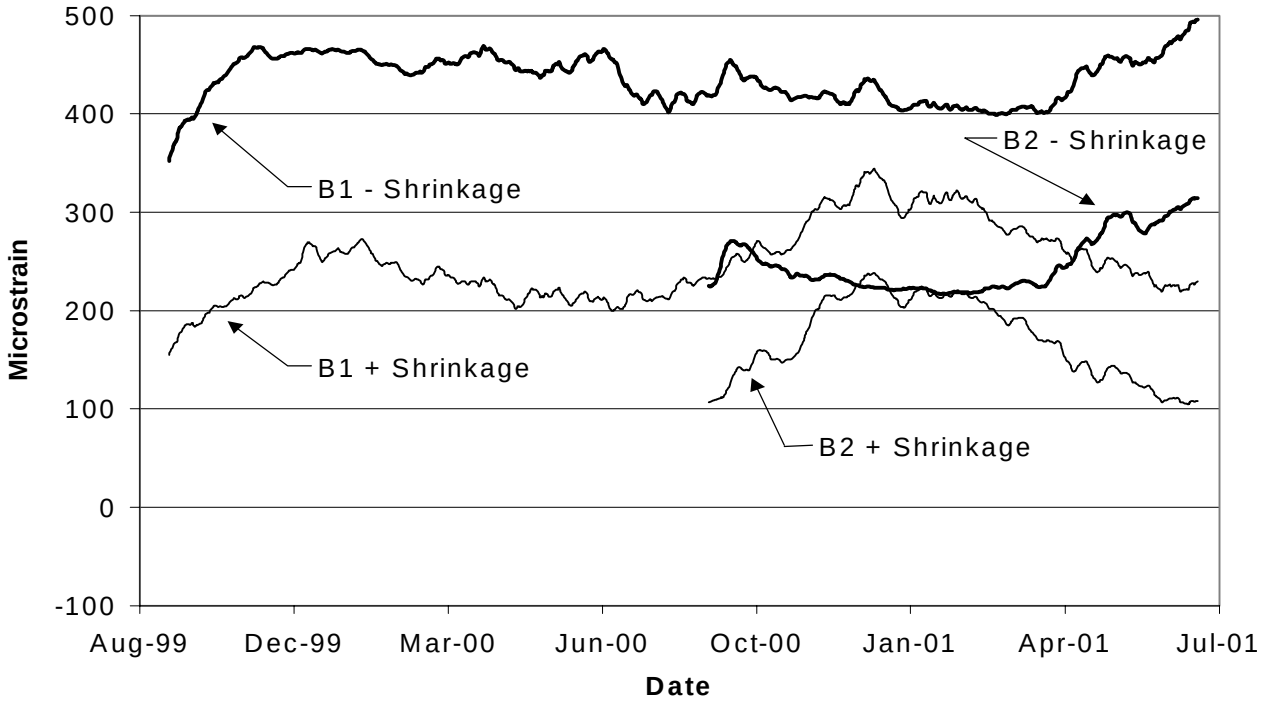

Figure 4.21: Bridges 1 and 2, mid-thickness deck strain at the bent.

Table 4.12 Bridge no 1 and 2, Summary crack data (Surveys of August 2001).

	Bridge no. 1		Bridge no. 2	
	No. of Cracks	Spacing (ft.)	No. of Cracks	Spacing (ft.)
North Span	38	6.0	17	12.9
Middle Span	82	3.3	49	5.4
South Span	43	5.5	27	8.1
Overall Data	163	4.5	93	7.6

Unit Conversions: 1 ft = 0.3048 m

4.13 Temperature analysis:

There are a large number of temperature sensors in each of these two bridges. Only summary information is presented here because detailed analyses have not been completed. The maximum temperature that was observed in the instrumented girders during the initial hydration of the concrete was essentially the same for each girder and was about 60 ^{o}C (140 ^{o}F). This peak

temperature was achieved about 16 hours after the concrete was placed. The fabricator applied supplementary heat in the form of hot water that was circulated through pipes that are directly under the beam forms. Insulating blankets were used to retain the heat in the girders.

The highest temperature that was observed during the curing of the decks was about 52.8 ^{o}C (127 ^{o}F) in the silica fume deck and about 46.1 ^{o}C (115 ^{o}F) in the fly ash deck. The high temperature in the silica fume deck was achieved about 23 hours after concrete placement. The high temperature in the fly ash deck was achieved about 27 hours after the deck was initially placed. Since silica fume hydrates very rapidly and contributes significantly to early strength gain, one would expect the silica fume mix to exhibit a higher peak temperature than the fly ash mix.

The average girder and deck temperature for bridge 1 during the summer and winter of 2000 are provided in Figures 4.22 and 4.23, respectively. Averaging all temperature transducers in the deck and performing a similar average for the girders generates these curves. The individual values are daily averages, for this reason they do not reflect the diurnal variation over the day. In addition to the data, a trend line has been imposed. As would be expected the girders are cooler than the deck.

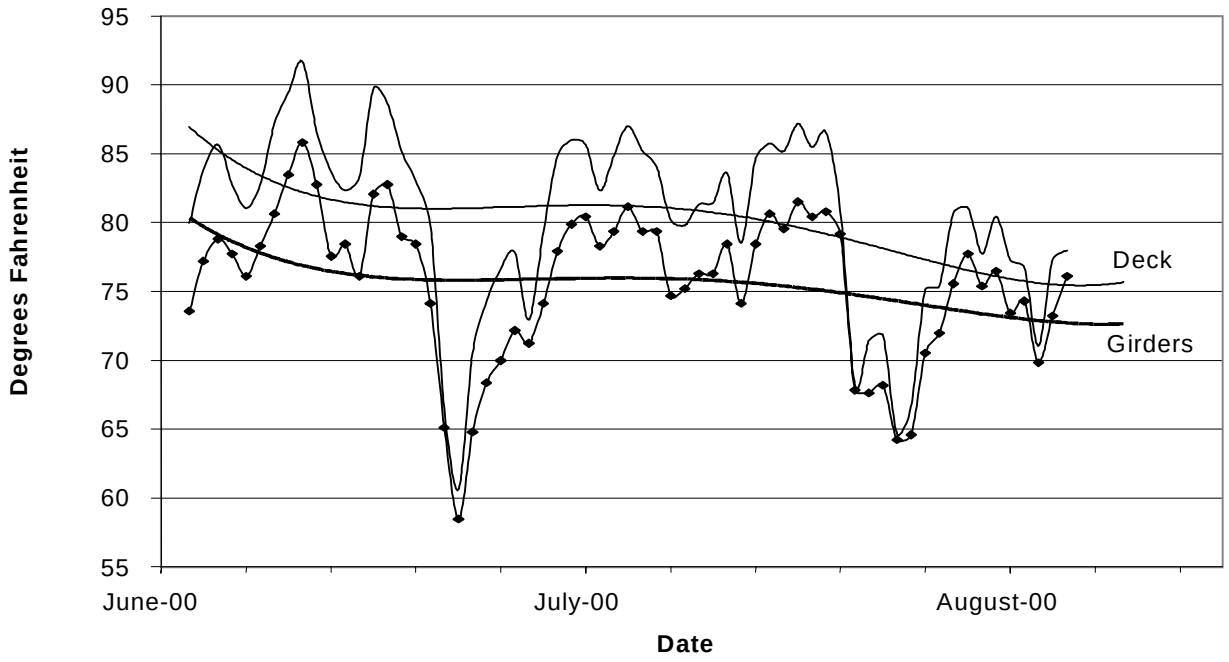

Figure 4.22: Bridge 1, average daily deck and girder temperatures during the summer of 2000.

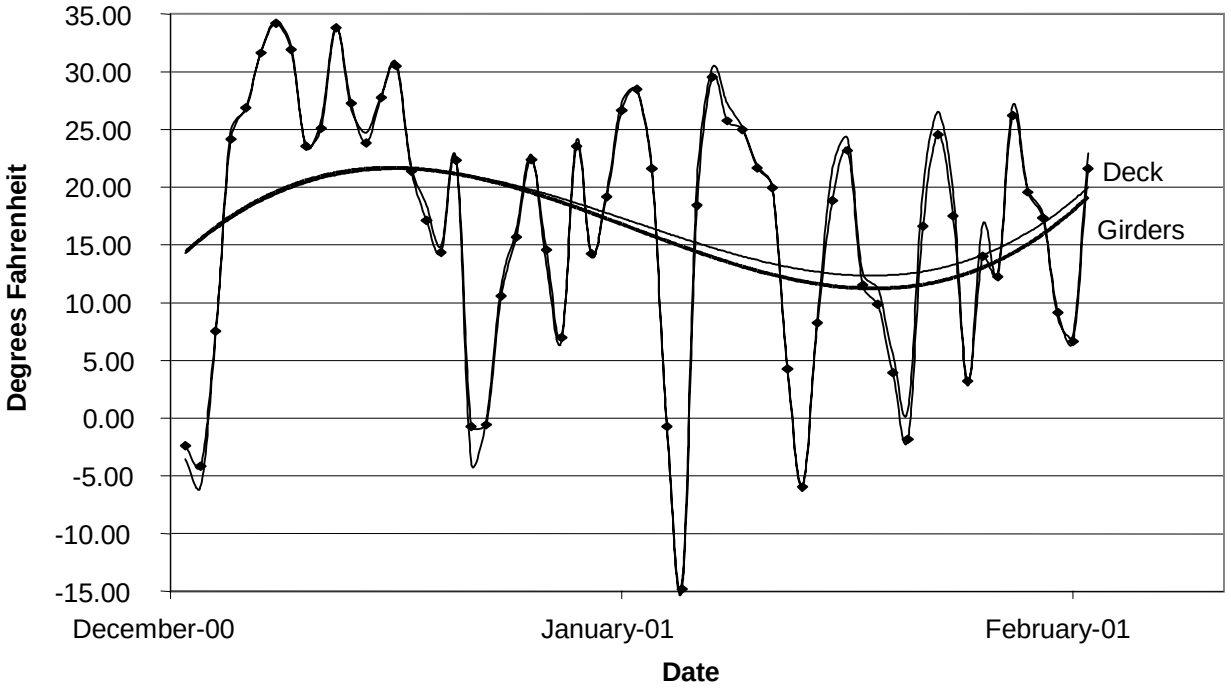

Figure 4.23: Bridge 1, average daily deck and girder temperatures during the winter of 2000.

By examining the trend line, it can be seen that in the summer the girders are about 9 ^{o}C (5 ^{o}F) cooler than the deck. This difference causes thermal gradients and will give rise to thermal stresses.

A similar graph is presented for the winter of 2000. Winter 2000 was a significant winter. It was very long and a record duration of continuous snow cover was recorded. The winter was not extremely cold, though significant stretches of cold weather occurred. As was the case in the summer, the girders are cooler than the deck. The difference though is not very much, being on the order of 1 ^{o}C (2 ^{o}F) degrees. What can not be seen in the data is the diurnal effect. This would be expected to be more significant in the deck than in the girders. The data does show that on an average basis the girders are not too much different in temperature than the deck.

4.14 Rapid Chloride Permeability

Durability of the concrete in bridge decks has a major impact on maintenance costs and the material design is of utmost importance. One of the most severe problems is the corrosion of the bridge deck reinforcing steel, aggravated by chloride ions. Penetration of the chloride ions

into and through the deck concrete, to the reinforcing steel, is a critical parameter to be controlled. The major purpose of this project is to develop the concrete mixture proportions to minimize the transport of chloride ions.

The specimens fabricated from the actual concretes used in the bridge decks, prestressed girders and trial mixes were tested for rapid chloride permeability as per ASTM C 1202. The individual test results are given in Tables 3.2 and 3.3 in Task 11. A total of 92 specimens were tested and the average values of rapid chloride permeability for the trial mix concrete, the girder concrete and bridge deck concrete are given in Table 4.13 for bridge 1 constructed in the summer of 1999 and the corresponding values obtained for bridge 2 constructed during the summer of 2000 are given in Table 4.14.

4.14.1 Bridge Deck Concrete

The comparison of the permeabilities measured for various batches of the concrete used in the construction of bridge 1 in the summer of 1999 is shown in Fig. 4.24. For this deck silica fume HPC mix was used. The values ranged from 393 to 621 coulombs. This is a very low variation, which is due to the better quality control used in the production of concrete. A similar comparison for the various batches of deck concrete used for the construction of the bridge 2 during the summer of 2000 is shown in Fig. 4.25. For this deck silica fume was omitted and fly ash was added as partial replacement for cement. The permeabilities varied from 708 to 1404 coulombs, which is again a low variability for field concrete. It shows that the same quality control was also maintained for the construction of this bridge.

The main objective of developing a HPC mix for the bridge deck construction was to reduce the chloride permeability of the concrete so that the corrosion potential of the steel reinforcement is reduced. The project' s requirement stated that "The bridge deck permeability should be reduced by a significant amount (50%) as compared to the SDDOT' S standard bridge deck mix. The average values of permeabilities for all the concretes used during the construction of both bridges are compared in Fig. 4.26. The rapid chloride permeability (average of 24 specimens) for the HPC silica fume concrete used in bridge 1 is 462 coulombs whereas the permeability of SDDOT' s standard bridge deck mix was 4158 coulombs. According to ASTM C1202, the chloride ion penetrability is "High" for SDDOT' s standard concrete and it is "Very Low" for HPC bridge concrete. This is a 88.9% reduction which has far exceeded the required 50% reduction. The chloride permeability (an average of 24 specimens) of the concrete

used for the second bridge is 1038 coulombs.

Table 4.13: Bridge 1 (Summer 1999) - Average Chloride Permeabilities of Samples taken at different times

Girder Fabrication		
Source	No. of Specimens	Total Charge Passed (Coulombs) - Average
Trial Mix 1	3	161
Trial Mix 2	5	109
Average of 8 specimens		135
Girder Fabrication 1	4	42
Girder Fabrication 2	4	75
Girder Fabrication 3	4	69
Girder Fabrication 4	4	61
Girder Fabrication 5	4	81
Girder Fabrication 6	4	61
Average of 24 specimens		65

Bridge Deck Concrete		
Source	No. of Specimens	Total Charge Passed (Coulombs) - Average
Deck Trial Placement	4	558
Deck Placement 1	4	317
Deck Placement 2	4	461
Deck Placement 3	4	621
Deck Placement 4	4	393
Deck Placement 5	4	516
Average of 24 specimens		462

There was a reduction of 75% in the chloride permeability, which is again greater than suggested. However the permeability of this fly ash mix was 123 % higher than that of the HPC mix that contained 7 percent silica fume.

Table 4.14: Bridge 2 (Summer 2000) - Average Chloride Permeabilities of Samples taken at different times

Girder Fabrication		
Source	No. of Specimens	Total Charge Passed (Coulombs) - Average
Girder Fabrication 2	4	96
Girder Fabrication 3	4	77
Girder Fabrication 5	4	89
Average of 12 specimens		87

Bridge Deck Concrete		
Source	No. of Specimens	Total Charge Passed (Coulombs) - Average
Deck Placement 1	4	782
Deck Placement 2	4	708
Deck Placement 3	4	1404
Deck Placement 4	4	1307
Deck Placement 5	4	988
Average of 24 specimens		1038

According to ASTM C1202, the chloride ion penetrability is "low" for the fly ash HPC mix used in Bridge 2. Therefore, it can be assumed that the potential for the rebar corrosion is very low for bridge 1 and low in bridge 2.

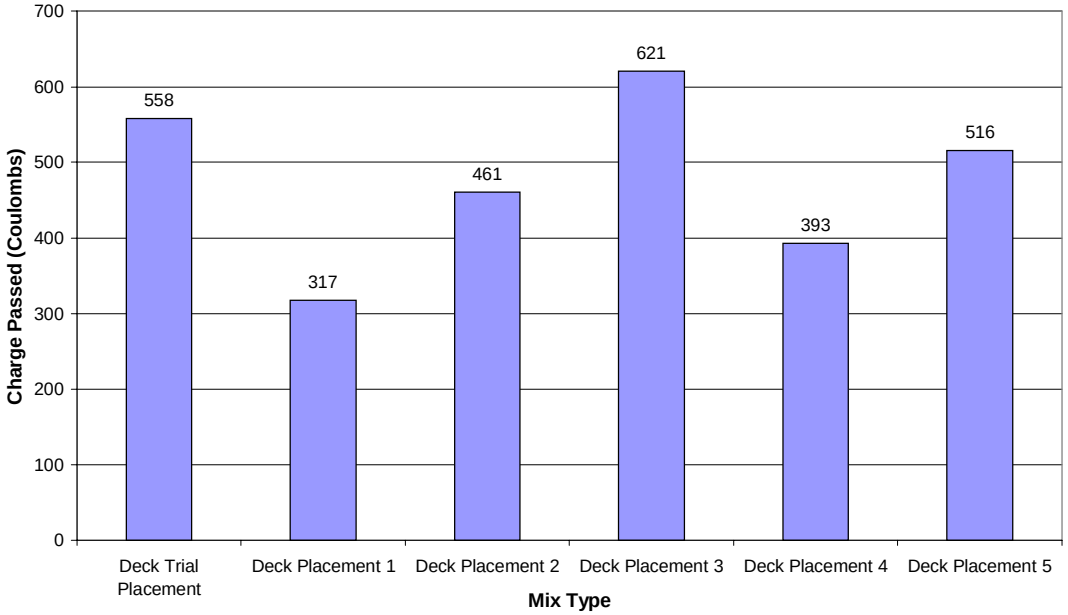

Fig 4.24: Comparison of Permeabilities for various Batches of Silica Fume Bridge Deck Concrete - Bridge 1 (Summer 1999)

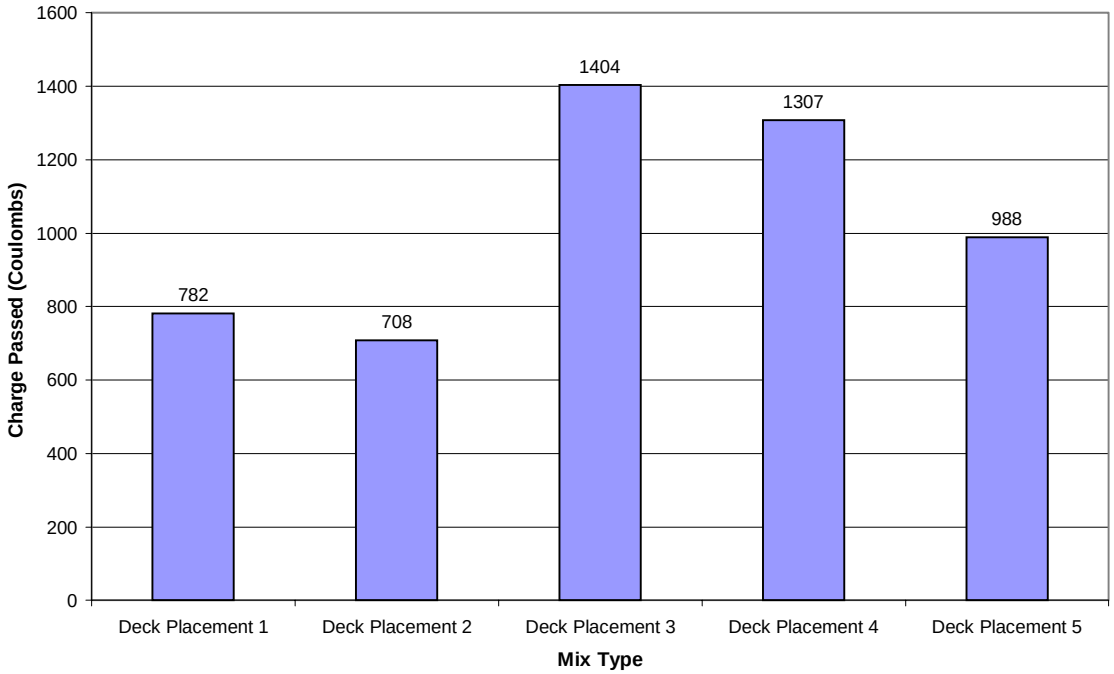

Fig. 4.25: Comparison of Permeabilities for Various Batches of Fly Ash Bridge Deck Concrete for Deck No. 2 (Summer 2000)

4.14.2 Bridge Girder Concrete

The average values of the permeabilities of concretes used in the fabrication of prestressed girders for bridge 1 and 2 are compared in Fig. 4.27 and 4.28 respectively. The permeabilities varied from 42 to 81 in bridge 1 and 77 to 96 in bridge 2. This variation can be considered reasonable for field concrete and it can be assumed that the silica fume distributed properly in the concrete. The quality control obtained in the production of HPC was good. The permeability (average of 24 specimens) for bridge 1 is 65 coulombs and the permeability (average of 12 specimens) for bridge 2 is 87 coulombs. According to ASTM C 1202 the chloride ion penetrability is classified as "Negligible". Therefore the high strength HPC could be considered as impermeable and the corrosion potential of the prestressed steel tendons is negligible.

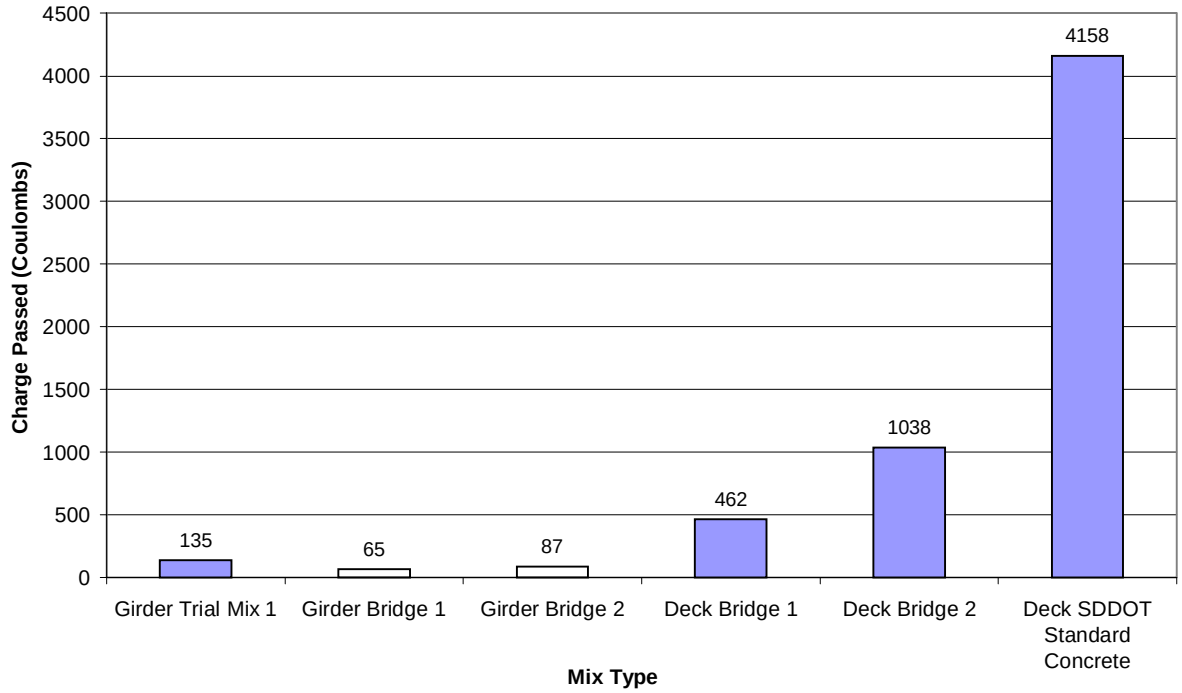

Fig. 4.26: Average Permeabilities of Bridge Deck and Girder Concrete for Bridges 1 & 2

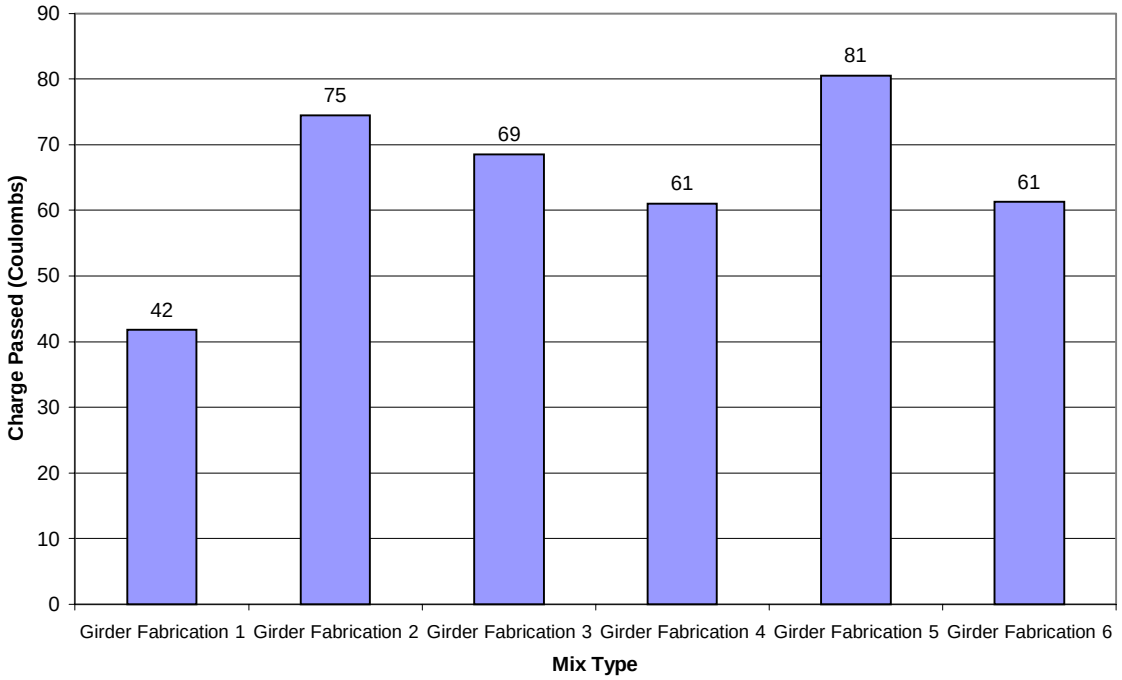

Fig. 4.27: Comparison of Permeabilities for various Batches of HPC Girder Concrete (Bridge 1 - Summer 1999)

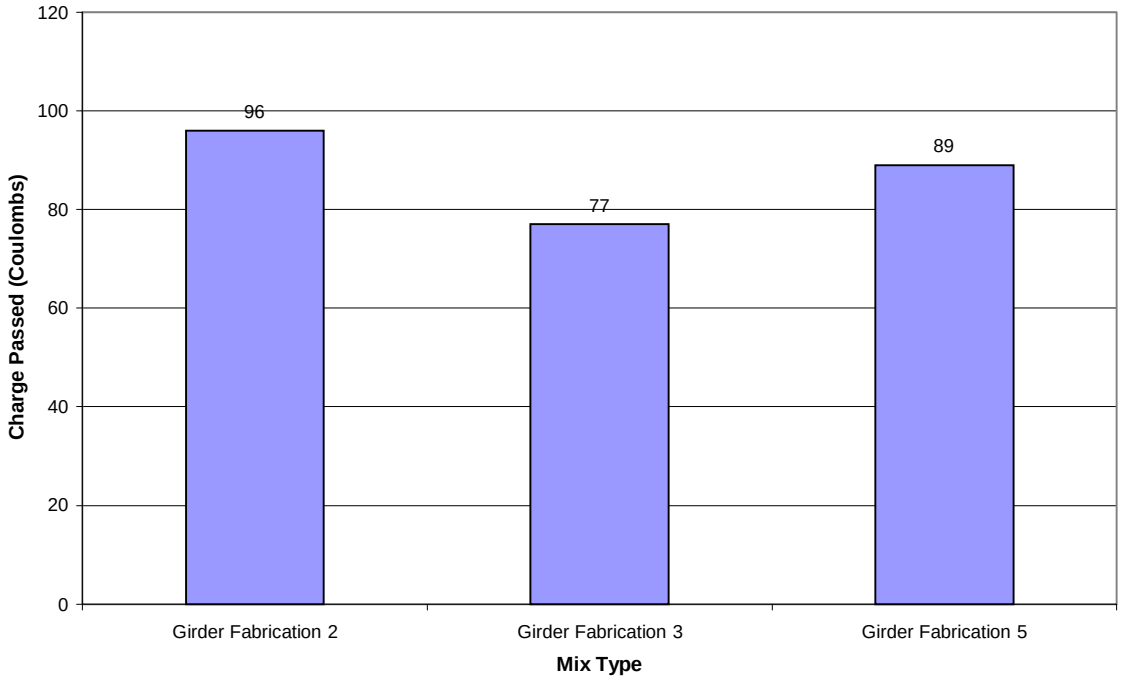

Fig. 4.28: Comparison of Permeabilities for Various Batches of HPC Girder Concrete (Bridge 2-Summer 2000)

4.14.3 Accelerated Rapid Chloride Test

Currently the 90 day rapid chloride permeability (ASTM C 1202) results are specified for bridge deck concretes by various DOT' s (14). This is too long a period to wait to know the results. Therefore accelerated curing of the specimens at a higher temperature and then testing them within a few days to determine the permeability is quicker way to get the same result. This procedure had been suggested by the Virginia DOT (14) and Malhotra (21). In this project, a comprehensive testing program was conducted to prove that it is possible to predict the 90-day rapid chloride permeability at a 7 day testing by using the accelerated curing of concrete specimens before testing for permeability. The following procedure was used for accelerated curing. The specimens were demolded after 24 hours following the ASTM specification and they were placed in an accelerated curing tank containing water maintained at a constant temperature of 38^0 C (100^0 F) for 3 days. Then they were tested for the rapid chloride permeability using the ASTM C 1202 test procedure.

4.14.4 Test Program and Regression Model: Ten mixes with quartzite aggregate with various quantities of silica fume and fly ash were made and eight specimens from each mix were fabricated from these mixes. Four specimens were subjected to accelerated curing mentioned above and tested after 7 days for rapid chloride permeability. The remaining four specimens were standard cured for 90 days and were then tested for rapid chloride permeability. The test results are given in Table 4.15.

A log-log linear model for predicting the relationship between the accelerated permeability (Y), a dependent variable, and the 90-day permeability value (X), an independent variable is presented.

$$\text{Log}(Y) = b_0 + b_1 \text{Log}(X)$$

In the above equation the constants b_0 and b_1 are evaluated by regression analysis and they are equal to -0.8307 and 1.2245 respectively. Hypothesis testing was also done to determine whether a strong and significant relation existed between Y and X. Adequacy of the regression model was assessed using the values of coefficient of correlation, conditional estimation of standard deviation and the significance-F (p-value) of the hypothesis test. Complete details of the analysis are given in Appendix C.

Table 4.15: Predicted 90 Day Permeability Values using Log-Log Linear Model

Proposed Logarithmic Model: Log Y= b_0+b_1Log X						
90 Days Coulombs (X)	**Accelerated Coulombs (Y)**	**Log X**	**Log Y**	**Pred Log Y**	**Standard Residuals**	**Pred Y**
323	132	2.51	2.12	2.24	-0.84	174.51
812	692	2.91	2.84	2.73	0.75	539.56
1207	533	3.08	2.73	2.94	-1.50	876.67
1219	1337	3.09	3.13	2.95	1.24	887.35
1774	1559	3.25	3.19	3.15	0.31	1404.85
1943	1642	3.29	3.22	3.20	0.13	1570.44
3475	4088	3.54	3.61	3.51	0.74	3200.25
4158	5566	3.62	3.75	3.60	1.01	3986.66
4704	4059	3.67	3.61	3.67	-0.40	4636.83
6831	4548	3.83	3.66	3.86	-1.44	7321.69

Table 4.16: Regression Statistics of Model for Predicting 90 Day Permeability

Proposed Logarithmic Model: Log Y= b_0+b_1Log X						
Std Deviation Sy/x	b_0 (Intercept)	b_1 (X Variable)	Coef of Correlation r	R Square	Significance F-P value	f
0.15	-0.83	1.22	0.96	0.92	1.07E-05	93.95

Table 4.16 gives the regression statistics of the developed model. The normal probability plot of the residuals is shown in Figure 4.29. The logarithmic line fit plot of permeability in coulombs due to accelerated curing (Y) with permeability in coulombs due to standard 90-day curing (X) is shown in Fig. 4.30.

This equation can be used to predict the 90-day permeability for the quartzite aggregate concretes used in this project for any compressive strength, if the accelerated permeability value is known for that concrete. This is highly advantageous because we need not wait for 90 days to know the permeability of concrete used. Some preliminary tests done with limestone aggregate seemed to agree with the suggested equation, however further extensive testing is needed to develop a universal equation applicable to all aggregates.

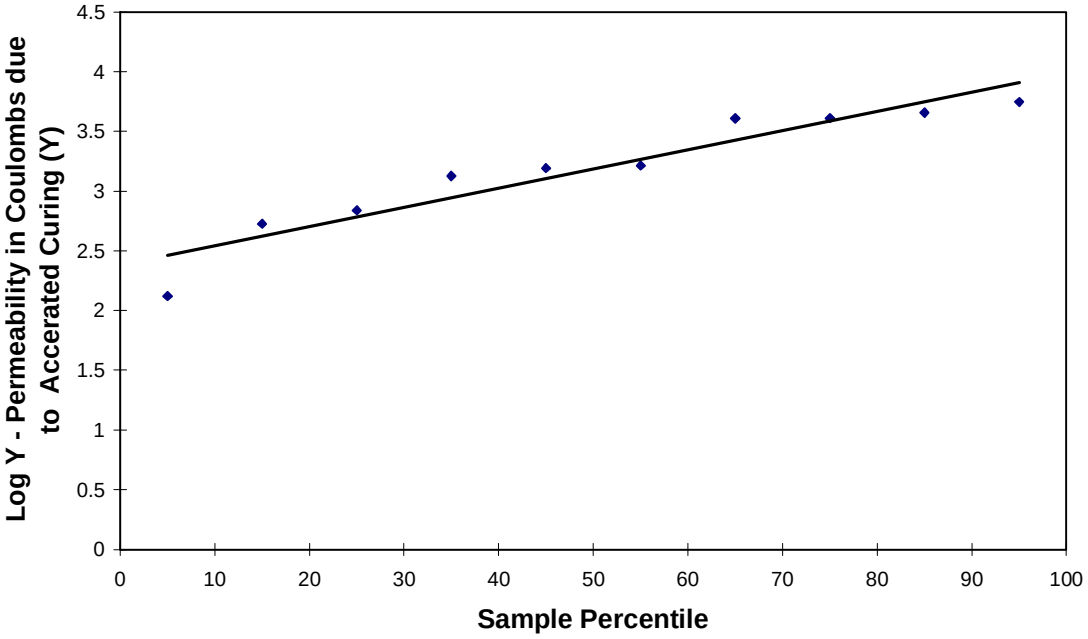

Fig 4.29: Normal Probability Plot

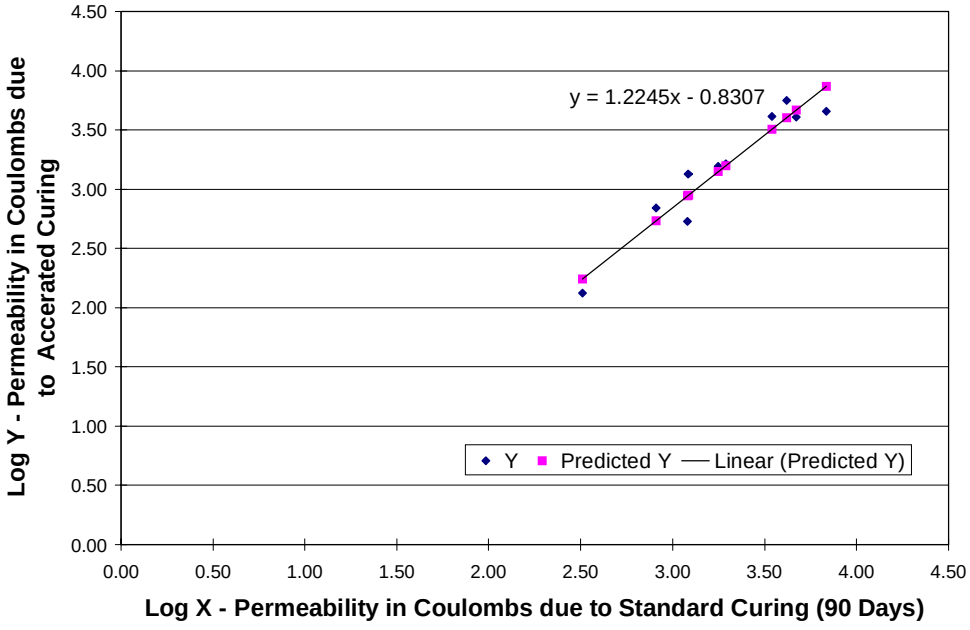

Fig. 4.30: Logarithmic Line Fit Plot of Permeability in Coulombs due to Accelerated Coulombs (Y) with Permeability in Coulombs due to Standard Curing (X)

4.15 Conclusions

Based on the test results and the observations made during the course of this investigation, the following conclusions are offered.

4.15.1 High Strength HPC Mix and Performance of Prestressed Girders

- The silica fume high strength HPC mix developed by the laboratory trial mixes and slightly modified for the field conditions and used in the fabrication of prestressed girders performed well both in the fresh and hardened states. The selected mix had 403.24 kg/m^3 (680 lb/cu.yd) cement and 49.81 kg/m^3 (84 lb/cu.yd) of silica fume with a water to cement ratio of 0.28 and water to cement + silica fume ratio of 0.25. This mix gave the required 127 to 178 mm (5 to 7 inches) slump and 4.0±1.0 % air. The coarse aggregates consisted of 19 mm (3/4 inch) Sioux falls quartzite aggregate. There was a significant increase in the compressive strength due to the addition of silica fume. This mix exceeded the specified design strength requirements of 56.9 MPa (8520 psi) at release of the strands and 68.3 MPa (9900 psi) at 28 days. This mix developed a range in stress at 28 days of 89.64 MPa (13, 000 psi) to 108.25 MPa (15,700 psi). Based on the results obtained from the field concrete used in the fabrication of the girders this high strength HPC mix could be used with design strength (28 days) conservatively set at 82.7 MPa (12,000 psi). This predicts that 95 percent of the results would break at, or higher than the design strength. This statement assumes that three cylinders be used and averaged to produce one test result, and that the test results are normally distributed.
- The modulus of elasticity of the high strength HPC mix with quartzite aggregate was higher than the SDDOT standard mixes used for prestressed girders. The modulus of elasticity for this mix can be estimated by the recommended ACI 363 equation with the substitution in this equation of 13790 MPa (2,000,000 psi) for the 6895 MPa (1,000,000 psi) constant.
- The modulus of elasticity of the high strength HPC mix with quartzite aggregate was higher than the SDDOT standard mixes used for prestressed girders. The current equation that is recommended for evaluating the modulus of elasticity of HSC is the ACI 363 equation. It has the form-

ACI equation 363:

$$E_C = \left(40{,}000\sqrt{f_c'} + 1{,}000{,}000\right)\left(\frac{w_C}{145}\right)^{1.5} \qquad \text{eq. 4-2}$$

An equation to predict the modulus of elasticity for HSC is not provided in either the current AASHTO or ACI 318 specifications. Based on the tests conducted as part of this research, and limited to mixes containing Sioux Quartzite aggregate, it is concluded that the above equation be used with the modification that the 1,000,000 constant be changed to 2,000,000. The resulting form is –

$$E_c = \left(40{,}000\sqrt{f_c'} + 2{,}000{,}000\right)\left(\frac{w_c}{145}\right)^{1.5} \qquad \text{eq. 4-3 .}$$

- The girders in bridge 1 exhibited a maximum early age (first 100 days) shrinkage of 150 με, the corresponding value for the girders of bridge 2 was 200 με. This is a variation of 25 to 30 percent. It is likely to be indicative of the variation in shrinkage that can be expected in silica fume high strength HPC. This was observed to be about half of that predicted for "so-called", standard concrete (Using the recommendations as suggested by the ACI 209 committee.)
- The loss in initial prestress for the girders due to the combined effect of creep and relaxation up to the time the deck was cast, was about 6 percent for the girders in bridge 1, and about 14 percent for the girders in bridge 2. The girders in bridge 2 exhibited an additional 4.8 percent loss from the time that the deck was placed up to the time that the girders were one year of age. Due to the form of the data record for bridge 1 it is not possible to estimate the losses in bridge 1 after the deck placement (More data is needed as the record is developing a possible periodic component). It is expected that additional losses (It is believed that their magnitude is not large.) have occurred, but their magnitude cannot be estimated at this time. Additional data and further analysis will be needed to determine a more reliable estimate of the time-dependent losses in these girders.
- The long-term curvature in bridge 2 is about double the curvature exhibited in bridge 1. This conclusion is consistent with the measured deflections. With the decks in place, these structures have not shown a tendency to develop increasing long-term deflections. It can be

concluded that this is due to the shrinkage that is occurring in the deck, which counteracts the tendency for the girders to exhibit increased camber. This conclusion is based on limited data.

- The measured curvatures taken in the gap between the girders at the bent demonstrate significant reduction over time. In bridge 1 it has been reduced from 9.5 to 4.0 (Curvature units in^{-1}, the values have been multiplied by 10^6.) over a two year time period. The results for bridge 2 show a similar trend but it is not as dramatic. The problem is that only one year of data is available from bridge 2 and more data will be needed to assess this behavior. The trend in the curvatures at the bents is difficult to explain.
- The average chloride permeability for the girders in bridges 1 and 2 were 65 and 87 coulombs respectively. According to ASTM C 1202, the chloride ion penetrability for both bridge girders is "Negligible". Therefore the high strength HPC could be considered as impermeable and the corrosion potential of the prestressed steel tendons is negligible.

4.15.2 Bridge Deck Concrete and Performance of the Decks

Based on the analysis of the trial mixes the following conclusions are made:

- The compressive strengths of concretes containing silica fume and fly ash were significantly higher when compared to plain concretes at the same w/c ratio and age. The increase in strength due to the addition of mineral admixtures was more prominent at later ages (28 day).
- There was no significant change in the modulus of rupture values for concretes containing silica fume and fly ash when compared to plain concretes at the same w/c ratio.
- The increase in static modulus values was more prominent in concretes containing just silica fume when compared with plain concrete at the same w/c ratios.
- There was no significant change in the compressive strength due to variation in the type of coarse aggregate used. Almost all the mixes containing limestone aggregate showed higher modulus of rupture values when compared to the same mixes containing quartzite aggregate.
- There was a significant reduction in the chloride permeability values in concretes containing silica fume when compared to plain concretes at the same w/c ratios. The reduction was more prominent in the concretes containing just silica fume than the concretes containing a combination of silica fume and fly ash. Concretes containing just fly ash showed higher

chloride permeabilities when compared to concretes with silica fume but lower chloride permeabilities when compared to plain concretes.

- The results of the rapid chloride permeability tests carried out on specimens, subjected to accelerated curing showed a good correlation with the results obtained from the tests carried out at 90-days.
- All mixes containing mineral admixtures showed low workability and hence water reducers were used to obtain the required workability. The addition of the water reducers did not affect the strength.

Based on the test results of the field concrete used in bridge 1 and 2, the following conclusions are offered:

- The 28 day compressive strengths obtained were, silica fume trial mix 61.5 MPa (8910 psi), silica fume mix for bridge 1- 48.8 MPa (7070 psi), fly ash mix for bridge 2 - 46.6 MPa (6760 psi). At 90 days, both concretes had the same compressive strength 53.5 MPa (7760 psi). The 1-year compressive strengths were silica fume mix for bridge 1-57.6 MPa (8350 psi), fly ash mix for bridge 2- 62.4 MPa (9040 psi). Both mixes had much higher strength than the design 28-day strength 31 MPa (4500 psi). This is about 50% higher strength than the required strength. At 28 days, the silica fume mix used in the bridge deck yielded a 5 percent greater strength than the fly ash mix used in bridge deck no. 2. At one year the fly ash mix yielded compressive strength results 7 percent higher than the silica fume mix. This was as expected.
- The silica fume deck concrete exhibited 1.6 times more early age shrinkage strain than the fly ash concrete mix. This contributed to the greater deck cracking than was observed in the fly ash deck concrete.
- Both decks tended to develop significant tensile strains. On average the silica fume deck developed average tensile strains 1.9 times greater than the average tensile strains that were measured in the fly ash deck.
- There was a higher heat of hydration and higher temperatures during the early curing period in silica fume concrete as compared to the fly ash concrete.
- A coefficient of thermal expansion of $13.5 \times 10^{-6}\ ^{o}C^{-1}$ ($7.5 \times 10^{-6}\ ^{o}F^{-1}$) can be used with confidence for silica fume and fly ash mixes representative of those studied in this research.

- The crack survey data demonstrate that there was 1.7 times more cracking in the silica fume deck as compared to the fly ash deck. This is in general agreement with the deck tensile strain data.
- The fly ash mix is considered to be better for deck use than the silica fume mix because of the fly ash concrete' s tendency to develop lower shrinkage strains and thus develop fewer cracks. A further negative for the silica fume mix is that it requires much more care during the placing and curing of the concrete. For this reason, silica fume concrete is likely to cost more than fly ash concrete.
- The rapid chloride permeabilities as measured from the ASTM C 1202 test for the silica fume bridge deck concrete ranged from 393 to 621 coulombs and for fly ash concrete used in bridge deck 2 varied from 708 to 1404 coulombs. The average permeability (24 specimens) for silica fume concrete was 462 coulombs whereas the permeability of SDDOT' s standard bridge deck concrete was 4158 coulombs. This is 88.9 % reduction which had far exceeded the required 50% reduction. The average permeability (24 specimens) for the fly ash concrete was 1038 coulombs which was a reduction of 75%. The permeability of fly ash concrete was 123 % higher than that of the silica fume concrete containing 7 percent silica fume.
- According to ASTM C1202, the chloride ion penetrability is "very low" for the silica fume concrete and "low" for the fly ash concrete. It is concluded that the potential for rebar corrosion is low for both silica fume and fly ash concretes.

4.15.3 Cost

- The cost of the superstructure for the bridges was the same on a first cost basis for both the HPC bridge and the normal concrete SDDOT present design bridge. However the life cycle cost might be cheaper for the HPC bridge because of the anticipated longer life and reduced maintenance cost.
- The use of HPC allowed designers to reduce the number of girders in each span from five to four. However the thicker deck needed due to the wider girder spacing negated the savings realized in the girders.

4.16 Recommendations

Prestressed Girders:

1. For the fabrication of prestressed girders, when compressive strengths greater than 62 MPa (9000 psi) are required, the high strength silica fume HPC should be specified. The 28-day design compressive strength could be specified as high as 82.7 MPa (12,000 psi), but the fabricator would want the concrete to reach the release strength in a few days for production purposes. Therefore the mix should be designed to reach the fabricator' s required release strength in the specified number of days.

   The feasibility of producing and using high strength silica fume HPC mix had been successfully demonstrated in this project. The concrete was almost impermeable and hence the corrosion potential was eliminated. The anticipated benefits are less number of girders, less deflection, less prestress loss due to creep and shrinkage.

2. Based on extensive testing of trial mixes and analysis, the following mix proportions are recommended for high strength girder concrete. This mix was used for a design strength (f_c') of 68.3 MPa (9900 psi) and the average strength obtained was 99.3 MPa (14,400 psi). The fabricator wanted to achieve the specified strand release strength of 56.9 MPa (8250 psi) in 3 days.

Cement (Type II)	403.24 kg/m^3	680 lbs./pcy
Water included from Silica fume slurry and HRWR	112.67 kg/m^3	190 lbs./pcy
Coarse aggregate (3/4" quartzite)	1082.23 kg/m^3	1825 lbs./pcy
Fine aggregate (S.S.D)	683.16 kg/m^3	1200 lbs./pcy
Silica fume	49.81 kg/m^3	84 lbs./pcy
Air Content	4.0±1.0%	4.0±1.0%
Water to Cement ratio	0.28	0.28
Water/C+S.F. ratio	0.25	0.25

Note: The recommended slump was 127 to 178 mm (5 to 7 inches). The dosage of High Range Water Reducer (HRWR) and/or water reducer should be adjusted according to the field conditions to achieve the specified slump. The 19mm (3/4 inch) quartzite aggregate used in this project conformed to the standard specifications for Roads and Bridges, Section 820 for Size No. 1 (SDDOT). The mixing water should be adjusted taking into account the excess water present in the silica fume slurry and the high range and mid range water reducers.

3. The equation currently recommended for calculation of modulus of elasticity (E_c) for HSC is the ACI 363 equation:

$$E_c = \left(40{,}000\sqrt{f_c'} + 1{,}000{,}000 \right)\left(\frac{w_c}{145} \right)^{1.5}$$

Based on the modulus of elasticity (ASTM C469) tests conducted as part of this research and limited to mixes containing Sioux Quartzite aggregate, it is recommended that the above equation be modified by changing the 1,000,000 constant to 2,000,000. Therefore the recommended formula becomes:

$$E_c = \left(40{,}000\sqrt{f_c'} + 2{,}000{,}000\right)\left(\frac{w_c}{145}\right)^{1.5}$$

It is recommended that the ACI 363 equation be used without modification for mixes containing limestone aggregates since the research was not conducted on mixes containing limestone aggregate.

Bridge Deck:

4. For the construction of bridge decks, the Class F fly ash concrete which was successfully used in the construction of bridge deck 2, should be specified for future deck concrete. Compared to plain deck concrete, the benefits of using fly ash deck concrete as demonstrated in this project, are substantial reduction in the chloride ion penetrability (a "low" value as per ASTM C1202), reduced corrosion potential, higher modulus concrete, reduced plastic shrinkage, reduced drying shrinkage, reduced restrained shrinkage cracking in the underside of the deck slabs, reduced early temperature rise due to the hydration activity, less micro-cracking, higher durability, better workability, and good finishability. This fly ash concrete developed smaller tensile stress in the deck than the silica fume concrete. All these benefits could be realized without an increase in cost.
5. The recommended bridge deck concrete mix proportions are given below.

Cement (Type I/II)	349.87 kg/m^3	590 lbs./cu.yd.
Fly ash (Class F)	74.53 kg/m^3	124 lbs./cu.yd.
Water	151.22 kg/m^3	255 lbs./cu.yd.
Fine aggregate (sand)	724.65 kg/m^3	1222 lbs./cu.yd.
Coarse aggregate (rock)	968.96 kg/m^3	1634 lbs./cu.yd.
Percent air	6.5%±1.0%	6.5%±1.0%
Water/C ratio	0.432	0.432
Water/C+FA ratio	0.357	0.357

Note: Appropriate quantity of water reducer either mid range or high range should be used to obtain the specified slump. The mixing water should be adjusted taking into account the excess water in the water reducer used. An appropriate amount of air entraining agent should be used to obtain an air content of 6.5±1 %.

The 28-day design compressive strength could be specified as 37.9 MPa (5500 psi) because this mix gave an average compressive strength of 46.2 MPa (6700 psi) at 28 days. According to ACI 318, for a design strength (f_c') of 37.9MPa (5500 psi), the required average strength

would be (5500+1200) 6700 psi. This higher design strength could be used in the design of the deck slab to reduce the thickness. Based on the performance of the bridge decks in bridges 1 and 2, the fly ash mix is deemed better for deck use than silica fume mix. There is apparently no economical way to efficiently control the shrinkage, and thus the tendency to produce cracks in the silica fume mix.

6. Where higher strength concrete is not needed and when the design compressive strength of 31 MPa (4500 psi) is required then the following Class F fly ash concrete could be used for both limestone and quartzite aggregate. This recommendation is based on the ongoing research "Determination of Optimized Fly Ash Content in Bridge Deck and Bridge Deck Overlay Concrete: SD00-06". When this mix is used the chloride ion permeability at 90 days (ASTM C1202) would be reduced more than 50 percent compared to Class A bridge deck concrete currently used.

Cement Type I/II	291 kg/m^3	491 lbs./cu.yd.
Fine Aggregate	652 kg/m^3	1100 lbs./cu.yd.
Coarse Aggregate	1023 kg/m^3	1725 lbs./cu.yd.
Water	155 kg/m^3	262 lbs./cu.yd.
Fly Ash	97 kg/m^3	164 lbs./cu.yd.
Percent air	6.5%±1.0%	6.5%±1.0%
Water to Cement ratio	0.53	0.53
Water/C+S.F. ratio	0.40	0.40

Note: The appropriate amount of air entraining agent should be used by the contractor to obtain the specified air content.

7. For bridge deck concrete, the rapid chloride permeability at 90 days, as determined by the ASTM C 1202 test, should be specified for accepting the concrete. The specification should require that the charge passed should be less than 2000 coulombs at 90 days testing, which ensures the "low" chloride ion penetrability. The major objective of this project was to develop a mix proportion to reduce the chloride permeability by 50 percent. The fly ash deck concrete used in the project achieved a 75% reduction in the chloride permeability.
8. In cases where the w/c ratios are very low (in the range of 0.28 to 0.32) and mineral admixtures such as silica fume and fly ash are in use, high range water reducers are recommended. In cases where the w/c ratio is around 0.40, mid range water reducers may be sufficient. Addition of large quantities of mid range water reducers lowers the rate of strength gain.
9. It is strongly recommended that, whenever silica fume is used in bridge deck concrete, a proper 100% humid curing for 5 to 7 days is necessary to minimize shrinkage cracking. This

could be achieved with continuous water sprays or misting and/or fogging devices. The same construction procedures for mixing, transporting, placing, consolidating, finishing and tining used for construction with standard concrete should be followed. The same construction techniques and equipment without major modification could be used for the construction of HPC bridge decks.

General:

10. When silica fume is used in a slurry form, the slurry should be sampled and tested while being continuously agitated, before use and at specified intervals during the concrete production. The amount of silica fume in the slurry could be determined by the hydrometer test. Because the silica fume is suspended in water (not dissolved), there is an inevitable tendency for the silica fume to settle to the bottom. To avoid this a continuous agitation of the liquid with proper instruments is recommended. The water in the slurry should be accounted for and the mix water should be adjusted.
11. When HPC mixes are used, it is recommended that the following quality control tests should be conducted in the field using ASTM test procedures for the fresh concrete: slump, unit weight, air content, and the concrete temperature. The ambient temperature, humidity, and the wind velocity should be recorded during the bridge deck concrete placement or the fabrication of the prestressed girders. The compressive strength and static modulus tests should be conducted on the field samples collected and cured according to the ASTM standard procedures at 28 days. When HPC is used for fabricating prestressed girders, it is recommended that companion cylinders (preferably 102 mm × 204 mm (4" × 8")) should be placed near the girder and cured under identical conditions as the girders, to determine when the prestressed strands can be released as per specifications. When chloride permeability is specified, the hardened concrete samples made from the actual concrete placed should be tested for rapid chloride permeability at 90 days as per ASTM C 1202. The cylinder samples can be made in the field and cured as per standard ASTM procedures for 28 days.
12. These two bridges should continue to be monitored by using the already installed instrumentation and by visual observation. Only limited data, (one-year for bridge 2, and two years for bridge 1) have been gathered. To determine the long term behavior, several years of monitoring is required.

References

1. Edward G. Nawy., “Fundamentals of High-Performance Concrete”, Second Edition., John Wiley & sons, Inc , 2001
2. Zia, Paul., Leming, M.L., Ahmad, S., H., “High Performance Concrete, A State – of – the – Art Report”, SHRP-C/FR-91-103.
3. Ramakrishnan, V., “Evaluation of Non-Metallic Fiber Reinforced Concrete in PCC Pavements and Structures”, Interim Report SD94-04, submitted to SDDOT, September 1995.
4. Russell, H.G., "ACI Defines High-Performance Concrete", From the Technical Activities Committee, Concrete International, *ACI Journal*, V.21, No.2, Feb. 1999, pp.56-57.
5. Russell, H.G., "High strength Concretes in Bridges- History And Challenges", Proceedings of the PCI/FHWA, *International Symposium on High Performance Concrete*, New Orleans, Luisiana, October 20-22, 1997, pp.27-38.
6. Aiticin, P., C., Baalbaki, M., "Candian Experience in Producing and Testing HPC", International Workshop on High Performance Concrete, Publication SP-159, ACI Bangkok, Thailand, November 1994, pp. 295-308.
7. Leming, M.L., Ahmad, S.H.;Zia,P.; Schemmel, J.J,; Elliot, R.P., and Naaman, A.E.,. "High Performance Concretes: An Annotated Bibliography 1974-1989" SHRP-C307, Strategic Highway Research Program, National Research Council, Washington, D.C. 1990.
8. Russell,H.G., “High Performance concrete Applications in North America”, International Conference on High Performance High Strength Concrete: Material Properties, Structural Behaviour and Field Applications, Perth, Australia, 1998.
9. Zia, P, Leming, M.L., Ahmad, S.H.; "Research on High Performance Concrete", Proceedings of Conference on the United States Strategic Highway Research Program. The Institution of Civil Engineers, London, October 29-31, 1990, pp.63-75.
10. Aiticin, P.-C., and Nivelle, A., "High Performance Concrete Demystified", Concrete International, *ACI Journal*, V.15, No.1, Jan. 1993, pp.21-26.
11. Ozyildirim, C., "HPC Bridge Decks in Virginia", Concrete International, *ACI Journal*, V.21, No.2, Feb. 1999, pp.58.
12. Waszczuk, M.C., and Juliano, M.L.,"Application of HPC in a New Hampshire Bridge", Concrete International, *ACI Journal*, V.21, No.2, Feb. 1999, pp.60.
13. Beacham,M., "HPC Bridge Deck in Nebraska", *University and government join forces*, Concrete International, *ACI Journal*, V.21, No.2, Feb. 1999, pp.66.
14. Ozyildirim, C., "Permeability Specification for High Performance Concrete Bridge Deck", A Report Virginia Transportation Research Council
15. Ralls,M.L, "Texas HPC Bridge Decks ”, New durable mix specification used", Concrete International, *ACI Journal*, V.21, No.2, Feb. 1999, pp.63.
16. Russell, H.G., “Long-term Properties of High-strength concretes,” Concrete Technology today, Portland Cement Association, Vol.14, No.3, November 1993, pp. 1-3.
17. ACI Committee 363, “State-of-the-art Report on High-strength Concrete” (ACI 363 R-84), American Concrete Institute, Detroit, 48 pp.
18. Nawy,E.G., “Fundamentals of High Strength High Performance Concrete”, Longman Group Limited,1996
19. ACI Committee 226, " Use of Fly Ash in concrete", *ACI Report 226.3R-87* American Concrete Institute, Detroit, 1990, pp. 1-29.
20. Berry, E.E., and Malhotra,V.M.,"Fly Ash for use in Concrete-A critical Review", *Proceedings, ACI Journal*, Vol.77 No.2, American Concrete Institute, Detroit, pp.59-73.
21. Sivasundaram, V.,Carette,G.G., and Malhotra, V.M.,"Mechanical Properties, Creep, and Resistance to Diffusion of chloride Ions of concrete Incorporating High Volumes of ASTM Class F Fly Ash From Different Sources", *MSL Diviision Report 89-126 (J)*, Energy, Mines, Resources Canada, Ottawa,1989.
22. Sivasundaram, V.,Carette,G.G., and Malhotra, V.M., "Properties of Concrete Incorporating Low quantity of Cement and High Volumes of Low-Calcium Fly Ash", *ACI SP114* Vol.1, ed. V.M.Malhotra, ACI Detroit, pp.45-71.
23. Carette,C.G., and Malhotra,V.M., "Long-Term strength Development of silica Fume Concrete", *Proceedings CANMET/ACI 4th International Conference on Fly Ash, silica Fume, Slag and Natural Pozzolans in Concrete*, Istanbul. ACI SP-132 Vol.2, ed. V.M.Malhotra, ACI, Detroit, pp.1017-1044.

24. Ramakrishnan, V., "Properties and Applications of Latex Modified Concrete", *Proceedings CANMET International Conference on Advances in Concrete Technology*, ed. V.M.Malhotra, Ottawa, Ontario, 1992, pp.839-890.
25. ASTM C 1202-94, "Standard Test Method for Electrical Indication of Concrete's Ability to Resist Chloride Ion Penetration", *ASTM Standards*, June 1994, pp.622-627.
26. Proove it, " Instruction and Maintenance Manual, PR-1090, Version 1.2", Germann Instruments, Inc.
27. Whiting, D., "Permeability of Selected Concretes," Permeability of Concrete, SP-108, American concrete Institute, Detroit, 1988, pp.195-222.
28. Perraton, D.,Aiticin, P.C., and Vezina, D.,"Permeabilities of Silica Fume Concrete," Permeability of Concrete, SP-108, American concrete Institute, Detroit, 1988, pp.63-84.
29. Ozyildirim, C., Halstead, W., "Resistance to Chloride Ion Penetration of Concretes containing Fly Ash, Silica Fume or Slag," Permeability of Concrete, SP-108, American concrete Institute, Detroit, 1988, pp.35-62.
30. Mobasher, B., Mitchell, T.,M., "Laboratory Experience with The Rapid Chloride Permeability Test," Permeability of Concrete, SP-108, American concrete Institute, Detroit, 1988, pp.117-144.
31. Marusin, S.,L.," Influence of Superplasticizers, Polymer Admixtures, and Silica Fume in Concrete on Chloride Ion Permeability", Permeability of Concrete, SP-108, American concrete Institute, Detroit, 1988, pp.19-34.
32. Janssen, D.,J., "Laboratory Permeability Measurement," Permeability of Concrete, SP-108, American concrete Institute, Detroit, 1988, pp.145-158.
33. NCHRP Report 410,"Silica fume Concrete for Bridge Decks", National Cooperative Highway Research Program, TRB, Washington, D.C.,1998
34. Smith, D. C. "The Promise of High-Performance Concrete." Business Insurance, 31 (14), 1997, pp. 31-39.
35. Adelman, D., and Cousins, T.E. "Evaluation of the Use of High Strength Concrete Bridge Girders in Louisiana." PCI Journal, (2), 1990, pp. 70-78.
36. Goodspeed, C. H., Vanikar, S., and Cook, R.A. "High Performance Concrete Defined for Highway Structures." Concrete International, 18 (2), 1996, pp. 62-67.
37. Mehta, P.K. and Monteiro, P.J.M., Concrete: Structure, Properties, and Materials 2nd Ed. (Prentice-Hall, Englewood Cliffs, New Jersey, 1993, pp. 154-159.
38. Pauw, A. "Static Modulus of Elasticity of Concrete as Affected by Density." ACI Journal, 57 (6), 1960, pp. 679-687.
39. Carrasquillo, R., Nilson, A., and Slate, F. "Properties of High Strength Concrete Subject to Short-Term Loads." ACI Journal, 78 (3), 1981, pp. 171-178.
40. Iravani, S. "Mechanical Properties of High-Performance Concrete." ACI Materials Journal, 93 (5), 1996, pp. 416-426.
41. Imbsen, R.A. "Thermal Effects in Concrete Bridge Superstructures", Transportation Research Board, National Research Council, Washington, D.C., 1985.
42. Mindess, S., and Young, F.J., Concrete, Prentice-Hall, Inc., Englewood Cliffs, NJ, 1981, 671 PP.
43. Smadi, M. M., Slate, F. O., and Nilson, A. H., "Shrinkage and Creep of High-, Medium-, and Low-Strength Concretes, Including Overloads." ACI Materials Journal, 84 (3), 1987, pp. 224-234.
44. Lachemi, M., Bois, A., Miao, B. Lessard, M., and Aitcin, P. "First Year Monitoring of the First Air-Entrained High-Performance Bridge in North America." ACI Structural Journal, 93 (4), 1996, pp. 379-386.
45. Yonezawa T., Mitsui K., Tezuka M., and Kinoshita M. "Application of 100 MPa High-Strength, High-Fluidity Concrete for a Prestressed Concrete Bridge with Span-Depth Ratio of 40." PCI/FHWA International Symposium on High Performance Concrete, New Orleans, Louisiana; Ed. by Johal, L. S., Precast/Prestressed Concrete Institute, Chicago, Illinois, 1997.
46. Shing, P. B., Cooke, D., Frangopol, D. M., Leonard, M. A., McMullen, M.L., and Hutter, W. "Colorado Showcase on HPC Box-Girder Bridge: Development and Transfer Length Tests." PCI/FHWA International Symposium on High Performance Concrete, New Orleans, Louisiana; Ed. by Johal, L. S., Precast/Prestressed Concrete Institute, Chicago, Illinois, 1997.
47. Nabil Bouzoubaa and Mohan Malhotra. V., "Performance of Lab-Produced HVFA-Blended Cements in Concrete", Volume 23, No.4, Concrete International, April 2001, pp. 29.
48. Nabil Bouzoubaa.; Zhang, M.H.; Bilodeau, A.; and Malhotra. M. V., "Effect of the grinding on the Physical Properties of Fly Ashes", Cement and Concrete Research, V. 27, No.12, Dec. 1997, pp. 1861-1874.
49. Bilodeau, A.; and Malhotra. M. V., "High Performance Concrete Incorporating Large Volumes of ASTM Class F Fly Ash", High Performance Concrete: Proceedings, ACI International Conference, Singapore, SP-149, V. M. Malhotra, ed., American Concrete Institute, Farmington Hills, Mich., Nov. 1994, pp. 177-193.

50. Nabil Bouzoubaa.; Zhang, M.H.; Bilodeau, A.; and Malhotra. M. V., "High-Volume Fly Ash-Blended Cement: Status Report", EPRI Report TE-114025, Electric Power Research Institute, Palo Alto, Calif., Oct. 1999, pp. 25.
51. Nabil Bouzoubaa.; Zhang, M.H.; Bilodeau, A.; and Malhotra. M. V., "Mechanical Properties and Durability of Concrete made with High-Volume FlyAsh-Blended Cement Using a Coarse Fly Ash", CANMET Report MTL 99-19(J), NATURAL Resources Canada, Ottawa, July 1999, pp. 25.
52. A. Peled; M. F. Cyr; and S. P. Shah., "High Content of Fly Ash (Class F) in Extruded Cementitious Composites", ACI Materials Journal, Vol. 97 No. 5, Sept-Oct 2000, pp. 509.
53. V. M. Malhotra; M. H. Zhang; P. H. Read; and J. Ryell., "Long Term Mechanical Properties and Durability Characteristics of High Strength/High Performance Concrete Incorporating Supplementary Cementing Materials under Outdoor Exposure Conditions", ACI Materials Journal, Vol. 97 No. 5, Sept-Oct 2000, pp. 518.
54. Khayat. K. H., "Optimization and Performance of Air-Entrained, Self Consolidating Concrete" ACI Materials Journal, Vol. 97 No.5, Sept-Oct 2000, pp. 526-535.
55. Malhotra V. M., and Ramezaniapour A.A., "Fly Ash in Concrete, Second Edition", Applications and Case Histories, CANMET, September 1994, pp 236-237.

ADDITIONAL BIBLIOGRAPHY

56. Aiticin, P.C., and Mehta, P.K., "Effect of Coarse Aggregates Characteristics on Mechanical Properties of High-strength Concrete", *ACI Materials Journal,* V.87, No.2, Mar.-Apr. 1990,pp.103-107.
57. Aiticin, P.-C., and Lessard, M., "Canadian Experience with Air-entrained, High Performance Concerte", *ACI Concrete International,* V.16, No.10, October 1994, pp.35-38.
58. Beacham,M.,"High Performance Concrete Lead state Team Activities- An Overview", Presented at the 1999 Spring Convention, ACI, Chicago Illinois, March 14-19, 1999.
59. Bush,T.D.,Russell,B.W.,Freyne,S.F.,"High Performance Concretes Using Oklahoma Aggregates", Proceedings of the PCI/FHWA ,*International Symposium on High Performance Concrete,* New Orleans, Luisiana, October 20-22, 1997, pp.84-95.
60. Evans, E.P.," High Perfromance Concrete from Laboratory to Construction Site", International Conference on High Performance High Strength Concrete: Material Properties, Structural Behaviour and Field Applications, Perth, Australia, 1998.
61. Fidjestol, P., Kojundic,T.," High-Performance Prefabricated Silica Fume Concrete for Infrastruture", Proceedings of the PCI/FHWA, *International Symposium on High Performance Concrete,* New Orleans, Luisiana, October 20-22, 1997, pp.159-171.
62. Hoff, G.C.,"The Hibernia Offshore Platform – A major application of High-Performance Concrete", International Conference on High Performance High Strength Concrete: Material Properties, Structural Behaviour and Field Applications, Perth, Australia, 1998.
63. Lwin,M.M.,"Use of High Performance Concrete in Highway Bridges in Washington State", Proceedings of the PCI/FHWA,*International Symposium on High Performance Concrete,* New Orleans, Luisiana, October 20-22, 1997, pp.657-668.
64. Malhotra,V.M.,"High-Performance High-Volume Fly Ash Concrete", International Conference on High Performance High Strength Concrete: Material Properties, Structural Behaviour and Field Applications, Perth, Australia, 1998.
65. Mather, B.,"Concrete in Transportation: Desired Performance and Specifications",Transactions No. 1382, Transportation Research Board, National Research Council, Washington, D.C., 1993, pp.5-10.
66. Mitchell,D., Aiticin,P.C., Bickley,J.A.," High-Performance Concrete Bridges: The Canadian Experience", Proceedings of the PCI/FHWA,*International Symposium on High Performance Concrete,* New Orleans, Luisiana, October 20-22, 1997, pp.355-367.
67. Moore, J.A.,"High-Performance Concrete for Bridge Decks", *Introduction: HPC Lead State Teams share data,* Concrete International, *ACI Journal,* V.21, No.2, Feb. 1999, pp.58.
68. Myers,J.J., Touma, W.E., Carrasquillo, R.L.," Permeability of High Performance Concrete: Rapid Chloride Ion Test Versus Chloride Ponding Test", Proceedings of the PCI/FHWA,*International Symposium on High Performance Concrete,* New Orleans, Luisiana, October 20-22, 1997, pp.268-282.
69. Navalurkar, R.K., and Ansari, F.,"Tensile Properties of High-Performance Concrete", International Workshop on High Performance Concrete, Publication SP-159, ACI Bangkok, Thailand, November 1994, pp. 283-294.

70. Ramakrishnan. V.,"Flexural Fatigue Performance Characteristics of High Performance Lightweight Concrete", International Conference on High Performance High Strength Concrete: Material Properties, Structural Behaviour and Field Applications, Perth, Australia, 1998.
71. Rangan,B.V.,"High-Performance High-Strength Concrete: Design Recommendations", *State-of-the-Art in HPHSC,* Concrete International, *ACI Journal,* V.20, No.11, Nov. 1998, pp.63-68.
72. Zia, P.,"State-Of-The-Art Of HPC: An International Perspective", Proceedings of the PCI/FHWA, *International Symposium on High Performance Concrete,* New Orleans, Luisiana, October 20-22, 1997, pp.49-59.
73. Zia, P, Leming, M.L.; Ahmad, S.H.; "Mechanical Behaviour of High Performance Concretes, Volume I, Summary Report", SHRP C-361, Strategic Highway Research Program, National Research Council, Washington D.C. 1993.
74. Adam Neville.; "Standard Test Methods: Avoid the Free-For-All", Volume 23, No.5, Concrete International, May 2001, pp 60.
75. Neville, A.M.; *Properties of Concrete*, 4th Edition John Wiley and Addison Wesley Longman, 1996.
76. "Fly Ash – Types and Benefits',Url. http://www.flyash.com/I_flyash.htm.
77. "Fly Ash in Ready Mix Concrete", Url. http://www.irmca.com/tipofthe/tipofo4.htm.
78. "Fly Ash Concrete", Sustainable Building Source Book, Url. http://www.greenbuilder.com/sourcebook/flyash.html11#CSI.
79. "Concrete, Fly Ash, and the Environment", Environmental Building News, Url. www.buildinggreen.com/features/flyash/shell.html.
80. Russell, H.G., " High-Strength Concrete Research for Buildings and Bridges," International Workshop on High Performance Concrete, Publication SP-159, ACI Bangkok, Thailand, November 1994, pp. 375-383.
81. Ahmad, S., H., and Zia, Paul, "High Performance Concretes for Highway Applications," International Workshop on High Performance Concrete, Publication SP-159, ACI Bangkok, Thailand, November 1994, pp. 335-350.
82. Davis, R. E., Carlson, R.W., Kelly, J.W., and Davis, H.E. 1937 "Properties of cements and concretes containing fly ash" Journal of the American Concrete Institute, 33: 577-612.
83. Stanton, T. E. "Expansion of concrete through reaction between cement and aggregate", Transactions of the American Society of Civil Engineers, Part 2, 1942, pp.68-85.
84. Bloem, D.L. "Effect of fly ash in concrete", National Ready Mixed Concrete Association, Silver Springs, MD, Bulletin 48, 1954.
85. Davis, R.E. "Pozzolanic material- With special reference to their use in concrete pipe", American Concrete Pipe Association, Technical Memo, 1954.
86. Brink, R.H., and Halstead, W.J. "Studies relating to the testing of fly ash for use in concrete", Proceedings of the American Society for Testing and Materials, 1956, pp. 56: 1161-1206.
87. Welsh, G.B., and Burton, J. R. "Sydney fly ash in concrete" Commonwealth Engineer (Jan.), 1958, pp. 62-67.
88. Pepper, L., and Mather, B. "Effectiveness of mineral admixtures in preventing excessive expansion of concrete due to alkali- aggregate reaction", Proceedings of American Society of Testing and Materials, 1959, pp. 59: 1178-1202.
89. Campbell, L. "Aggregate and fly ash in concrete for Barkley Lock", Proceedings of American Society for Civil Engineers, 1961, pp. 87: 1-16.
90. Grieb, W.E., and Woolf, D.O. "Concrete containing fly ash as a replacement for portland blast furnace slag cement", Proceedings of American Society of the American Society for Testing and Materials, 1961, pp. 1143-1153.
91. ASTM Committee m-H. "Co-operative tests of fly ash as an admixture in portland cement concrete", Proceedings of American Society of the American Society for Testing and Materials, 1962, pp. 314-348.
92. Tynes, W .0 "Fly ash and water reducing admixtures for articulated concrete mattress" U .S Army Corps of Engineers, Waterways Experiment Station, Vicksburg, MS, Miscellaneous Paper, 1962, pp. 6-473
93. ACI Committee 201. "Durability of concrete in service" Journal of the American Concrete Institute, 1962, pp. 59: 1771-1784.
94. Larson, T.D. "Air entrainment and durability aspects of fly ash concrete", Proceedings of American Society of the American Society for Testing and Materials, 1964, pp. 866-886.
95. Daniels, F., and Alberty, R., Physical Chemistry, 3rd Edition, Chapter 11, pp. 394-397, Wiley, New York, 1967.
96. Dikeou, J.T. "Fly ash increases resistance of concrete to sulphate attack", Bureau of Reclamation, Denver, Co, Water Resources Technical Publication, Research Report 23, 1970.
97. Lovewell, C.E. and Hyland, E. J. "Effects of combining two or more admixtures in concrete", 50th Annual Meeting of the Highway Research Board, Washington, DC, Jan.1971, Ctte. A2-E5.

98. Rehsi, S.S. "Studies on Indian fly ashes and their use in structural concrete", Proceedings 3rd lnternational Ash Utilization Symposium, Pittsburgh, PA, Mar. 13-14, 1973, Bureau of Mines, Washington, DC, Information Circular IC 8640,pp. 231-245.
99. Elfert, R.J. "Bureau of Reclamation experiences with fly ash and other pozzolans in concrete" Proceedings, 3rd International Ash Utilization Symposium, Pittsburgh, PA, Mar. 13-14, 1973, Bureau of Mines, Washington, DC, Information Circular IC 8640,pp. 80-93.
100. Samarin, A., and Ryan, W.G.J. "Experience in use of admixtures in concrete containing cement and fly ash" Proceedings, Workshop on the Use of Chemical Admixtures in Concrete, University of New South Wales, Sydney, Australia, Dec.1975, pp.91-112.
101. Gebler, S and Klieger, P. "Effect of fly ash on the air-void stability of concrete" In Proceedings, 1st International Conference on the Use of Fly Ash, Silica Fume,Slag, and Other Mineral By- products in Concrete, Montebello, PQ, July 31- Aug.5, 1983. Edited by V.M. Malhotra. American Concrete Institute, Detroit, MI, Special Publication SP-79, pp.103-142.
102. Dunstan, E. R. "Performance of lignite and sub-bituminous fly ash in concrete" - A progress report, Bureau of Reclamation, Denver, Co, Report REC- ERC -76-1, 1976.
103. Clear, K.C., "Time-to-Corrosion of Reinforcing Steel in Concrete Slabs", Report No.FHWA-RD-76-70, April, 1976.
104. Slater, I., Lankard, D., and Moreland, P.I., "Electro-Chemical Removal of Chlorides from Concrete Bridge Decks", Materials Performance, Vol. 15, No.11, 1976, pp. 21-26.
105. Morrison, G.L., Virmani, Y.P., Stratten, F.W., and Gilliand, W.I., "Chloride Removal and Monomer Impregnation of Bridge Deck Concrete by Electro-Osmosis", Report No.FHWA KS-RD-71-1, 1976.
106. Owens, P. L. "Fly ash and its usage in concrete", Concrete: The journal of the Concrete Society, 1979, 13: 21-26.
107. Stuart, K.D., Anderson, D.A., and Cady, P.D. "Compressive strength studies of portland cement motors containing fly ash and superplasticers", Cement and Concrete Research, 1980, 10: 823-832.
108. Oberholster, R.E., and Westra, W. B. "The effectiveness of mineral admixtures in reducing expansion due to alkali- aggregate reaction with Malmesbury Group aggregates", Proceedings, 5th International Conference on Alkali- Aggregate Reactions in Concrete, Cape Town, South Africa, 1981, Mar.30- Apr. 3.
109. Whiting, D., "Rapid Determination of the Chloride permeability of Concrete", Report No. FHW A-RD-811119, Federal highway Administration, Washington, D. C, 1981.
110. Goro, S., and Roy, D.M., "Diffusion of ions Through Hardened Cement Paste", Cement and Concrete Research., Vol. 11, No.516, 1981, pp. 751-757.
111. Manmohan, D., and Mehta, P.K. "Influence of pozzolanic, slag and chemical admixtures on pore size distribution and permeability of hardened cement pastes", Cement, Concrete and Aggregates, 1981, 3: 63-67.
112. Ramakishnan, V., Coyle, W.V., Brown, J., Tlustus, A., and Venkataramanujam, "Performance characteristics of concretes containing fly ash", In Proceedings Symposium on Fly Ash Incorporating in Hydrated Cement Systems. Edited by S.Diamond. Materials Research Society, Boston, MA, 1981. pp. 233-243.
113. Short, N. R., and Page, C. L. "The diffusion of chloride ions through portland and blended cement pastes", Silicates industriels, 1982, 47: 237-240.
114. Kantitakis, I.M. "Permeability of concrete containing pulverized fuel ash", Proceedings of 5th International Symposium on Concrete Technology, Nuevo Leon, Mexico, Mar. 1981, Department of Civil Engineering, University of Nuevo Leon, Monterrey, Mexico, 1982, pp. 311-322.
115. Brown, J.H. "The strength and workability of concrete with PFA substitution", Proceedings of the International Symposium on the Use of PFA in Concrete, University of Leeds, Leeds, U.K, Apr.14-16, 1982. Edited by J.G. Cabrera and A.R Cusens.Department of Civil Engineering, University of Leeds, Leeds, U.K, pp. 151-161.
116. Mather, K. "Current research in sulphate resistance at the Waterways Experiment Station", Proceedings of George Verbeck Symposium on Sulphate Resistance of Concrete. American Concrete Institute. Detroit, MI, Special Publication SP- 77, 1982, pp. 63-74.
117. Perenchio, W .F., and Marusin, S.L., "Short -Term Chloride Penetration into Relatively Impermeable Concretes", Concrete International, Vol. 5, No.4, April, 1983, pp. 37-41.
118. Whiting, D., "In Situ Measurement of the Permeability of Concrete to Chloride Ions", SP 82-25, Proceedings CANMET/ACI International Conference on In Situ/Nondestructive Testing of Concrete, ed. v. M. Malhotra, Ottawa, Canada, October, 1984, pp. 501-524.
119. Kasai, Y., Matsui, I., Fukushima, U., and Kamohara, H. "Air permeability and carbonation of blended cement mortars", Proceedings of 1st International Conference on the Use of Fly Ash, Silica Fume, Slag, and Other

Mineral By- products in Concrete, Montebello, PQ, July 31- Aug.5, 1983. Edited by V.M. Malhotra. American Concrete Institute, Detroit, MI, Special Publication SP-79, 1983, pp.435-451.

120. Sturrup, V.R., Hooton, R.D., and Clendenning, T.G. "Durability of fly ash concrete", In Proceedings, 1st International Conference on the Use of Fly Ash, Silica Fume, Slag, and Other Mineral By- products in Concrete, Montebello, PQ, July 31-Aug.5, 1983. Edited by V.M. Malhotra. American Concrete Institute, Detroit, MI,Special Publication SP- 79, pp.47-69.
121. Virtanen,j. "Freeze-thaw resistance of concrete containing blast furnace slag, fly ash and condensed silica fume", Proceedings of 1st International Conference on the Use of Fly Ash, Silica Fume, Slag, and Other Mineral By- products in Concrete,Montebello, PQ, July 31- Aug.5, 1983. Edited by V.M. Malhotra. American Concrete Institute, Detroit, MI, Special Publication SP- 79, 1983, pp.923-942.
122. Helmuth, R. A. "Water- reducing properties of fly ash in cement pastes, mortars,and concretes: Causes and test methods" Proceedings of Silica Fume, Slag, and Natural Pozzolans in Concrete, Madrid, Spain, Apr.21-25, 1986. Edited by V.M.Malhotra. American Concrete Institute, Detroit, MI, Special Publication SP-91, pp. 723-737.
123. Klieger, P., and Gebler, S. "Fly ash and concrete durability", Proceedings of Katharine and Bryant Mather International Conference on Concrete Durability, Atlanta, GA, Apr. 27- May 1, 1987. Edited by J .M. Scanlon. American Concrete Institute, Detroit, MI, Special Publication SP-100, Vol. 1, pp.1043-1069.
124. Farbiarz, J., and Carrasquillo, R. "Alkali- aggregate reaction in concrete containing fly ash", Proceedings of Katharine and Bryant Mather International Conference on Concrete Durability, Atlanta, GA, Apr. 27- May 1, 1987. Edited by J .M. Scanlon. American Concrete Institute, Detroit, MI, Special Publication SP-100, Vol. 1, pp.1787-1808.
125. Sivasundaram, V., Carette, G.G., and Malhotra, V.M "Structural concrete incorporating high volumes of ASTM Class F fly ash", ACI Materials Journal, 1989, 86(5): 507-514.
126. Carette, G.C., and Langley, W.S. "Evaluation of de-icing salt scaling of fly ash concrete", Proceedings, International Workshop on Alkali- Aggregate Reactions in Concrete: Occurrences, Testing and Control, Halifax, NS, 1990, CANMET, Ottawa, ON.
127. Sivasundaram, V., Carette, G.G., and Malhotra, V.M "Long term strength development of high volume fly ash concrete", Cement & Concrete Composites, 1990, 12: 263-270.
128. Dhir. R.K., Jones, M.R., Ahmed, H.E.H., and Seneviratne, A.M.G., "Rapid estimation of Chloride Diffusion Coefficient in Concrete", Magazine of Concrete Research, Vol.42, No.152, September, 1990, pp. 177-185.
129. Lemming, M.L., Ahroad, S.H., Zia,P., Schemmel, J.J, Elliot, R.P., and Naaman, A.E., "High Performance Concretes: An Annotated Bibliography 1974-1989", SHRP-C307,Strategic Highway Research Program, National Research Council, Washington, D.C.1990.
130. Suprenant, Bruce A., "Testing for Chloride Permeability of Concrete", Concrete Construction, July 1991,pp. 8-12.
131. Zia, P, Leming, M.L., Ahmad, S.H. "High Performance Concrete: A State-of-the-Art Report", SHRP-C317, Strategic Highway Research Program, National Research Council, Washington D.C.1991.
132. American Society for Testing Materials "Standard specifications for fly ash and raw or calcined natural pozzolan for use as a mineral admixture in portland cement concrete", ASTM, 1992, Philadelphia, PA, ASTM C 618-92a.
133. Nasser, K.W., and Lai, P.S.H. "Resistance of fly ash concrete to freezing and thawing", Proceedings of the 4th CANMET/ACI International Conference on the Use of Fly Ash, Silica Fume, Slag, and Other Mineral By-products in Concrete, Istanbul,Turkey, May 3- 8, 1992. Edited by V .M. Malhotra. American Concrete Institute, Detroit, MI, Special Publication SP-132, Vol. 1, pp.205-226.
134. Ramakrishnan, V ., Suheyl Akman, M., "Fly Ash, Silica fume, Slag and Natural Pozzolans in Concrete", Proceedings US -Turkey Workshop, Istanbul, May 9, 1992, pp.94-98.
135. Malhotra, V.M., Ramezanianpour, A.A., "Fly Ash in Concrete", MSL Division Report 94 -95 (IR), CANMET, Canada, 1994, pp.135 -140.
136. Naik, T .R.,Singh S.S, and Ramme, B., “Effect of Source and Amount of Fly Ash on Mechanical and durability Properties of Concrete” Durability of Concrete: Proceedings of Fourth CANMET / ACI International Conference, SP-170, V .M.Malhotra, ed., American Concrete Institute, Farmington Hills, Mich., 1997, pp.157-188.
137. Cahn, D.et al, "Atmospheric Co2and the U.S. Cement Industry", World Cement, August 1997, pp.64-68.
138. Naik, T .R.,Singh S.S, and Ramme, B., " Effect of Source and Amount of Fly Ash on Mechanical and durability Properties of Concrete", II Durability of Concrete:Proceedings of Fourth CANMETI ACI International

Conference, SP-170, V .M.Malhotra, ed., American Concrete Institute, Farmington Hills, Mich., 1997, pp.157-188.

139. Naik, T.R.,Singh S.S, and Ramme, B., "Effect of Source and Amount of Fly Ash on Mechanical and durability Properties of Concrete," Durability of Concrete:Proceedings of Fourth CANMENT/ACI International Conference, SP-170, V.M.Malhotra, ed., American Concrete Institute, Farmington Hills, Mich., 1997, pp.157-188.
140. ASTM Designation C 1202-97, Test method for Electrical Indication of Concrete' s Ability to Resist Chloride Ion Penetration, Annual Book of ASTM Standards, Section 4, Construction, Vol. 04.02, Concrete and Concrete Aggregates, ASTM,Philadelphia, PA, 1998.
141. Baweja, D., Roper, H., and Sirivivatnanon, V., "Chloride Induced Steel Corrosion in Concrete: Part I-Corrosion Rates, Corrosion Activity, and Attack Areas", Materials Journal, American Concrete Institute, Detroit, Volume 95, Issue 3, 1998.
142. Ghafoori, N., and Cesar A. Garcia M., "Compacted Non Cement Concrete Utilizing Fluidized Bed And Pulverized Coal Combustion By-Products", Materials Journal,American Concrete Institute, Detroit, Volume 95, Issue 5, 1998.
143. Berg, E.R., and Neal, 1.A., "Concrete Masonry Unit Mix Designs Using Municipal Solid Waste Bottom Ash", Materials Journal, American Concrete Institute, Detroit,Volume 95, Issue 4,1998.
144. Naik, T.R., and Singh, S.S., and Ramme, B.W., "Mechanical Properties and Durability of Concrete Made with Blended Fly Ash", Materials Journal, American Concrete Institute, Detroit, Volume 95, Issue 4, 1998.
145. Taikalsky, P .1., Smith, E., and Regan, R., "Proportioning Spent Casting Sand in Controlled-Low Strength Materials", Materials Journal, American Concrete Institute, Detroit, Volume 95, Issue 6, 1998.
146. Salem, R.M., and Burdette, E.G., "Role of Chemical and Mineral Admixtures on the Physical Properties and Frost-Resistance of Recycled Aggregate Concrete", Materials Journal, American Concrete Institute, Detroit, Volume 95, Issue 5, 1998.
147. Ghafoori, N., and Zhang, Z., "Sulfate Resistance of Roller Compacted Concrete", Materials Journal, American Concrete Institute, Detroit, Volume 95, Issue 4, 1998.
148. Shi, C., Stegemann, 1.A., and Caldwell, R.1., "Effect of Supplementary Cementing Materials on the Specific Conductivity of Pore Solution and Its Implications on the Rapid Chloride Permeability Test (AASHTO T277 and ASTM C1202) Results", Materials Journal, American Concrete Institute, Detroit, Volume 95, Issue 4; 1998.
149. Malhotra, V. M., Materials Technology Laboratory "Role of Supplementary Cementing Materials in reducing Greenhouse Gas Emissions", CANMET, pp.4-9,1998
150. Naik, T.R.,Singh S.S, Karus,R.N, and Hossain, M.M, "Deicing Salt Scaling Resistance of High-Volume Fly Ash Concrete Using Various Sources of Fly Ashes," Fly Ash, Silica Fume, Slag, and natural Pozzolans in Concrete: Proceedings of Sixth CANMET/ACI international Conference, SP-178,V.M.Malhotra, ed., American concrete Institute, Farmington Hills, Mich., 1998, pp.77-111.
151. Naik, T.R.,Singh S.S, Karus,R.N, and Hossain, M.M, "Deicing Salt Scaling Resistance of High- Volume Fly Ash Concrete Using Various Sources of Fly Ashes," Fly Ash, Silica Fume, Slag, and natural Pozzolans in Concrete: Proceedings of Sixth CANMENT/ACI international Conference, SP-178,V.M.Malhotra, ed., American concrete Institute, Farmington Hills, Mich., 1998, pp.77-111.
152. Baweja, D., Roper, H., and Sirivivatnanon, V., "Chloride Induced Steel Corrosion in Concrete: Part 2-Gravimetric and Electrochemical Comparisons", Materials Journal, American Concrete Institute, Detroit, Volume 95, Issue 3, 1999.
153. Zhang, M.H., Bilodeau, A., Malhotra, V.M., Kim, K.S., and Kim, l.C., "Concrete Incorporating Supplementary Cementing Materials: Effect of Curing on Compressive Strength and Resistance to Chloride-Ion Penetration", Materials Journal, American Concrete Institute, Detroit, Volume 96, Issue 2, 1999.
154. Arino, A.M., and Mobasher, B., "Effect of Ground Copper Slag on Strength and Toughness of Cementitious Mixes", Materials Journal, American Concrete Institute, Detroit, Volume 96, Issue 1, 1999.
155. Li, Z., Peng,. l., and Ma, B., "Investigation of Chloride Diffusion for High-Performance Concrete Containing Fly Ash, Microsilica, and Chemical Admixtures", Materials Journal, American Concrete Institute, Detroit, Volume 96, Issue 3, 1999.
156. Whiting, D., and Nagi, M., "Laboratory Evaluation of Nuclear Gage for Measurement of Water and Cement Content of Fresh Concrete", Materials Journal, American Concrete Institute, Detroit, Volume 96, Issue 1, 1999.
157. Zhao, T.l., Zhu, l.Q., and Chi P.Y., "Modification of Pore Chemicals in Evaluation of High-Performance Concrete Permeability", Materials Journal, American Concrete Institute, Detroit, Volume 96, Issue 1, 1999.

158. Gu, J., Beaudoin, J.J., Zhang, M.H., and Malhotra, V.M., "Performance of Steel Reinforcement in Portland Cement and High- Volume Fly Ash Concretes", Materials Journal, American Concrete Institute, Detroit, Volume 96, Issue 5, 1999.
159. Shi, C., "Pozzolanic Reaction and Microstructure of Chemical Activated Lime-Fly Ash Pastes", Materials Journal, American Concrete Institute, Detroit, Volume 95, Issue 5, 1999.
160. Baweja, D., Roper, H., Sirivivatnanon, V., "Specifications of Concrete For Marine Environments: A Fresh Approach", Materials Journal, American Concrete Institute, Detroit, Volume 96, Issue 4, 1999.
161. Hearn, N., "Effect of Shrinkage and Load-lnduced Cracking on Water Permeability of Concrete", Materials Journal, American Concrete Institute, Detroit, Volume 96, Issue 2, 1999.
162. Srinivas Yenamandra., " Properties of High Performance Concrete for Bridge Deck and Prestressed Girders", Master of Science Thesis, South Dakota School of Mines and Technology, 1999.
163. Bilodeau, A., and Malhotra, V.M., "High-Volume Fly Ash System: Concrete Solution for Sustainable Development", Materials Journal, American Concrete Institute, Detroit, Volume 97, Issue 1, 2000.
164. Myers, L.L., and Carrasquillo, R.L., "Mixture Proportioning for High-Strength High-Performance Concrete Bridge Beams", Special Publication, American Concrete Institute, Detroit, Volume 189,2000.
165. MacDonald, K.A., and Northwood, D.O., "Rapid Estimation of Water-Cementitious Ratio and Chloride Ion Diffusivity in Hardened and Plastic Concrete by Resistivity Measurement", Special Publication, American Concrete Institute, Detroit, Volume 191, 2000.
166. Parrott, L.1., "Curing Time Estimator for Portland and Portland/Fly Ash Concretes", Special Publication, American Concrete Institute, Detroit, Volume 192, 2000.
167. Vieira, M., A1meida, I.R., and Goncalves, A.F., "Influence of Moisture Curing on Durability of Fly Ash Concrete for Road Pavements", Special Publication, American Concrete Institute, Detroit, Volume 192,2000.
168. Saricimen, H., Maslehuddin, M., Shameem, M., AlGhamdi, A.J., and Barry, M.S., "Effect of Curing and Drying on Strength and Absorption of Concretes Containing Fly Ash and Silica Fume", Special Publication, American Concrete Institute, Detroit, Volume 192, 2000.
169. Collpardi, S., Corinaldesi, V., Moricone, G., Bonora, G., and Collepardi, "Durability of High-Performance Concretes with Pozzolanic and Composite Cements", Special Publication, American Concrete Institute, Detroit, Volume 192, 2000.
170. lain Bilodeau, V. Mohan Malhotra., "High-Volume Fly Ash System: Concrete Solutions for Sustainale Development", ACI Materials Journal, V .97, No.1,Jan-Feb2000, pp.41
171. Gretchen, K. Hoffman, " Western region Ash Group", fly Ash Usage in the Western United States, Url. http://www.wrashg.orglwestuse.htm.
172. Cahn, D. et al, "Atmospheric Co2 and the U.S. Cement Industry", World Cement,August 1997, pp.64-68.
173. ACI Committee 209, “Prediction of Creep, Shrinkage, and Temperature Effects in Concrete.” ACI 209R-92, Manual of Concrete Practice, American Concrete Institute, Detroit, MI, 1994.
174. Alfes, C. “Modulus of Elasticity and Drying Shrinkage of High-Strength Concrete Containing Silica Fume.” Fly Ash, Silica Fume, Slag, and Natural Pozzolansin Concrete. Proceedings of the Fourth International Conference, Istanbul Turkey; Ed. by Malhotra. V.M. (1992). American Concrete Institute, Detroit, Michigan.
175. Bloom, R., and Benture, A. “Free and Restrained Shrinkage for Normal and High Strength Concretes.” ACI Materials Journal, 1995, 92 (2), pp. 211-217.
176. Browne, R. D., “Thermal Movement of Concrete.” Concrete, 1972, 6 (11), pp. 51-53.
177. Fiorato, A. E. “PCA Research on High-Strength Concrete.” Concrete International, 1989, 11 (4), pp. 44-50.
178. Ngab, A. S., Slate, F.O., and Nilson, A. H. “Microcracking and Time-Dependent Strains in High Strength Concrete.” ACI Journal, 1981, 78 (4), pp. 262-268.
179. Shah, S.P., and Ahmad, S.H. "High Performance Concrete: Properties and Applications", McGraw-Hill Inc., New York, 1994.
180. Weiss, W. J., Yang, W., and Shah, S. P. “Shrinkage Cracking of Restrained Concrete Slabs.” Journal of Engineering Mechanics, 1998, 124 (7), pp. 765-774.
181. Wiegrink, K., Marikunte, S., and Shah, S. P. “Shrinkage Cracking of High-Strength Concrete.” ACI Materials Journal, 1996, 93 (5), pp. 409-415
182. Wolsiefer, J., Sivasundaram, V., Carette, G.G., and Malhotra, V.M., "Performance of Concretes Incorporating Various Forms of Silica Fume," Fifth Canmnet / ACI International Conference, Milwaukee, WI, 1995.
183. Vijaya Rangan, B., "High-Performance High-Strength Concrete: Design Recommendations", Concrete International, November 1998, Volume 20, No. 11, pp. 63-68.
184. Vijaya Rangan, B., and Yau Seng Hwee., "Studies on Commercial High-Strength Concretes", ACI Materials Journal, V. 87, No. 5, September-October 1990, pp. 440-445.

APPENDIX A

Details of Trial Mixes for Fresh and Hardened Concrete Properties for Bridge Deck Concrete

Note:

The following mix designation scheme is used. The first letter refers to the type of aggregate used: Q-Quartzite, L-Limestone, H-High Strength Girder Concrete. The second letter indicates a number that indicates the mix number. The next letters indicate whether the mix contains fly ash and/or silica fume: F-Fly Ash, S- Silica Fume. The number following S or F indicates the percentage of cement replaced with fly ash and/or silica fume. A zero indicates no fly ash or silica fume. The last letter with W indicates the water to cement ratio. All control mixes are referred to as CONTROL followed by the water to cement ratio.

Examples:

Q1CONTROLW0.4 - Mix no 1, with quartzite aggregate, with no cement replacement: Control, with water to cement ratio of 0.4.

Q2F15S7W0.52 - Mix no 2, with quartzite aggregate, with 15% of cement by weight replaced by fly ash, and with 7% of cement by weight replaced by silica fume, with water to cement ratio of 0.52.

L9F0S10W0.45 - Mix no 9, with limestone aggregate, with no fly ash, and with 10% of cement by weight replaced by silica fume, with water to cement ratio of 0.45

Table A1: Mixture Designations for Mixes with Quartzite Aggregate

Mixture Designation	Description
Q1CONTROLW0.4	Mix with no cement replacement : Control
Q2F15S7W0.52	Mix with 7% of cement by weight replaced by silica fume and 15% by fly ash
Q3F15S5W0.50	Mix with 5% of cement by weight replaced by silica fume and 15% by fly ash
Q4F20S5W0.54	Mix with 5% of cement by weight replaced by silica fume and 20% by fly ash
Q5F15S0W0.47	Mix with 15% of cement by weight replaced by fly ash
Q6F20S0W0.50	Mix with 20% of cement by weight replaced by fly ash
Q7F25S0W0.54	Mix with 25% of cement by weight replaced by fly ash
Q8F0S7W0.43	Mix with 7% of cement by weight replaced by silica fume
Q9F0S10W0.45	Mix with 10% of cement by weight replaced by silica fume
Q10F0S12W0.46	Mix with 12% of cement by weight replaced by silica fume

Note: Multiplication factor of 1.2 used for volume correction for fly ash addition

Table A2: Mixture Proportions for Mixes with Quartzite Aggregate

Mixture Designation	Mixture Proportions (lbs/cubic yard)							w/(c+f+sf)
	Cement pcy	Fly Ash pcy	Silica Fume pcy	Coarse Aggregate pcy	Fine Aggregate pcy	Water pcy	w/c	
Q1CONTROLW0.4	655	0	0	1725	1100	264	0.40	0.40
Q2F15S7W0.52	511	118	55	1725	1100	264	0.52	0.39
Q3F15S5W0.50	524	118	39	1725	1100	264	0.50	0.39
Q4F20S5W0.54	491	157	39	1725	1100	264	0.54	0.38
Q5F15S0W0.47	557	118	0	1725	1100	264	0.47	0.39
Q6F20S0W0.50	524	157	0	1725	1100	264	0.50	0.39
Q7F25S0W0.54	491	197	0	1725	1100	264	0.54	0.38
Q8F0S7W0.43	610	0	55	1725	1100	264	0.43	0.40
Q9F0S10W0.45	590	0	78	1725	1100	264	0.45	0.40
Q10F0S12W0.46	577	0	94	1725	1100	264	0.46	0.39

* Conversion Factor: pcy x 0.59 = kg/m^3

Table A3: Fresh Concrete Properties for Mixes with Quartzite Aggregate

Mixture Designation	Unit Weight		Air	Slump	
	lbs/ft^3	kg/m^3	%	inches	mm
Q1CONTROLW0.4	139.2	2229.6	8.0	4.00	102
Q2F15S7W0.52	141.2	2261.6	5.4	7.50	191
Q3F15S5W0.50	144.4	2312.9	4.4	5.25	133
Q4F20S5W0.54	140.8	2255.2	6.8	8.25	210
Q5F15S0W0.47	140.8	2255.2	7.0	7.50	191
Q6F20S0W0.50	140.8	2255.2	7.2	8.25	210
Q7F25S0W0.54	139.6	2236.0	7.6	9.00	229
Q8F0S7W0.43	143.6	2300.0	5.8	7.00	178
Q9F0S10W0.45	146.4	2344.9	4.8	4.25	108
Q10F0S12W0.46	144.4	2312.9	4.4	6.00	152

Table A4: 14- Day Compressive Strength and Static Modulus (Quartzite Aggregate)

Spec.	Age	Length		Diameter		Unit Weight		Static Mod. psi	Static Mod. Mpa	Compressive Strength	
ID #	days	in.	mm	in.	mm	pcf	Kg/m^3	(x10^6)	(x10^4)	psi	Mpa
Q1CONTROLW0.4-C1	14	12.00	304.8	6.01	152.6	142.2	2277.9	4.2	2.9	4955	34.2
Q1CONTROLW0.4-C2	14	12.00	304.9	6.00	152.5	145.1	2323.4	4.2	2.9	5320	36.8
*Q1CONTROLW0.4-C3	14	12.00	304.8	6.00	152.5	145.0	2322.8	5.3	3.7	5250	36.3
Averages		**12.00**	**304.8**	**6.00**	**152.5**	**144.1**	**2308.0**	**4.2**	**3.2**	**5175**	**35.8**
Q2F15S7W0.52-C1	14	12.00	304.8	6.00	152.4	145.2	2324.9	4.2	2.9	5110	35.3
Q2F15S7W0.52-C2	14	12.00	304.8	6.01	152.5	144.9	2321.0	4.2	2.9	5120	35.4
Q2F15S7W0.52-C3	14	12.00	304.8	6.00	152.5	145.0	2322.0	4.2	2.9	5175	35.8
Averages		**12.00**	**304.8**	**6.00**	**152.5**	**145.0**	**2322.6**	**4.2**	**2.9**	**5135**	**35.5**
Q3F15S5W0.50-C1	14	12.00	304.8	6.00	152.5	147.6	2364.1	4.2	2.9	5640	39.0
*Q3F15S5W0.50-C2	14	12.00	304.8	6.01	152.5	147.5	2361.7	4.2	2.9	4275	29.5
Q3F15S5W0.50-C3	14	12.00	304.8	6.01	152.5	150.0	2402.4	3.9	2.7	6020	41.6
Averages		**12.00**	**304.8**	**6.00**	**152.5**	**148.3**	**2376.1**	**4.1**	**2.8**	**5830**	**36.7**
Q4F20S5W0.54-C4	14	12.00	304.8	6.00	152.4	142.6	2284.0	4.2	2.9	4600	31.8
Q4F20S5W0.54-C5	14	12.00	304.8	6.00	152.4	142.6	2284.0	4.2	2.9	4795	33.1
*Q4F20S5W0.54-C6	14	12.00	304.8	6.00	152.4	142.6	2284.3	4.2	2.9	4050	28.0
Averages		**12.00**	**304.8**	**6.00**	**152.4**	**142.6**	**2284.1**	**4.2**	**2.9**	**4698**	**31.0**
Q5F15S0W0.47-C3	14	12.00	304.8	6.00	152.4	142.6	2284.0	4.7	3.2	5025	34.7
Q5F15S0W0.47-C4	14	12.00	304.8	6.00	152.4	142.6	2283.2	4.7	3.2	4900	33.9
Q5F15S0W0.47-C5	14	12.00	304.8	6.00	152.4	142.6	2283.2	4.7	3.3	4860	33.6
Averages		**12.00**	**304.8**	**6.00**	**152.4**	**142.6**	**2283.5**	**4.7**	**3.3**	**4928**	**34.1**

Table A4: 14- Day Compressive Strength and Static Modulus (Quartzite Aggregate)…continued

Spec. ID #	Age days	Length in.	Length mm	Diameter in.	Diameter mm	Unit Weight pcf	Unit Weight Kg/m^3	Static Mod. psi ($x10^6$)	Static Mod. Mpa ($x10^4$)	Compressive Strength psi	Compressive Strength Mpa
Q6F20S0W0.50-C2	14	12.00	304.8	6.00	152.4	142.6	2284.0	4.2	2.9	4420	30.5
Q6F20S0W0.50-C3	14	12.00	304.8	6.00	152.5	142.5	2282.6	4.2	2.9	4435	30.6
*Q6F20S0W0.50-C4	14	12.00	304.8	6.00	152.4	142.6	2283.2	4.2	2.9	4065	28.1
Averages		**12.00**	**304.8**	**6.00**	**152.4**	**142.6**	**2283.3**	**4.2**	**2.9**	**4428**	**29.8**
Q7F25S0W0.54-C2	14	12.00	304.8	6.00	152.4	140.0	2242.5	3.5	2.4	4175	28.8
Q7F25S0W0.54-C3	14	12.00	304.8	6.00	152.4	140.1	2243.2	3.5	2.4	3785	26.2
Q7F25S0W0.54-C5	14	12.00	304.8	6.00	152.4	140.0	2242.5	3.5	2.4	3430	23.7
Averages		**12.00**	**304.8**	**6.00**	**152.4**	**140.0**	**2242.8**	**3.5**	**2.4**	**3797**	**26.2**
Q8F25S0W0.54-C2	14	12.00	304.8	6.02	152.9	144.4	2312.7	4.7	3.2	6490	44.8
Q8F25S0W0.54-C3	14	12.00	304.8	6.01	152.7	144.5	2314.8	4.7	3.2	6410	44.3
Q8F25S0W0.54-C4	14	12.00	304.8	6.01	152.7	144.2	2309.0	4.7	3.2	6485	44.8
Averages		**12.00**	**304.8**	**6.01**	**152.7**	**144.4**	**2312.2**	**4.7**	**3.2**	**6462**	**44.7**
Q9F0S10W0.45-C3	14	12.00	304.8	6.01	152.6	147.3	2359.6	4.7	3.2	7230	50.0
Q9F0S10W0.45-C4	14	12.00	304.8	6.01	152.7	147.1	2356.1	4.7	3.2	7045	48.7
Q9F0S10W0.45-C5	14	12.00	304.8	6.01	152.7	147.2	2357.7	4.7	3.2	7050	48.7
Averages		**12.00**	**304.8**	**6.01**	**152.7**	**147.2**	**2357.8**	**4.7**	**3.2**	**7108**	**49.1**
Q10F0S12W0.46-C2	14	12.00	304.8	6.00	152.5	147.5	2362.5	5.0	3.4	8655	59.8
Q10F0S12W0.46-C3	14	12.00	304.8	6.00	152.5	147.6	2363.3	5.0	3.4	8835	61.0
Q10F0S12W0.46-C6	14	12.00	304.8	6.01	152.5	147.5	2361.7	5.0	3.4	8405	58.1
Averages		**12.00**	**304.8**	**6.00**	**152.5**	**147.5**	**2362.5**	**5.0**	**3.4**	**8632**	**59.6**

Note: *Specimen Not considered for calculation of average value as it is an outlier.

Table A5: 14-Day Flexural Strength (Quartzite Aggregate)

Spec. ID #	Age	Length		Breadth		Depth		Unit Weight		Maximum Load		Flexural Strength	
	days	in.	mm	in.	mm	in.	mm	pcf	kg/m^3	lbs	kgs	psi	Mpa
Q1CONTROLW0.4-B1	14	14.00	355.6	4.00	101.6	4.00	101.7	150.4	2408.4	3900.0	1769.0	730	5.0
*Q1CONTROLW0.4-B3	14	14.00	355.6	4.00	101.7	4.01	101.8	146.2	2341.3	3260.6	1479.0	610	4.2
*Q1CONTROLW0.4-B5	14	14.00	355.6	3.97	100.9	4.01	101.8	147.4	2361.2	4484.8	2034.3	840	5.8
Q1CONTROLW0.4-B6	14	14.00	355.6	4.01	101.8	4.00	101.7	146.2	2341.5	3750.1	1701.0	703	4.9
Averages		**14.00**	**355.6**	**4.00**	**101.5**	**4.01**	**101.7**	**147.5**	**2363.1**	**3848.9**	**1745.8**	**717**	**5.0**
*Q2F15S7W0.52-B1	14	14.00	355.6	4.04	102.6	4.05	102.9	143.3	2296.0	4300.7	1950.8	780	5.4
Q2F15S7W0.52-B2	14	14.00	355.6	4.07	103.3	4.06	103.1	142.0	2275.2	3579.7	1623.7	635	4.4
Q2F15S7W0.52-B3	14	14.00	355.6	3.98	101.2	4.03	102.4	146.0	2339.2	3353.6	1521.2	635	4.4
*Q2F15S7W0.52-B4	14	14.00	355.6	4.09	103.9	4.02	102.0	142.7	2286.5	3190.4	1447.1	580	4.0
Averages		**14.00**	**355.6**	**4.05**	**102.7**	**4.04**	**102.6**	**143.5**	**2299.2**	**3606.1**	**1635.7**	**635**	**4.4**
Q3F15S5W0.50-B1	14	14.00	355.6	4.03	102.2	4.00	101.7	146.0	2339.1	3830.3	1737.4	715	4.9
*Q3F15S5W0.50-B2	14	14.00	355.6	4.01	101.8	4.01	101.8	146.0	2338.6	3681.7	1670.0	690	4.8
Q3F15S5W0.50-B3	14	14.00	355.6	4.00	101.7	4.02	102.0	145.9	2336.7	3989.9	1809.8	740	5.1
Q3F15S5W0.50-B4	14	14.00	355.6	4.01	101.7	4.01	101.8	149.9	2401.9	4101.1	1860.2	765	5.3
Averages		**14.00**	**355.6**	**4.01**	**101.9**	**4.01**	**101.8**	**147.0**	**2354.0**	**3900.8**	**1769.3**	**740**	**5.1**
Q4F20S5W0.54-B1	14	14.00	355.6	4.00	101.6	4.00	101.6	142.7	2285.6	3300.0	1496.9	620	4.3
Q4F20S5W0.54-B2	14	14.00	355.6	4.00	101.6	4.01	101.7	142.5	2283.3	3100.0	1406.1	580	4.0
Q4F20S5W0.54-B3	14	14.00	355.6	4.00	101.7	4.00	101.7	142.4	2281.6	3100.0	1406.1	580	4.0
Averages		**14.00**	**355.6**	**4.00**	**101.6**	**4.00**	**101.7**	**142.6**	**2283.5**	**3166.7**	**1436.4**	**593**	**4.1**

Table A5: 14-Day Flexural Strength (Quartzite Aggregate)…continued

Spec. ID #	Age	Length		Breadth		Depth		Unit Weight		Maximum Load		Flexural Strength	
	days	in.	mm	in.	mm	in.	mm	pcf	kg/m^3	lbs	kgs	psi	Mpa
Q5F15S0W0.47-B1	14	14.00	355.6	4.00	101.6	4.00	101.6	146.5	2346.3	3991.7	1810.6	750	5.2
*Q5F15S0W0.47-B2	14	14.00	355.6	4.00	101.6	4.00	101.7	142.6	2284.2	2919.7	1324.4	545	3.8
Q5F15S0W0.47-B3	14	14.00	355.6	4.00	101.6	4.00	101.6	146.5	2347.0	3725.5	1689.9	700	4.8
*Q5F15S0W0.47-B4	14	14.00	355.6	4.00	101.6	4.00	101.7	142.6	2283.5	3425.6	1553.8	640	4.4
Averages		**14.00**	**355.6**	**4.00**	**101.6**	**4.00**	**101.7**	**144.6**	**2315.3**	**3515.6**	**1594.7**	**725**	**5.0**
*Q6F20S0W0.50-B1	14	14.00	355.6	4.00	101.6	4.00	101.6	139.6	2235.8	3200.4	1451.7	600	4.1
*Q6F20S0W0.50-B2	14	14.00	355.6	4.00	101.6	4.00	101.6	139.6	2235.8	4057.3	1840.4	760	5.3
Q6F20S0W0.50-B3	14	14.00	355.6	4.01	101.8	4.01	101.9	138.9	2224.6	3625.2	1644.4	675	4.7
Q6F20S0W0.50-B4	14	14.00	355.6	4.00	101.7	4.00	101.7	139.4	2232.4	3612.5	1638.6	675	4.7
Averages		**14.00**	**355.6**	**4.00**	**101.7**	**4.00**	**101.7**	**139.4**	**2232.2**	**3623.9**	**1643.7**	**675**	**4.7**
*Q7F25S0W0.54-B1	14	14.00	355.6	4.00	101.6	4.00	101.6	142.6	2284.7	3424.7	1553.4	640	4.4
Q7F25S0W0.54-B2	14	14.00	355.6	4.00	101.6	4.00	101.6	142.7	2285.1	3013.6	1366.9	565	3.9
Q7F25S0W0.54-B3	14	14.00	355.6	4.00	101.6	4.00	101.7	142.6	2284.2	2932.4	1330.1	550	3.8
Q7F25S0W0.54-B7	14	14.00	355.6	4.00	101.6	4.00	101.6	142.7	2285.1	3020.0	1369.8	565	3.9
Averages		**14.00**	**355.6**	**4.00**	**101.6**	**4.00**	**101.6**	**142.6**	**2284.8**	**3097.7**	**1405.1**	**560**	**3.9**
*Q8F25S0W0.54-B1	14	14.00	355.6	4.03	102.3	4.03	102.4	144.4	2313.2	4137.5	1876.7	760	5.3
Q8F25S0W0.54-B4	14	14.00	355.6	4.02	102.2	4.03	102.3	144.7	2317.3	4655.3	2111.6	855	5.9
Q8F25S0W0.54-B5	14	14.00	355.6	4.00	101.6	4.01	101.9	150.0	2402.7	4669.0	2117.8	870	6.0
Q8F25S0W0.54-B7	14	14.00	355.6	4.00	101.6	4.01	101.8	146.3	2343.0	4474.8	2029.7	835	5.8
Averages		**14.00**	**355.6**	**4.01**	**101.9**	**4.02**	**102.1**	**146.3**	**2344.0**	**4484.2**	**2034.0**	**853**	**5.9**

Table A5: 14-Day Flexural Strength (Quartzite Aggregate)…continued

Spec. ID #	Age	Length		Breadth		Depth		Unit Weight		Maximum Load		Flexural Strength	
	days	in.	mm	in.	mm	in.	mm	pcf	kg/m^3	lbs	kgs	psi	Mpa
Q9F0S10W0.45-B1	14	14.00	355.6	4.02	102.2	4.02	102.1	148.8	2383.2	4739.2	2149.7	875	6.0
Q9F0S10W0.45-B2	14	14.00	355.6	4.06	103.1	4.02	102.2	147.4	2360.6	4368.1	1981.3	800	5.5
Q9F0S10W0.45-B3	14	14.00	355.6	4.00	101.6	4.01	101.8	150.1	2404.6	4348.1	1972.3	815	5.6
Q9F0S10W0.45-B4	14	14.00	355.6	4.01	101.9	4.01	101.8	149.7	2397.3	4185.8	1898.6	780	5.4
Averages		**14.00**	**355.6**	**4.02**	**102.2**	**4.01**	**102.0**	**149.0**	**2386.4**	**4410.3**	**2000.5**	**818**	**5.6**
*Q10F0S12W0.46-B1	14	14.00	355.6	4.01	101.9	4.01	101.8	149.8	2399.2	4307.1	1953.7	805	5.6
Q10F0S12W0.46-B2	14	14.00	355.6	4.00	101.7	4.01	101.7	150.1	2404.0	4753.7	2156.2	890	6.1
*Q10F0S12W0.46-B3	14	14.00	355.6	4.00	101.7	4.00	101.7	150.2	2405.8	4445.6	2016.5	835	5.8
Q10F0S12W0.46-B5	14	14.00	355.6	4.00	101.7	4.00	101.7	150.1	2404.6	4894.1	2219.9	915	6.3
Averages		**14.00**	**355.6**	**4.01**	**101.7**	**4.00**	**101.7**	**150.1**	**2403.4**	**4600.1**	**2086.6**	**903**	**6.2**

Note: *Specimen not considered for the calculation of average value as it is an outlier.

Table A6: 28- Day Compressive Strength and Static Modulus (Quartzite Aggregate)

Spec. ID #	Age	Length		Diameter		Unit Weight		Static Mod.		Compressive Strength	
								psi	Mpa		
	days	in.	mm	in.	mm	pcf	Kg/m^3	(x10^6)	(x10^4)	psi	Mpa
Q1CONTROLW0.4-C4	28	12.14	308.4	6.01	152.5	142.4	2280.2	4.7	3.2	5685	39.3
Q1CONTROLW0.4-C5	28	12.16	308.9	6.00	152.5	142.4	2281.0	4.7	3.2	5935	41.0
*Q1CONTROLW0.4-C6	28	12.08	306.8	6.01	152.5	142.4	2280.2	4.2	2.9	5775	39.9
Averages		**12.13**	**308.0**	**6.00**	**152.5**	**142.4**	**2280.4**	**4.7**	**3.2**	**5798**	**40.1**
Q2F15S7W0.52-C4	28	12.09	307.1	6.01	152.7	142.1	2276.5	4.7	3.2	6170	42.6
Q2F15S7W0.52-C5	28	12.10	307.3	6.01	152.7	142.0	2274.7	4.7	3.2	6000	41.5
Q2F15S7W0.52-C6	28	12.12	307.8	6.01	152.8	144.5	2314.0	4.7	3.2	6250	43.2
Averages		**12.10**	**307.4**	**6.01**	**152.7**	**142.9**	**2288.4**	**4.7**	**3.2**	**6140**	**42.4**
Q3F15S5W0.50-C4	28	12.30	312.4	6.01	152.7	147.1	2356.3	5.3	3.6	7395	51.1
Q3F15S5W0.50-C5	28	12.14	308.4	6.01	152.7	147.2	2357.7	5.3	3.7	7225	49.9
Q3F15S5W0.50-C6	28	12.16	308.9	6.01	152.7	147.2	2356.9	5.3	3.6	7045	48.7
Averages		**12.20**	**309.9**	**6.01**	**152.7**	**147.2**	**2357.0**	**5.3**	**3.7**	**7222**	**49.9**
*Q4F20S5W0.54-C1	28	12.16	308.9	6.01	152.6	139.6	2236.6	4.0	2.8	5290	36.6
Q4F20S5W0.54-C2	28	12.14	308.4	6.01	152.7	139.5	2234.9	4.7	3.2	5570	38.5
Q4F20S5W0.54-C3	28	12.20	309.9	6.01	152.7	139.5	2235.0	4.7	3.2	5655	39.1
Averages		**12.17**	**309.0**	**6.01**	**152.7**	**139.6**	**2235.5**	**4.7**	**3.2**	**5505**	**38.0**
Q5F15S0W0.47-C1	28	12.02	305.2	6.02	152.8	141.7	2269.6	4.7	3.2	5810	40.1
Q5F15S0W0.47-C2	28	12.13	308.1	6.01	152.7	141.9	2273.5	4.7	3.2	5495	38.0
Q5F15S0W0.47-C6	28	12.15	308.6	6.02	152.8	141.7	2269.4	4.7	3.2	5560	38.4
Averages		**12.10**	**307.3**	**6.01**	**152.8**	**141.8**	**2270.8**	**4.7**	**3.2**	**5622**	**38.8**

Table A6: 28- Day Compressive Strength and Static Modulus (Quartzite Aggregate)…continued

Spec. ID #	Age	Length		Diameter		Unit Weight		Static Mod.		Compressive Strength	
								psi	Mpa		
	days	in.	mm	in.	mm	pcf	Kg/m^3	(x10^6)	(x10^4)	psi	Mpa
Q6F20S0W0.50-C1	28	12.15	308.6	6.02	153.0	141.3	2263.7	4.4	3.1	5175	35.8
Q6F20S0W0.50-C5	28	12.11	307.6	6.02	152.9	141.6	2268.0	4.7	3.2	5185	35.8
Q6F20S0W0.50-C6	28	12.16	308.9	6.02	153.0	143.9	2304.2	4.4	3.1	5000	34.6
Averages		**12.14**	**308.4**	**6.02**	**153.0**	**142.3**	**2278.6**	**4.5**	**3.1**	**5120**	**35.4**
Q7F25S0W0.54-C6	28	12.18	309.4	6.02	153.0	138.9	2224.0	4.2	2.9	4685	32.4
Q7F25S0W0.54-C1	28	12.10	307.3	6.01	152.8	139.4	2232.0	4.2	2.9	4875	33.7
Q7F25S0W0.54-C4	28	12.08	306.8	6.02	152.9	139.1	2228.0	4.2	2.9	4710	32.5
Averages		**12.12**	**307.8**	**6.02**	**152.9**	**139.1**	**2228.0**	**4.2**	**2.9**	**4757**	**32.9**
Q8F25S0W0.54-C5	28	12.11	307.6	6.01	152.6	144.6	2315.6	5.3	3.7	6840	47.3
Q8F25S0W0.54-C6	28	12.11	307.6	6.01	152.7	144.5	2314.8	5.3	3.7	7420	51.3
Q8F25S0W0.54-C1	28	12.01	305.0	6.01	152.7	141.9	2272.5	5.3	3.7	7045	48.7
Averages		**12.08**	**306.7**	**6.01**	**152.7**	**143.7**	**2300.9**	**5.3**	**3.7**	**7102**	**49.1**
Q9F0S10W0.45-C2	28	12.02	305.3	6.02	152.8	146.7	2350.2	5.3	3.6	8445	58.4
Q9F0S10W0.45-C1	28	12.08	306.8	6.01	152.7	146.9	2352.7	5.3	3.6	7925	54.8
Q9F0S10W0.45-C6	28	12.09	307.1	6.01	152.7	146.9	2352.9	5.3	3.6	7710	53.3
Averages		**12.06**	**306.4**	**6.01**	**152.7**	**146.8**	**2351.9**	**5.3**	**3.6**	**8027**	**55.5**
Q10F0S12W0.46-C4	28	12.01	305.1	6.02	153.0	144.0	2305.6	6.0	4.2	9130	63.1
Q10F0S12W0.46-C1	28	12.01	305.1	6.01	152.7	144.4	2312.7	6.0	4.2	8875	61.3
Q10F0S12W0.46-C5	28	12.23	310.6	6.02	152.9	144.0	2306.8	6.0	4.2	9070	62.7
Averages		**12.08**	**307.0**	**6.02**	**152.9**	**144.1**	**2308.4**	**6.0**	**4.2**	**9025**	**62.4**

Note: *Specimen not considered for the caluulation of average value as it is an outlier.

Table A7: 28-Day Flexural Strength (Quartzite Aggregate)

Spec. ID #	Age	Length		Breadth		Depth		Unit Weight		Maximum Load		Flexural Strength	
	days	in.	mm	in.	mm	in.	mm	pcf	kg/m^3	lbs	kgs	psi	Mpa
*Q1CONTROLW0.4-B4	28	14.00	355.6	4.00	101.6	4.00	101.7	146.5	2345.8	5138	2330	730	5.0
Q1CONTROLW0.4-B8	28	14.00	355.6	4.00	101.6	4.00	101.7	146.5	2346.5	5534	2510	1035	7.2
*Q1CONTROLW0.4-B2	28	14.00	355.6	4.00	101.6	4.00	101.7	146.5	2346.3	4193	1902	785	5.4
Q1CONTROLW0.4-B7	28	14.00	355.6	4.00	101.6	4.00	101.6	146.5	2347.0	5043	2287	945	6.5
Averages		**14.00**	**355.6**	**4.00**	**101.6**	**4.00**	**101.6**	**146.5**	**2346.4**	**4977**	**2257**	**990**	**6.8**
*Q2F15S7W0.52-B7	28	14.00	355.6	4.02	102.2	4.05	102.9	147.7	2366.0	4314	1957	785	5.4
Q2F15S7W0.52-B5	28	14.00	355.6	4.01	101.8	4.01	102.0	145.7	2334.2	4383	1988	810	5.6
*Q2F15S7W0.52-B6	28	14.00	355.6	4.02	102.2	4.02	102.1	148.9	2384.3	4037	1831	745	5.1
Q2F15S7W0.52-B8	28	14.00	355.6	4.02	102.2	4.05	102.9	143.9	2305.3	4765	2161	865	6.0
Averages		**14.00**	**355.6**	**4.02**	**102.1**	**4.03**	**102.5**	**146.6**	**2347.5**	**4375**	**1984**	**838**	**5.8**
*Q3F15S5W0.50-B8	28	14.00	355.6	4.02	102.2	4.02	102.1	148.8	2382.5	5017	2276	715	4.9
Q3F15S5W0.50-B5	28	14.00	355.6	4.01	102.0	4.01	101.9	149.5	2393.7	4297	1949	800	5.5
*Q3F15S5W0.50-B6	28	14.00	355.6	4.01	101.9	4.01	101.9	149.6	2395.7	5132	2328	955	6.6
Q3F15S5W0.50-B7	28	14.00	355.6	4.02	102.1	4.02	102.2	148.9	2385.4	4592	2083	850	5.9
Averages		**14.00**	**355.6**	**4.02**	**102.0**	**4.02**	**102.0**	**149.2**	**2389.3**	**4759**	**2159**	**825**	**5.7**
*Q4F20S5W0.54-B8	28	14.00	355.6	4.01	101.8	4.01	101.8	142.2	2277.9	4524	2052	845	5.8
Q4F20S5W0.54-B5	28	14.00	355.6	4.01	101.9	4.01	101.9	141.8	2271.7	3862	1752	720	5.0
Q4F20S5W0.54-B6	28	14.00	355.6	4.01	101.9	4.01	101.9	141.9	2272.8	4246	1926	790	5.5
Q4F20S5W0.54-B7	28	14.00	355.6	4.01	101.9	4.01	101.9	141.9	2272.2	3876	1758	720	5.0
Averages		**14.00**	**355.6**	**4.01**	**101.9**	**4.01**	**101.9**	**142.0**	**2273.7**	**4127**	**1872**	**743**	**5.1**

Table A7: 28-Day Flexural Strength (Quartzite Aggregate)...continued

Spec. ID #	Age	Length		Breadth		Depth		Unit Weight		Maximum Load		Flexural Strength	
	days	in.	mm	in.	mm	in.	mm	pcf	kg/m^3	lbs	kgs	psi	Mpa
*Q5F15S0W0.47-B5	28	14.00	355.6	4.02	102.0	4.01	101.8	145.7	2334.2	4026	1826	750	5.2
Q5F15S0W0.47-B8	28	14.00	355.6	4.01	101.9	4.01	101.8	145.9	2336.6	4695	2129	875	6.0
*Q5F15S0W0.47-B6	28	14.00	355.6	4.01	101.9	4.01	101.9	145.7	2333.5	3970	1801	740	5.1
Q5F15S0W0.47-B7	28	14.00	355.6	4.01	101.9	4.01	102.0	145.6	2331.9	4823	2188	895	6.2
Averages		**14.00**	**355.6**	**4.01**	**101.9**	**4.01**	**101.8**	**145.7**	**2334.0**	**4378**	**1986**	**885**	**6.1**
Q6F20S0W0.50-B8	28	14.00	355.6	4.01	101.9	4.01	101.9	141.9	2272.2	3962	1797	735	5.1
Q6F20S0W0.50-B6	28	14.00	355.6	4.02	102.0	4.01	101.9	141.8	2270.4	3584	1625	665	4.6
Q6F20S0W0.50-B7	28	14.00	355.6	4.01	101.9	4.02	102.1	141.6	2267.7	3640	1651	675	4.7
*Q6F20S0W0.50-B5	28	14.00	355.6	4.01	101.9	4.01	101.9	141.8	2271.7	3277	1486	610	4.2
Averages		**14.00**	**355.6**	**4.01**	**101.9**	**4.01**	**101.9**	**141.8**	**2270.5**	**3616**	**1640**	**692**	**4.8**
*Q7F25S0W0.54-B6	28	14.00	355.6	4.02	102.2	4.01	101.9	141.6	2267.7	2954	1340	550	3.8
Q7F25S0W0.54-B5	28	14.00	355.6	4.01	102.0	4.01	102.0	141.7	2269.9	3571	1620	665	4.6
Q7F25S0W0.54-B8	28	14.00	355.6	4.02	102.1	4.01	102.0	141.6	2267.7	3431	1556	635	4.4
*Q7F25S0W0.54-B4	28	14.00	355.6	4.02	102.1	4.02	102.1	141.3	2263.7	3863	1752	715	4.9
Averages		**14.00**	**355.6**	**4.02**	**102.1**	**4.01**	**102.0**	**141.6**	**2267.2**	**3455**	**1567**	**650**	**4.5**
Q8F25S0W0.54-B8	28	14.00	355.6	4.02	102.1	4.03	102.3	144.8	2318.6	4578	2076	845	5.8
Q8F25S0W0.54-B2	28	14.00	355.6	4.01	101.9	4.02	102.1	145.4	2328.9	4666	2117	865	6.0
Q8F25S0W0.54-B3	28	14.00	355.6	4.01	101.9	4.02	102.1	145.4	2329.0	4520	2050	835	5.8
Q8F25S0W0.54-B7	28	14.00	355.6	4.01	102.0	4.02	102.2	149.1	2387.3	4754	2156	880	6.1
Averages		**14.00**	**355.6**	**4.02**	**102.0**	**4.02**	**102.2**	**146.2**	**2341.0**	**4630**	**2100**	**856**	**5.9**

Table A7: 28-Day Flexural Strength (Quartzite Aggregate)...continued

Spec. ID #	Age	Length		Breadth		Depth		Unit Weight		Maximum Load		Flexural Strength	
	days	in.	mm	in.	mm	in.	mm	pcf	kg/m^3	lbs	kgs	psi	Mpa
Q9F0S10W0.45-B5	28	14.00	355.6	4.02	102.0	4.02	102.0	145.4	2328.4	5539	2512	1025	7.1
Q9F0S10W0.45-B8	28	14.00	355.6	4.02	102.0	4.01	101.9	145.6	2331.3	5409	2454	1005	6.9
Q9F0S10W0.45-B6	28	14.00	355.6	4.01	102.0	4.02	102.0	149.3	2391.3	5289	2399	980	6.8
*Q9F0S10W0.45-B7	28	14.00	355.6	4.02	102.0	4.01	101.9	145.5	2330.6	5097	2312	945	6.5
Averages		**14.00**	**355.6**	**4.02**	**102.0**	**4.01**	**102.0**	**146.4**	**2345.4**	**5334**	**2419**	**1003**	**6.9**
Q10F0S12W0.46-B4	28	14.00	355.6	4.03	102.3	4.03	102.4	148.2	2373.1	5340	2422	980	6.8
Q10F0S12W0.46-B7	28	14.00	355.6	4.03	102.4	4.03	102.4	144.4	2312.9	5628	2553	1030	7.1
Q10F0S12W0.46-B8	28	14.00	355.6	4.03	102.4	4.03	102.4	148.2	2373.1	5518	2503	1010	7.0
*Q10F0S12W0.46-B6	28	14.00	355.6	4.03	102.4	4.03	102.3	148.2	2373.1	6496	2946	1190	8.2
Averages		**14.00**	**355.6**	**4.03**	**102.4**	**4.03**	**102.4**	**147.2**	**2358.0**	**5745**	**2606**	**1007**	**7.0**

Note: *Specimen not considered for the calculation of average value as it is an outlier.

Table A8: Mixture Designations for mixes with Limestone Aggregate

Mixture Designation	Description
L1CONTROLW0.4	Mix with no cement replacement : Control
L2F15S7W0.52	Mix with 7% of cement by weight replaced by silica fume and 15% by fly ash
L3F15S5W0.50	Mix with 5% of cement by weight replaced by silica fume and 15% by fly ash
L4F20S5W0.54	Mix with 5% of cement by weight replaced by silica fume and 20% by fly ash
L5F15S0W0.47	Mix with 15% of cement by weight replaced by fly ash
L6F20S0W0.50	Mix with 20% of cement by weight replaced by fly ash
L7F25S0W0.54	Mix with 25% of cement by weight replaced by fly ash
L8F0S7W0.43	Mix with 7% of cement by weight replaced by silica fume
L9F0S10W0.45	Mix with 10% of cement by weight replaced by silica fume
L10F0S12W0.46	Mix with 12% of cement by weight replaced by silica fume

Note: Multiplication factor of 1.2 used for volume correction for fly ash

Table A9: Mixture Proportions for Mixes with Limestone Aggregate

Mixture Designation	Mixture Proportions (lbs/cubic yard)						w/c	w/(c+f+sf)
	Cement pcy	Fly Ash pcy	Silica Fume pcy	Coarse Aggregate pcy	Fine Aggregate pcy	Water pcy		
L1CONTROLW0.4	655	0	0	1725	1100	264	0.40	0.40
L2F15S7W0.52	511	118	55	1725	1100	264	0.52	0.39
L3F15S5W0.50	524	118	39	1725	1100	264	0.50	0.39
L4F20S5W0.54	491	157	39	1725	1100	264	0.54	0.38
L5F15S0W0.47	557	118	0	1725	1100	264	0.47	0.39
L6F20S0W0.50	524	157	0	1725	1100	264	0.50	0.39
L7F25S0W0.54	491	197	0	1725	1100	264	0.54	0.38
L8F0S7W0.43	610	0	55	1725	1100	264	0.43	0.40
L9F0S10W0.45	590	0	78	1725	1100	264	0.45	0.40
L10F0S12W0.46	577	0	94	1725	1100	264	0.46	0.39

* Conversion Factor: pcy x 0.59 = kg/m^3

Table A10: Fresh Concrete Properties for Mixes with Limestone Aggregate

Mixture Designation	Unit Weight		Air	Slump	
	lbs/ft^3	kg/m^3	%	inches	mm
L1CONTROLW0.4	139.6	2236.0	9.6	7.25	184
L2F15S7W0.52	141.6	2268.0	6.2	5.50	140
L3F15S5W0.50	139.6	2236.0	8.0	8.00	203
L4F20S5W0.54	140.4	2248.8	7.4	7.00	178
L5F15S0W0.47	143.2	2293.6	6.2	7.50	191
L6F20S0W0.50	145.6	2332.1	5.2	6.00	152
L7F25S0W0.54	141.6	2268.0	6.8	7.00	178
L8F0S7W0.43	144.0	2306.4	6.4	4.88	124
L9F0S10W0.45	142.8	2287.2	5.6	4.50	114
L10F0S12W0.46	144.8	2319.3	5.2	3.00	76

Table A11: 14- Day Compressive Strength and Static Modulus (Limestone Aggregate)

Spec. ID #	Age days	Length in.	Length mm	Diameter in.	Diameter mm	Unit Weight pcf	Unit Weight Kg/m^3	Static Mod. psi $(x10^6)$	Static Mod. Mpa $(x10^4)$	Compressive Strength psi	Compressive Strength Mpa
L1CONTROLW0.4-C4	14	12.02	305.3	6.06	153.9	144.0	2305.8	5.3	3.6	5760	39.8
L1CONTROLW0.4-C1	14	12.02	305.2	6.06	153.8	143.3	2294.4	5.2	3.6	5415	37.4
Averages		**12.02**	**305.2**	**6.06**	**153.9**	**143.6**	**2300.1**	**5.2**	**3.6**	**5588**	**38.6**
L2F15S7W0.52-C5	14	12.02	305.2	6.02	152.9	142.2	2277.8	5.3	3.6	6380	44.1
L2F15S7W0.52-C6	14	12.01	305.1	6.02	153.0	143.9	2304.4	5.3	3.6	6385	44.1
L2F15S7W0.52-C4	14	12.01	305.1	6.02	153.0	143.9	2305.2	5.3	3.6	6460	44.6
Averages		**12.01**	**305.1**	**6.02**	**153.0**	**143.3**	**2295.8**	**5.3**	**3.6**	**6408**	**44.3**
L3F15S5W0.50-C4	14	12.02	305.2	6.02	153.0	143.8	2303.9	4.7	3.2	5300	36.6
L3F15S5W0.50-C5	14	12.02	305.3	6.02	153.0	143.8	2303.7	4.7	3.2	5440	37.6
L3F15S5W0.50-C6	14	12.02	305.2	6.02	153.0	141.3	2263.4	4.7	3.2	5265	36.4
Averages		**12.02**	**305.2**	**6.02**	**153.0**	**143.0**	**2290.3**	**4.7**	**3.2**	**5335**	**36.9**
L4F20S5W0.54-C6	14	12.01	305.1	6.03	153.2	141.1	2259.2	4.7	3.2	5095	35.2
L4F20S5W0.54-C4	14	12.01	305.1	6.03	153.2	143.4	2297.0	4.7	3.2	5070	35.0
L4F20S5W0.54-C3	14	12.00	304.8	6.03	153.2	141.1	2260.2	4.7	3.2	5075	35.1
Averages		**12.01**	**305.0**	**6.03**	**153.2**	**141.9**	**2272.1**	**4.7**	**3.2**	**5080**	**35.1**
L5F15S0W0.47-C4	14	12.01	305.1	6.02	153.0	141.4	2264.2	4.2	2.9	4390	30.3
L5F15S0W0.47-C5	14	12.01	305.1	6.03	153.2	143.6	2299.7	4.2	2.9	4395	30.4
*L5F15S0W0.47-C6	14	12.02	305.2	6.03	153.2	140.9	2257.3	4.2	2.9	4725	32.6
Averages		**12.01**	**305.1**	**6.03**	**153.1**	**142.0**	**2273.7**	**4.2**	**2.9**	**4393**	**30.4**

Table A11: 14- Day Compressive Strength and Static Modulus (Limestone Aggregate)….continued

Spec.	Age	Length		Diameter		Unit Weight		Static Mod. psi	Static Mod. Mpa	Compressive Strength	
ID #	days	in.	mm	in.	mm	pcf	Kg/m^3	(x10^6)	(x10^4)	psi	Mpa
L6F20S0W0.50-C3	14	12.02	305.2	6.02	152.9	144.1	2307.4	4.7	3.2	4955	34.2
L6F20S0W0.50-C1	14	12.01	305.1	6.02	152.8	146.8	2351.1	4.7	3.2	4890	33.8
*L6F20S0W0.50-C2	14	12.01	305.0	6.02	152.9	146.7	2349.9	4.7	3.2	4485	31.0
Averages		**12.01**	**305.1**	**6.02**	**152.8**	**145.9**	**2336.1**	**4.7**	**3.2**	**4923**	**34.0**
L7F25S0W0.54-C2	14	12.02	305.2	6.02	152.8	141.6	2268.2	4.7	3.2	4570	31.6
L7F25S0W0.54-C1	14	12.01	305.0	6.02	152.9	144.2	2309.5	4.7	3.2	4660	32.2
L7F25S0W0.54-C5	14	12.02	305.2	6.02	152.9	144.1	2308.0	4.7	3.2	4605	31.8
Averages		**12.01**	**305.1**	**6.02**	**152.8**	**143.3**	**2295.2**	**4.7**	**3.2**	**4612**	**31.9**
L8F0S7W0.43-C4	14	12.01	305.0	6.03	153.1	143.7	2301.6	5.3	3.6	6660	46.0
L8F0S7W0.43-C5	14	12.01	305.1	6.03	153.1	143.8	2302.6	5.3	3.6	6925	47.9
L8F0S7W0.43-C6	14	12.01	305.0	6.03	153.0	141.3	2263.8	5.3	3.6	6750	46.6
Averages		**12.01**	**305.0**	**6.03**	**153.1**	**142.9**	**2289.4**	**5.3**	**3.6**	**6778**	**46.8**
*L9F0S10W0.45-C3	14	12.01	305.1	6.02	152.9	141.6	2267.8	5.3	3.6	7345	50.8
L9F0S10W0.45-C1	14	12.01	305.0	6.02	152.8	144.3	2310.5	5.3	3.6	7125	49.2
L9F0S10W0.45-C2	14	12.01	305.1	6.02	152.9	146.7	2349.9	5.3	3.6	7175	49.6
Averages		**12.01**	**305.1**	**6.02**	**152.9**	**144.2**	**2309.4**	**5.3**	**3.6**	**7150**	**49.4**
L10F0S12W0.46-C1	14	12.01	305.1	6.02	152.8	149.3	2390.7	5.3	3.6	7560	52.2
L10F0S12W0.46-C3	14	12.01	305.1	6.02	152.9	149.2	2390.1	5.3	3.6	7560	52.2
*L10F0S12W0.46-C5	14	12.01	305.1	6.02	152.8	149.3	2390.7	5.3	3.6	7070	48.9
Averages		**12.01**	**305.1**	**6.02**	**152.8**	**149.2**	**2390.5**	**5.3**	**3.6**	**7560**	**52.2**

Note:* Specimen not considered for the calculation of average value as it is an outlier.

Table A12: 14-Day Flexural Strength (Limestone Aggregate)

Spec. ID #	Age	Length		Breadth		Depth		Unit Weight		Maximum Load		Flexural Strength	
	days	in.	mm	in.	mm	in.	mm	pcf	kg/m^3	lbs	kgs	psi	Mpa
L1CONTROLW0.4-B5	14	14.00	355.6	4.02	102.1	4.02	102.1	145.2	2325.1	4356.3	1976.0	805	5.6
*L1CONTROLW0.4-B6	14	14.00	355.6	4.02	102.2	4.02	102.2	144.9	2320.5	3819.4	1732.4	705	4.9
L1CONTROLW0.4-B3	14	14.00	355.6	4.02	102.1	4.02	102.1	145.1	2324.0	4737.3	2148.8	875	6.0
L1CONTROLW0.4-B2	14	14.00	355.6	4.02	102.1	4.02	102.2	145.0	2323.4	4658.9	2113.2	860	5.9
Averages		**14.00**	**355.6**	**4.02**	**102.1**	**4.02**	**102.2**	**145.0**	**2323.3**	**4393.0**	**1992.6**	**847**	**5.9**
*L2F15S7W0.52-B3	14	14.00	355.6	4.02	102.2	4.03	102.4	144.6	2315.8	5317.1	2411.8	975	6.7
L2F15S7W0.52-B4	14	14.00	355.6	4.03	102.3	4.03	102.4	144.4	2313.1	4466.6	2026.0	820	5.7
L2F15S7W0.52-B2	14	14.00	355.6	4.03	102.3	4.03	102.4	144.4	2313.6	4566.6	2071.4	840	5.8
L2F15S7W0.52-B1	14	14.00	355.6	4.03	102.3	4.03	102.4	144.4	2313.6	4466.6	2026.0	820	5.7
Averages		**14.00**	**355.6**	**4.03**	**102.3**	**4.03**	**102.4**	**144.5**	**2314.0**	**4704.2**	**2133.8**	**827**	**5.7**
L3F15S5W0.50-B5	14	14.00	355.6	4.04	102.5	4.04	102.7	143.8	2303.3	3998.6	1813.7	730	5.0
L3F15S5W0.50-B7	14	14.00	355.6	4.03	102.4	4.03	102.4	144.3	2311.8	4080.0	1850.7	750	5.2
L3F15S5W0.50-B6	14	14.00	355.6	4.03	102.4	4.04	102.5	147.9	2368.7	4215.1	1911.9	770	5.3
L3F15S5W0.50-B8	14	14.00	355.6	4.03	102.4	4.03	102.4	148.1	2372.7	4096.8	1858.3	750	5.2
Averages		**14.00**	**355.6**	**4.03**	**102.4**	**4.03**	**102.5**	**146.0**	**2339.2**	**4097.6**	**1858.6**	**750**	**5.2**
L4F20S5W0.54-B6	14	14.00	355.6	4.02	102.0	4.02	102.1	141.5	2266.8	3974.4	1802.8	735	5.1
*L4F20S5W0.54-B1	14	14.00	355.6	4.02	102.0	4.02	102.0	137.7	2205.5	4362.7	1978.9	810	5.6
L4F20S5W0.54-B5	14	14.00	355.6	4.02	102.1	4.02	102.2	137.4	2201.6	4224.1	1916.0	780	5.4
Averages		**14.00**	**355.6**	**4.02**	**102.0**	**4.02**	**102.1**	**138.9**	**2224.6**	**4187.1**	**1899.2**	**758**	**5.2**

Table A12: 14-Day Flexural Strength (Limestone Aggregate)...continued

Spec. ID #	Age	Length		Breadth		Depth		Unit Weight		Maximum Load		Flexural Strength	
	days	in.	mm	in.	mm	in.	mm	pcf	kg/m^3	lbs	kgs	psi	Mpa
*L5F15S0W0.47-B1	14	14.00	355.6	4.02	102.0	4.02	102.2	149.0	2386.1	3944.3	1789.1	730	5.0
L5F15S0W0.47-B2	14	14.00	355.6	4.02	102.2	4.02	102.1	144.9	2321.5	4522.2	2051.2	835	5.8
L5F15S0W0.47-B3	14	14.00	355.6	4.02	102.1	4.02	102.2	145.0	2322.6	4655.3	2111.6	860	5.9
L5F15S0W0.47-B4	14	14.00	355.6	4.03	102.2	4.02	102.1	145.0	2322.0	4522.2	2051.2	835	5.8
Averages		**14.00**	**355.6**	**4.02**	**102.2**	**4.02**	**102.1**	**146.0**	**2338.0**	**4411.0**	**2000.8**	**843**	**5.8**
L6F20S0W0.50-B7	14	14.00	355.6	4.03	102.3	4.04	102.5	148.0	2371.2	4397.3	1994.6	805	5.6
*L6F20S0W0.50-B8	14	14.00	355.6	4.03	102.3	4.03	102.4	144.4	2313.3	5007.2	2271.2	920	6.4
*L6F20S0W0.50-B6	14	14.00	355.6	4.03	102.5	4.03	102.3	144.3	2311.1	5198.6	2358.0	950	6.6
L6F20S0W0.50-B5	14	14.00	355.6	4.02	102.0	4.03	102.2	145.1	2323.7	4572.3	2074.0	845	5.8
Averages		**14.00**	**355.6**	**4.03**	**102.3**	**4.03**	**102.4**	**145.5**	**2329.8**	**4793.9**	**2174.5**	**825**	**5.7**
*L7F25S0W0.54-B3	14	14.00	355.6	4.04	102.7	4.04	102.7	147.3	2359.0	5188.6	2353.5	940	6.5
L7F25S0W0.54-B2	14	14.00	355.6	4.05	102.9	4.04	102.6	139.5	2234.7	4372.7	1983.4	795	5.5
L7F25S0W0.54-B1	14	14.00	355.6	4.05	102.8	4.04	102.7	143.8	2303.7	4679.0	2122.4	850	5.9
L7F25S0W0.54-B4	14	14.00	355.6	4.04	102.7	4.04	102.5	143.8	2303.1	4281.6	1942.1	780	5.4
Averages		**14.00**	**355.6**	**4.05**	**102.8**	**4.04**	**102.6**	**143.6**	**2300.1**	**4630.5**	**2100.3**	**808**	**5.6**
*L8F0S7W0.43-B4	14	14.00	355.6	4.03	102.3	4.03	102.3	144.6	2315.7	5601.5	2540.8	1030	7.1
*L8F0S7W0.43-B3	14	14.00	355.6	4.03	102.4	4.03	102.3	148.3	2376.0	5775.6	2619.8	1060	7.3
L8F0S7W0.43-B2	14	14.00	355.6	4.03	102.3	4.03	102.3	140.7	2254.2	5002.6	2269.1	915	6.3
L8F0S7W0.43-B1	14	14.00	355.6	4.02	102.2	4.03	102.3	144.7	2317.3	4892.3	2219.1	900	6.2
Averages		**14.00**	**355.6**	**4.03**	**102.3**	**4.03**	**102.3**	**144.6**	**2315.8**	**5318.0**	**2412.2**	**908**	**6.3**

Table A12: 14-Day Flexural Strength (Limestone Aggregate)...continued

Spec. ID #	Age	Length		Breadth		Depth		Unit Weight		Maximum Load		Flexural Strength	
	days	in.	mm	in.	mm	in.	mm	pcf	kg/m^3	lbs	kgs	psi	Mpa
L9F0S10W0.45-B1	14	14.00	355.6	4.03	102.3	4.03	102.4	148.2	2373.1	5459.3	2476.3	1000	6.9
L9F0S10W0.45-B2	14	14.00	355.6	4.03	102.4	4.04	102.5	148.0	2370.2	5215.0	2365.5	955	6.6
L9F0S10W0.45-B3	14	14.00	355.6	4.02	102.1	4.03	102.2	144.9	2321.3	5026.4	2279.9	930	6.4
L9F0S10W0.45-B4	14	14.00	355.6	4.02	102.1	4.02	102.2	145.0	2322.0	4862.2	2205.5	900	6.2
Averages		**14.00**	**355.6**	**4.02**	**102.2**	**4.03**	**102.3**	**146.5**	**2346.7**	**5140.7**	**2331.8**	**928**	**6.4**
L10F0S12W0.46-B2	14	14.00	355.6	4.02	102.2	4.02	102.0	141.3	2263.7	5495.8	2492.9	1015	7.0
L10F0S12W0.46-B3	14	14.00	355.6	4.02	102.2	4.02	102.1	145.0	2322.0	6148.4	2788.9	1135	7.8
L10F0S12W0.46-B4	14	14.00	355.6	4.02	102.2	4.01	101.9	141.5	2265.9	5312.5	2409.7	985	6.8
L10F0S12W0.46-B1	14	14.00	355.6	4.02	102.2	4.02	102.2	144.9	2320.9	6293.0	2854.5	1160	8.0
Averages		**14.00**	**355.6**	**4.02**	**102.2**	**4.02**	**102.0**	**143.2**	**2293.1**	**5812.4**	**2636.5**	**1074**	**7.4**

Note: *Specimen not considered for calculation of average value as it is an outlier.

Table A13: 28- Day Compressive Strength and Static Modulus (Limestone Aggregate)

Spec. ID #	Age	Length		Diameter		Unit Weight		Static Mod. psi	Static Mod. Mpa	Compressive Strength	
	days	in.	mm	in.	mm	pcf	Kg/m^3	(x10^6)	(x10^4)	psi	Mpa
L1CONTROLW0.4-C3	28	12.01	305.1	6.01	152.7	141.9	2273.1	5.3	3.6	6005	41.5
L1CONTROLW0.4-C2	28	12.01	305.1	6.02	152.9	144.1	2308.5	5.3	3.6	6135	42.4
Averages		**12.01**	**305.1**	**6.02**	**152.8**	**143.0**	**2290.8**	**5.3**	**3.6**	**6070**	**41.9**
L2F15S7W0.52-C1	28	12.00	304.9	6.02	152.8	144.4	2312.1	5.3	3.6	8445	58.4
L2F15S7W0.52-C2	28	12.01	305.1	6.02	152.9	141.5	2266.1	5.3	3.6	8150	56.3
L2F15S7W0.52-C3	28	12.01	305.0	6.02	152.9	144.1	2307.2	5.3	3.6	8255	57.0
Averages		**12.01**	**305.0**	**6.02**	**152.9**	**143.3**	**2295.1**	**5.3**	**3.6**	**8283**	**57.2**
L3F15S5W0.50-C1	28	12.02	305.2	6.02	152.9	144.0	2305.6	5.3	3.6	5795	40.0
*L3F15S5W0.50-C2	28	12.01	305.1	6.02	152.9	141.5	2266.9	5.3	3.6	4955	34.2
L3F15S5W0.50-C3	28	12.02	305.3	6.02	152.8	144.2	2309.3	5.3	3.6	5860	40.5
Averages		**12.02**	**305.2**	**6.02**	**152.9**	**143.2**	**2294.0**	**5.3**	**3.6**	**5828**	**40.3**
L4F20S5W0.54-C1	28	12.01	305.1	6.01	152.7	141.9	2273.1	4.7	3.2	6060	41.9
*L4F20S5W0.54-C5	28	12.01	305.1	6.01	152.7	141.9	2272.7	4.7	3.2	5725	39.6
L4F20S5W0.54-C2	28	12.01	305.1	6.01	152.7	142.0	2274.4	4.7	3.2	6080	42.0
Averages		**12.01**	**305.1**	**6.01**	**152.7**	**141.9**	**2273.4**	**4.7**	**3.2**	**6070**	**41.9**
*L5F15S0W0.47-C3	28	12.01	305.0	6.02	152.8	141.7	2270.2	5.3	3.6	4855	33.5
L5F15S0W0.47-C2	28	12.02	305.2	6.02	152.9	144.0	2305.8	5.3	3.6	5270	36.4
L5F15S0W0.47-C1	28	12.02	305.3	6.02	152.9	141.4	2265.0	5.3	3.6	5270	36.4
Averages		**12.01**	**305.1**	**6.02**	**152.9**	**142.4**	**2280.3**	**5.3**	**3.6**	**5270**	**36.4**

Table A13: 28- Day Compressive Strength and Static Modulus (Limestone Aggregate)…continued

Spec. ID #	Age	Length		Diameter		Unit Weight		Static Mod.		Compressive Strength	
								psi	Mpa		
	days	in.	mm	in.	mm	pcf	Kg/m^3	(x10^6)	(x10^4)	psi	Mpa
L6F20S0W0.50-C4	28	12.01	305.1	6.02	152.8	146.8	2351.1	5.3	3.6	5490	37.9
L6F20S0W0.50-C6	28	12.02	305.2	6.02	152.8	146.7	2349.4	5.3	3.6	5630	38.9
L6F20S0W0.50-C5	28	12.01	305.1	6.02	152.9	146.7	2349.7	5.3	3.6	5365	37.1
Averages		**12.01**	**305.1**	**6.02**	**152.8**	**146.7**	**2350.1**	**5.3**	**3.6**	**5495**	**38.0**
L7F25S0W0.54-C4	28	12.01	305.1	6.02	152.9	144.2	2309.3	4.7	3.2	5485	37.9
L7F25S0W0.54-C3	28	12.02	305.3	6.02	153.0	143.9	2304.7	4.7	3.2	5265	36.4
L7F25S0W0.54-C6	28	12.01	305.0	6.02	152.9	146.8	2350.5	4.7	3.2	5415	37.4
Averages		**12.01**	**305.1**	**6.02**	**152.9**	**144.9**	**2321.5**	**4.7**	**3.2**	**5388**	**37.2**
*L8F0S7W0.43-C2	28	12.01	305.2	6.02	152.9	144.0	2305.8	5.3	3.6	8500	58.7
L8F0S7W0.43-C1	28	12.02	305.2	6.02	152.8	144.2	2308.9	5.3	3.6	8090	55.9
L8F0S7W0.43-C3	28	12.01	305.1	6.02	153.0	144.0	2306.0	5.3	3.6	7710	53.3
Averages		**12.01**	**305.2**	**6.02**	**152.9**	**144.0**	**2306.9**	**5.3**	**3.6**	**7900**	**54.6**
L9F0S10W0.45-C4	28	12.02	305.2	6.02	152.9	144.1	2307.6	5.3	3.6	8225	56.8
L9F0S10W0.45-C6	28	12.02	305.2	6.02	152.9	146.6	2347.8	5.3	3.6	8350	57.7
L9F0S10W0.45-C5	28	12.01	305.1	6.02	152.9	149.2	2390.1	5.7	3.9	8440	58.3
Averages		**12.01**	**305.2**	**6.02**	**152.9**	**146.6**	**2348.5**	**5.4**	**3.7**	**8338**	**57.6**
L10F0S12W0.46-C2	28	12.01	305.1	6.02	152.9	146.6	2347.5	6.0	4.2	8515	58.8
L10F0S12W0.46-C6	28	12.01	305.1	6.02	152.9	146.7	2349.4	6.0	4.2	8860	61.2
L10F0S12W0.46-C4	28	12.02	305.2	6.02	152.9	146.6	2347.3	6.0	4.2	8715	60.2
Averages		**12.01**	**305.1**	**6.02**	**152.9**	**146.6**	**2348.0**	**6.0**	**4.2**	**8697**	**60.1**

Note: *Specimen not considered for the calculation of average value as it is an outlier.

Table A14: 28-Day Flexural Strength (Limestone Aggregate)

Spec. ID #	Age	Length		Breadth		Depth		Unit Weight		Maximum Load		Flexural Strength	
	days	in.	mm	in.	mm	in.	mm	pcf	kg/m^3	lbs	kgs	psi	Mpa
L1CONTROLW0.4-B8	28	14.00	355.6	4.02	102.1	4.02	102.2	141.2	2262.3	4655.3	2111.6	860	5.9
L1CONTROLW0.4-B4	28	14.00	355.6	4.02	102.1	4.02	102.1	141.3	2263.9	4923.3	2233.2	910	6.3
*L1CONTROLW0.4-B1	28	14.00	355.6	4.02	102.1	4.03	102.3	141.2	2261.2	4364.5	1979.7	805	5.6
L1CONTROLW0.4-B7	28	14.00	355.6	4.02	102.1	4.02	102.1	145.2	2325.8	4703.6	2133.5	870	6.0
Averages		**14.00**	**355.6**	**4.02**	**102.1**	**4.02**	**102.2**	**142.2**	**2278.3**	**4661.7**	**2114.5**	**880**	**6.1**
*L2F15S7W0.52-B6	28	14.00	355.6	4.03	102.2	4.03	102.4	140.7	2254.3	6028.1	2734.3	1105	7.6
L2F15S7W0.52-B7	28	14.00	355.6	4.03	102.3	4.02	102.0	145.0	2322.9	5105.6	2315.9	945	6.5
L2F15S7W0.52-B5	28	14.00	355.6	4.03	102.4	4.04	102.7	136.3	2183.7	5350.8	2427.1	975	6.7
L2F15S7W0.52-B8	28	14.00	355.6	4.02	102.2	4.03	102.3	148.5	2379.3	5102.9	2314.6	940	6.5
Averages		**14.00**	**355.6**	**4.03**	**102.3**	**4.03**	**102.4**	**142.6**	**2285.0**	**5396.9**	**2448.0**	**953**	**6.6**
L3F15S5W0.50-B4	28	14.00	355.6	4.02	102.0	4.01	101.9	141.7	2270.2	5390.9	2445.3	1000	6.9
*L3F15S5W0.50-B3	28	14.00	355.6	4.02	102.0	4.01	101.8	141.9	2273.1	8049.0	3651.0	1495	10.3
L3F15S5W0.50-B2	28	14.00	355.6	4.02	102.1	4.02	102.2	145.0	2323.4	4684.5	2124.9	865	6.0
L3F15S5W0.50-B1	28	14.00	355.6	4.02	102.2	4.02	102.1	148.8	2384.1	4733.7	2147.2	875	6.0
Averages		**14.00**	**355.6**	**4.02**	**102.1**	**4.02**	**102.0**	**144.4**	**2312.7**	**5714.5**	**2592.1**	**913**	**6.3**
L4F20S5W0.54-B4	28	14.00	355.6	4.02	102.1	4.03	102.4	141.0	2257.9	4889.0	2217.6	900	6.2
*L4F20S5W0.54-B8	28	14.00	355.6	4.02	102.1	4.02	102.1	141.4	2265.1	4720.0	2141.0	875	6.0
L4F20S5W0.54-B3	28	14.00	355.6	4.02	102.1	4.02	102.1	141.4	2265.1	5050.0	2290.6	935	6.5
L4F20S5W0.54-B7	28	14.00	355.6	4.02	102.1	4.03	102.4	141.0	2257.9	5124.0	2324.2	940	6.5
Averages		**14.00**	**355.6**	**4.02**	**102.1**	**4.02**	**102.2**	**141.3**	**2262.7**	**4886.3**	**2216.4**	**925**	**6.4**

Table A14: 28-Day Flexural Strength (Limestone Aggregate) …..continued

Spec. ID #	Age	Length		Breadth		Depth		Unit Weight		Maximum Load		Flexural Strength	
	days	in.	mm	in.	mm	in.	mm	pcf	kg/m^3	lbs	kgs	psi	Mpa
L5F15S0W0.47-B7	28	14.00	355.6	4.03	102.3	4.01	101.9	145.2	2324.9	4824.0	2188.1	890	6.1
*L5F15S0W0.47-B6	28	14.00	355.6	4.02	102.1	4.02	102.0	141.4	2265.4	3798.0	1722.7	705	4.9
*L5F15S0W0.47-B8	28	14.00	355.6	4.02	102.2	4.04	102.6	148.1	2372.0	4058.0	1840.7	745	5.1
L5F15S0W0.47-B5	28	14.00	355.6	4.02	102.1	4.01	101.9	149.2	2390.4	4334.0	1965.9	800	5.5
Averages		**14.00**	**355.6**	**4.02**	**102.2**	**4.02**	**102.1**	**146.0**	**2338.2**	**4253.5**	**1929.4**	**845**	**5.8**
L6F20S0W0.50-B1	28	14.00	355.6	4.02	102.0	4.01	101.8	145.7	2333.0	4688.0	2126.4	870	6.0
L6F20S0W0.50-B3	28	14.00	355.6	4.01	101.9	4.01	101.9	149.4	2393.3	5100.0	2313.3	945	6.5
L6F20S0W0.50-B2	28	14.00	355.6	4.01	102.0	4.01	101.9	145.7	2333.0	4692.7	2128.6	870	6.0
*L6F20S0W0.50-B4	28	14.00	355.6	4.02	102.1	4.01	101.9	145.3	2327.8	4320.0	1959.5	800	5.5
Averages		**14.00**	**355.6**	**4.02**	**102.0**	**4.01**	**101.9**	**146.5**	**2346.8**	**4700.2**	**2132.0**	**895**	**6.2**
L7F25S0W0.54-B8	28	14.00	355.6	4.02	102.2	4.02	102.0	148.9	2384.9	4768.3	2162.9	880	6.1
*L7F25S0W0.54-B5	28	14.00	355.6	4.02	102.1	4.02	102.2	148.8	2383.2	5199.5	2358.5	960	6.6
L7F25S0W0.54-B6	28	14.00	355.6	4.02	102.1	4.02	102.1	145.2	2324.9	4838.5	2194.7	895	6.2
*L7F25S0W0.54-B7	28	14.00	355.6	4.02	102.1	4.02	102.0	149.0	2387.2	4530.4	2055.0	840	5.8
Averages		**14.00**	**355.6**	**4.02**	**102.1**	**4.02**	**102.1**	**148.0**	**2370.0**	**4834.2**	**2192.7**	**888**	**6.1**
L8F0S7W0.43-B5	28	14.00	355.6	4.02	102.2	4.02	102.0	149.0	2386.1	5717.3	2593.3	1055	7.3
*L8F0S7W0.43-B6	28	14.00	355.6	4.03	102.3	4.02	102.0	145.0	2323.1	5041.8	2286.9	930	6.4
*L8F0S7W0.43-B7	28	14.00	355.6	4.02	102.2	4.02	102.0	145.2	2325.5	6104.7	2769.0	1130	7.8
L8F0S7W0.43-B8	28	14.00	355.6	4.02	102.2	4.02	102.0	141.4	2264.3	5891.4	2672.3	1090	7.5
Averages		**14.00**	**355.6**	**4.02**	**102.2**	**4.02**	**102.0**	**145.1**	**2324.7**	**5688.8**	**2580.4**	**1073**	**7.4**

Table A14: 28-Day Flexural Strength (Limestone Aggregate) …..continued

Spec. ID #	Age	Length		Breadth		Depth		Unit Weight		Maximum Load		Flexural Strength	
	days	in.	mm	in.	mm	in.	mm	pcf	kg/m^3	lbs	kgs	psi	Mpa
L9F0S10W0.45-B8	28	14.00	355.6	4.02	102.1	4.02	102.1	148.9	2385.4	5378.2	2439.5	990	6.8
*L9F0S10W0.45-B6	28	14.00	355.6	4.02	102.1	4.02	102.1	145.1	2324.4	6280.6	2848.8	1160	8.0
L9F0S10W0.45-B7	28	14.00	355.6	4.02	102.1	4.02	102.1	145.1	2323.7	5393.7	2446.5	995	6.9
L9F0S10W0.45-B5	28	14.00	355.6	4.02	102.1	4.02	102.1	148.9	2385.4	5222.3	2368.8	965	6.7
Averages		**14.00**	**355.6**	**4.02**	**102.1**	**4.02**	**102.1**	**147.0**	**2354.7**	**5568.7**	**2525.9**	**983**	**6.8**
L10F0S12W0.46-B7	28	14.00	355.6	4.02	102.1	4.03	102.3	152.4	2441.2	5743.0	2605.0	1055	7.3
L10F0S12W0.46-B8	28	14.00	355.6	4.02	102.1	4.02	102.2	148.8	2383.8	6265.0	2841.8	1160	8.0
*L10F0S12W0.46-B5	28	14.00	355.6	4.02	102.2	4.02	102.2	152.5	2441.8	5425.0	2460.7	1000	6.9
L10F0S12W0.46-B6	28	14.00	355.6	4.02	102.1	4.01	101.9	153.0	2450.3	5625.4	2551.6	1040	7.2
Averages		**14.00**	**355.6**	**4.02**	**102.1**	**4.02**	**102.2**	**151.7**	**2429.3**	**5764.6**	**2614.8**	**1085**	**7.5**

Note: *Specimen not considered for the calculation of average value as it is an outlier.

Table A15: Chloride Permeability of Quartzite Mixes

Mix Id:	Age (days)	w/c	Cement		Fly Ash		Silica Fume		Air %	Coulombs	Average of Spec.	Cure History
			pcy	kg/m^3	pcy	kg/m^3	pcy	kg/m^3				
Q1CONTROLW0.4	14	0.403	655.0	388.4	0.0	0.0	0.0	0.0	8.0	7941	4	14 days continuos moist curing
Q2F15S7W0.52	14	0.403	655.0	388.4	118.0	70.0	55.0	32.6	5.4	6679	3	14 days continuos moist curing
Q3F15S5W0.50	17	0.403	524.0	310.7	118.0	70.0	39.0	23.1	4.4	3276	3	17 days continuos moist curing
Q4F20S5W0.54	16	0.403	491.0	291.2	157.0	93.1	39.0	23.1	6.8	6880	2	16 days continuos moist curing
Q5F15S0W0.47	15	0.403	557.0	330.3	118.0	70.0	0.0	0.0	7.0	10744	2	15 days continuos moist curing
Q6F20S0W0.50	14	0.403	524.0	310.7	157.0	93.1	0.0	0.0	7.2	11143	3	14 days continuos moist curing
Q7F25S0W0.54	14	0.403	491.0	291.2	197.0	116.8	0.0	0.0	7.6	14317	3	14 days continuos moist curing
Q1CONTROLW0.4	28	0.403	655.0	388.4	0.0	0.0	0.0	0.0	8.0	5719	3	28 days continuos moist curing
Q1CONTROLW0.4	37	0.403	655.0	388.4	0.0	0.0	0.0	0.0	8.0	5566	3	14 days continuos moist curing + air dried for 22 days + 1 day accelerated curing
Q2F15S7W0.52	47	0.403	655.0	388.4	118.0	70.0	55.0	32.6	5.4	533	2	Continuously moist cured for 28 days+air-dried for 7 days+12 day accelerated curing
Q2F15S7W0.52	43	0.403	655.0	388.4	118.0	70.0	55.0	32.6	5.4	713	2	Continuously moist cured for 28 days+air-dried for 7 days+12 day accelerated curing
Q3F15S5W0.50	51	0.403	524.0	310.7	118.0	70.0	39.0	23.1	4.4	1337	2	Continuously moist cured for 44 days + 7 days accelerated curing
Q4F20S5W0.54	49	0.403	491.0	291.2	157.0	93.1	39.0	23.1	6.8	1599	2	Continuously moist cured for 42 days + 7 days accelerated curing
Q5F15S0W0.47	48	0.403	557.0	330.3	118.0	70.0	0.0	0.0	7.0	4088	4	Continuously moist cured for 41 days + 7 days accelerated curing

Table A15: Chloride Permeability of Quartzite Mixes (...continued)

Mix Id:	Age (Days)	w/c	Cement		Fly Ash		Silica Fume		Air %	Coulombs	Average of Spec.	Cure History
			pcy	kg/m^3	pcy	kg/m^3	pcy	kg/m^3				
Q6F20S0W0.50	47	0.403	524.0	310.7	157.0	93.1	0.0	0.0	7.2	4548	2	Continuously moist cured for 40 days + 7 days accelerated curing
Q7F25S0W0.54	45	0.403	491.0	291.2	197.0	116.8	0.0	0.0	7.6	4059	3	Continuously moist cured for 38 days + 7 days accelerated curing
Q8F0S7W0.43	44	0.403	655.0	388.4	0.0	0.0	55.0	32.6	7.6	1642	3	Continuously moist cured for 39 days + 5 days accelerated curing
Q9F0S10W0.45	45	0.403	590.0	349.9	0.0	0.0	78.0	46.3	4.8	692	4	Continuously moist cured for 38 days + 7 days accelerated curing
Q10F0S12W0.46	43	0.403	577.0	342.2	0.0	0.0	94.0	55.7	4.4	132	3	Continuously moist cured for 36 days + 7 days accelerated curing

Conversion Factor:

1pcy = 0.593 * kg/m^3

Table A16: Chloride Permeability of Limestone Mixes

Mix Id:	Age days	w/c	Cement		Fly Ash		Silica Fume		Air %	Coulombs	Avg. of Spec.	ASTM Category	Cure History
			pcy	kg/m^3	pcy	kg/m^3	pcy	kg/m^3					
L1CONTROLW0.4	4	0.403	655.0	388.4	0.0	0.0	0.0	0.0	9.6	6340	3	High	3 days in water at 51 C
L2F15S7W0.52	4	0.403	655.0	388.4	118.0	70.0	55.0	32.6	6.2	481	2	Very Low	3 days in water at 46 C
L3F15S5W0.50	4	0.403	524.0	310.7	118.0	70.0	39.0	23.1	6.2	4478	2	High	3 days in water at 34 C
L4F20S5W0.54	5	0.403	491.0	291.2	157.0	93.1	39.0	23.1	7.4	2703	3	Moderate	3 days in water at 35 C
L5F15S0W0.47	4	0.403	557.0	330.3	118.0	70.0	0.0	0.0	6.2	4979	3	High	3 days in water at 40 C
L6F20S0W0.50	4	0.403	524.0	310.7	157.0	93.1	0.0	0.0	5.2	7249	3	High	3 days in water at 43 C
L7F25S0W0.54	4	0.403	491.0	291.2	197.0	116.8	0.0	0.0	6.8	7232	3	High	3 days in water at 44 C
L8F0S7W0.43	4	0.403	610.0	361.7	0.0	0.0	55.0	32.6	6.4	1089	3	Low	3 days in water at 44 C
L9F0S10W0.45	6	0.403	590.0	349.9	0.0	0.0	78.0	46.3	5.6	574	3	Very Low	5 days in water at 44 C
L10F0S12W0.46	5	0.403	577.0	342.2	0.0	0.0	94.0	55.7	5.2	354	3	Very Low	4 days in water at 44 C

Note :
Conversion Factor : I pcy = 0.593 x kg/m^3

Table A17: Chloride Permeability of Quartzite Mixes - 90 day tests

Mix Id:	Age days	w/c	Cement		Fly Ash		Silica Fume		Air %	Coulombs	Avg. of Spec.	ASTM Category	Cure History
			pcy	kg/m^3	pcy	kg/m^3	pcy	kg/m^3					
Q1CONTROLW0.4	97	0.403	655.0	388.4	0.0	0.0	0.0	0.0	8.0	4158	3	High	Continuously moist cured in water for 75 days:air dried for 22 days
Q2F15S7W0.52	102	0.403	655.0	388.4	118.0	70.0	55.0	32.6	8.0	1207	2	Low	Continuously moist cured in water for 73 days:air dried for 29 days
Q3F15S5W0.50	100	0.403	524.0	310.7	118.0	70.0	39.0	23.1	4.4	1219	3	Low	Continuously moist cured in water for 71 days:air dried for 29 days
Q4F20S5W0.54	100	0.403	491.0	291.2	157.0	93.1	39.0	23.1	6.8	1774	3	Low	Continuously moist cured in water for 69 days:air dried for 31 days
Q5F15S0W0.47	98	0.403	557.0	330.3	118.0	70.0	0.0	0.0	7.0	3475	2	Moderate	Continuously moist cured in water for 67 days:air dried for 31 days
Q6F20S0W0.50	99	0.403	524.0	310.7	157.0	93.1	0.0	0.0	7.2	6831	2	High	Continuously moist cured in water for 65 days:air dried for 34 days
Q7F25S0W0.54	96	0.403	491.0	291.2	197.0	116.8	0.0	0.0	7.6	4704	3	High	Continuously moist cured in water for 62 days:air dried for 34 days
Q8F0S7W0.43	97	0.403	610.0	361.7	0.0	0.0	55.0	32.6	5.8	1943	2	Low	Continuously moist cured in water for 60 days:air dried for 37 days
Q9F0S10W0.45	95	0.403	590.0	349.9	0.0	0.0	78.0	46.3	4.8	812	2	Very Low	Continuously moist cured in water for 58 days:air dried for 37 days
Q10F0S12W0.46	98	0.403	577.0	342.2	0.0	0.0	94.0	55.7	4.4	323	4	Very Low	Continuously moist cured in water for 55 days:air dried for 43 days

Note :
Conversion Factor : I pcy = 0.593 x kg/m^3

Table A18: Chloride Permeability of Limestone Mixes at 90-day

Mix ID:	Age (Days)	w/c	Cement		Fly Ash		Silica Fume		Air %	Coulombs	Avg. of Spec.	ASTM Category	Cure History
			pcy	kg/m^3	pcy	kg/m^3	pcy	kg/m^3					
L1CONTROLW0.4	96	0.403	655.0	388.4	0.0	0.0	0.0	0.0	9.6	6577	2	High	Continuously moist cured in water for 28 days:air dried for 68 days
L2F15S7W0.52	96	0.403	655.0	388.4	118.0	70.0	55.0	32.6	6.2	430	2	Very Low	Continuously moist cured in water for 28 days:air dried for 68 days
L3F15S5W0.50	95	0.403	524.0	310.7	118.0	70.0	39.0	23.1	8.0	615	3	Very Low	Continuously moist cured in water for 28 days:air dried for 67 days
L4F20S5W0.54	99	0.403	491.0	291.2	157.0	93.1	39.0	23.1	7.4	1785	3	Low	Continuously moist cured in water for 28 days:air dried for 71 days
L5F15S0W0.47	95	0.403	557.0	330.3	118.0	70.0	0.0	0.0	8.0	3553	3	Moderate	Continuously moist cured in water for 28 days:air dried for 67 days
L6F20S0W0.50	145	0.403	524.0	310.7	157.0	93.1	0.0	0.0	5.2	1455	3	Low	Continuously moist cured in water for 28 days:air dried for 117 days
L7F25S0W0.54	143	0.403	491.0	291.2	197.0	116.8	0.0	0.0	6.8	986	3	Very Low	Continuously moist cured in water for 28 days:air dried for 115 days
L8F0S7W0.43	154	0.403	610.0	361.7	0.0	0.0	55.0	32.6	6.8	685	4	Very Low	Continuously moist cured in water for 28 days:air dried for 126 days
L9F0S10W0.45	152	0.403	590.0	349.9	0.0	0.0	78.0	46.3	5.6	511	3	Very Low	Continuously moist cured in water for 28 days:air dried for 124 days
L10F0S12W0.46	154	0.403	577.0	342.2	0.0	0.0	94.0	55.7	5.2	373	4	Very Low	Continuously moist cured in water for 28 days:air dried for 126 days

Note :
Conversion Factor : I pcy = 0.593 x kg/m^3

Chloride Permeability

The results of all tests conducted for chloride permeability are tabulated in Tables A15 and A17 and bar charts are shown in Figures 3.19, 3.21, 3.23 (Chapter 3). Initially it was expected that a significant reduction in chloride permeability would occur between the ages of 14 and 28-day. Mixes Q1CONTROLW0.4 through Q7F25S0W0.54 were tested after being subjected to 14 days of normal moist curing in cold water and mix Q1CONTROLW0.4 was also subjected to 28-day testing under the same conditions of curing. As can be seen from the results of the tests on mix Q1CONTROLW0.4 (Table A15, Appendix A), which showed 7941, and 5719 coulombs at 14 and 28-day (both high values). These values were considerably higher than the normal values because sufficient curing and drying did not take place. Therefore it was decided to subject the specimens to accelerated curing for seven days before testing and the results are given in Table A15, Appendix A.

The same concretes were subjected to rapid chloride permeability tests again after 90-day curing. The specimens were subjected to an average of 28 days of continuos moist curing and then air-dried till they reached an age of 90-days. They were then tested for chloride permeability. The results of these tests are tabulated in Table A17, Appendix A. The bar charts for the permeability values obtained are shown in Figure 3.21, Chapter 3. A comparative analysis of the results of the accelerated curing and 90-day test results shows a good correlation (Q2F15S7W0.52, Q3F15S5W0.50, Q4F20S5W0.54, Q8F0S7W0.43, Q9F0S10W0.45, Q10F0S12W0.46). The comparative bar charts are shown in Figure 3.23, Chapter 3.

STATISTICAL MODELS

Probability distributions are useful for modeling and analyzing real-world process. In some cases theoretical distributions closely fits the historical data that has been collected about a process. In other cases we make judgements about the fundamental nature of the process and choose an appropriate theoretical distribution without collecting data. The field of statistics concerned with making inferences about populations and population characteristics. Experiments are conducted with results that are subject to changes. The compression testing of a number of concrete cylinders is an example of a ‘statistical experiment’; a term that is used to describe any process by which

Table C4: 95% Confidence Region for Predicting Y given X

X	Y	Upper Band	Lower Band
2.60	2.35	2.80	1.91
2.85	2.66	3.06	2.26
3.02	2.87	3.25	2.49
3.21	3.10	3.47	2.73
3.32	3.24	3.60	2.87
3.45	3.39	3.77	3.02
3.56	3.53	3.91	3.15
3.62	3.60	3.99	3.22
3.71	3.71	4.11	3.32
3.81	3.84	4.24	3.43

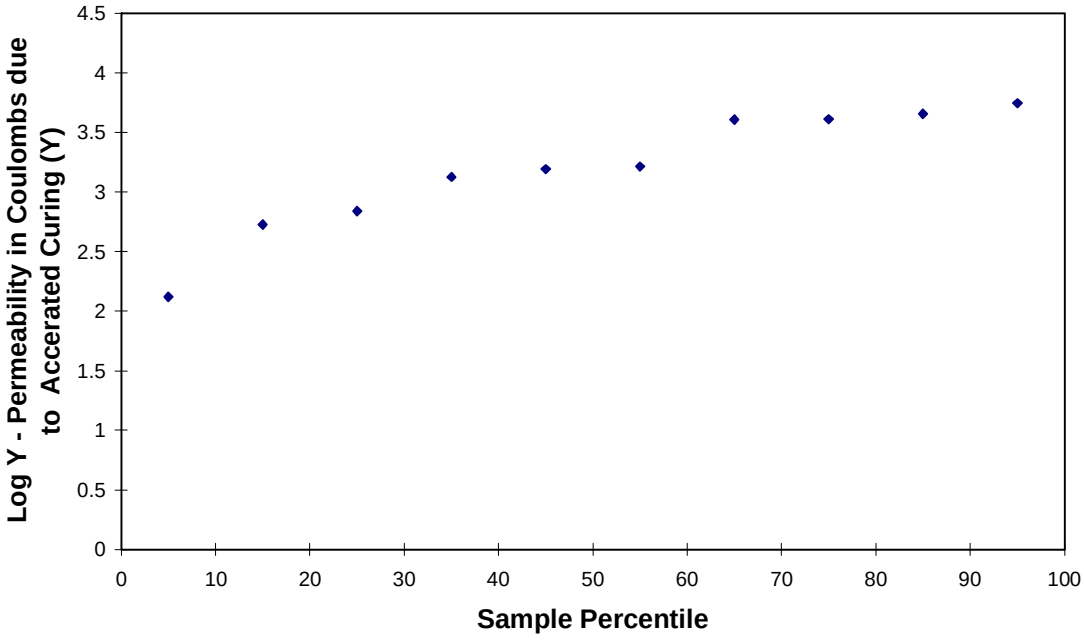

Fig C1: Normal Probability Plot of Residuals

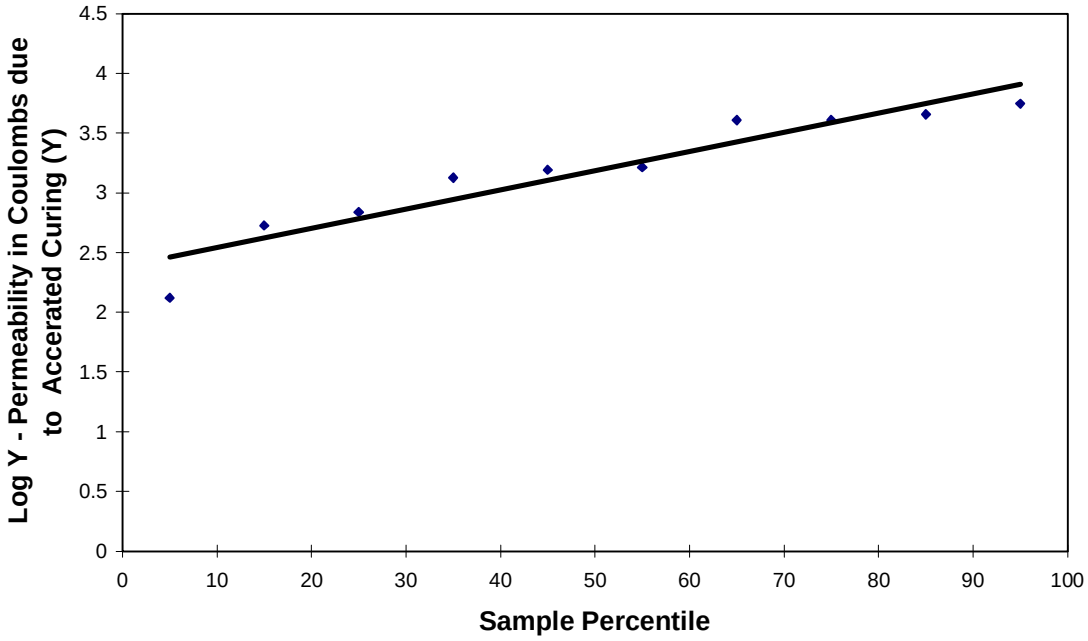

Fig C2: Fat Pencil Test on Normal Probability Plot

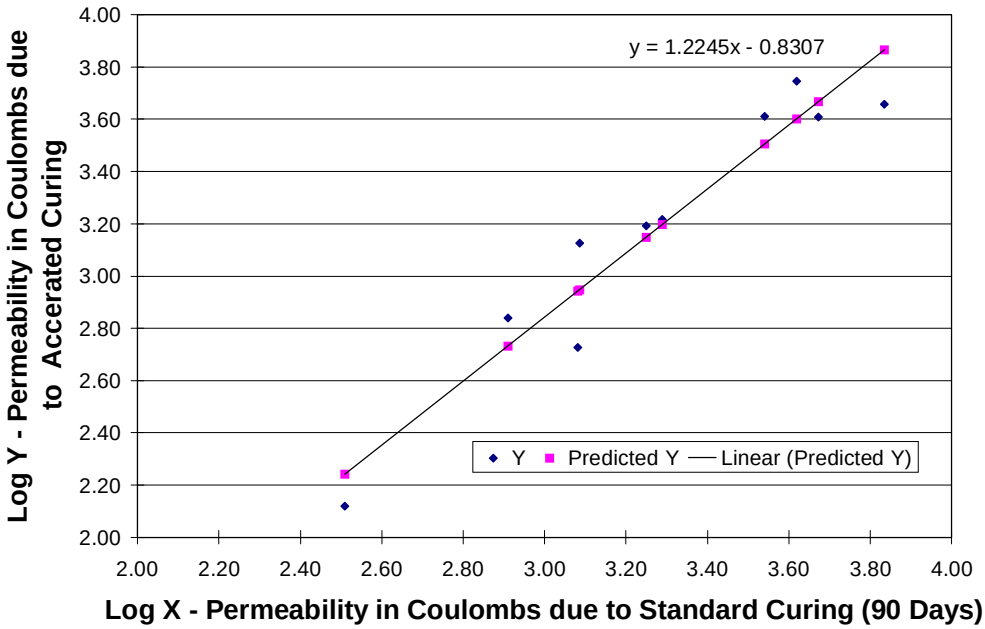

Fig. C3: Regression Analysis - Logarithmic Line Fit Plot

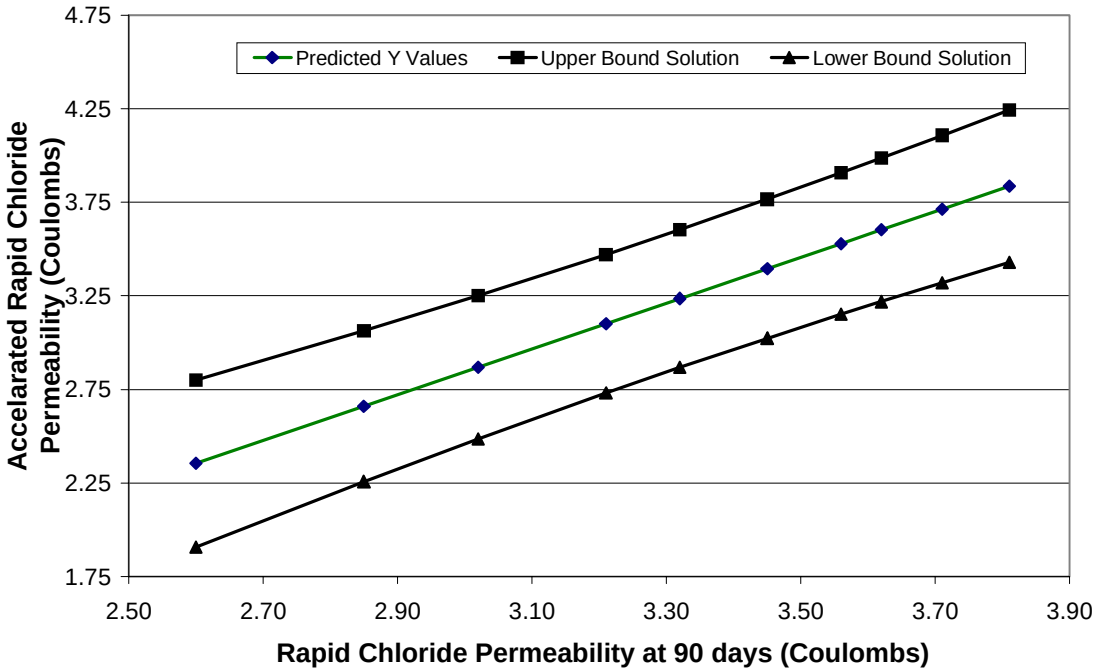

Figure C4: A confidence Band of a future value of Y (Accelerated Coulombs)

Dear Dr. Ramakrishnan,

I am sending you the report on the South Dakota Bridge that includes the final measurements using electromagnetic sensors am also attaching a supplement showing the calculation of losses in the high strength girder. I am sending you a copy of the same by fax and also sending you the final report by mail for your convenience. I am including few details of the final measurement in this letter.

A final set of measurements of the magnetoelastic sensors was attempted on 27 Nov 2001; readings for S3 and S4 were unambiguous and are summarized below. Data from sensor S1 9 nearest to the end of the beam) remained unavailable because of damage to the internal cable, sustained between 19 Jul 01 and 20 Jul 01, when the deck was poured and tamped. During the present visit difficulties were also experienced with sensor S2. The readings from S2 overranged , most likely due to an open circuit at some point. Because this sensor was functioning correctly after the pour on 20 Jul 01, the problem experienced with this sensor is probably due to factors related to external cable/connectors. However, due to deep snow, heavy winds, and freezing conditions on 27 Nov, no attempt was made to diagnose the location of the problem.

Readings for sensors S3 and S4 were obtained as follows. The steel/concrete temperature was measured using the type K thermocouple placed with the sensors during its fabrication. The measurement was made with a handheld thermocouple reader, yielding a value of –1.8 C. the discharge voltage was set to 150 V, the same as in previous measurements. The voltage set points between which the induced voltage was integrated were set to 0.574 and 0.757 volts, respectively, also matching the previous measurements. Three measurements of induced voltage were measured for each of the two sensors, as follows: S3 (2.6004,2.6022, 2.6013), and S4 (2.611,2.6121,2,6105). The mean values of 2.6013 and 2.6114 volts, respectively, were used in conjunction with the measured internal concrete/steel temperature to yield the following in-situ stresses: S3 =185.94 ksi and S4 = 187.88 ksi.

The corresponding forces in the cable are therefore 28447 and 28745 lbs , respectively. The average loss in prestress force is 5.5 % according to calculations from the measured values as shown in **Appendix I** .

It should be noted that the combination lock securing the instrumentation enclosure was frozen shut and all attempts of opening it failed. With the assistance of SDDOT personnel, the lock was removed with a bolt cutter. At the conclusion of the visit, SDDOT supplied a keyed lock , the keys to this lock were given to the lead project engineering in Sioux Falls, Mr. Craig Smith (SDDOT, P.O. Drawer L. Sioux falls, SD 57101-1927, 605 367 5680)

Please don't hesitate to contact me, if you need more information.

Yours sincerely,
Prof. Ming L. Wang
Director
Bridge Research Center
University of Illinois at Chicago
Chicago , IL –60607

Measurement of Prestressed Force of a High Strength Beam

By
Ming L. Wang
Department of Civil and Materials Engineering
University of Illinois – Chicago

Introduction

The field project in South Dakota demonstrates the application of magnetoelastic method to monitor strand stress in I-beams. These beams were fabricated by Gage Brothers Inc, SD, for a three span pre-tensioned concrete bridge. Figure 1 shows the cross-section of one of the I-beams. Each I-beam has 28 FW 0.5" 270 grade strands.

The purpose of this project was to develop a stress monitoring system for one strand of the beam shown in Fig. 1. Fig. 2 shows graphically the location of sensors along the strand. In order to avoid the possible damage and corrosion during construction and sensor's service period, a plastic dip (colored in yellow) was used to cover the steel covering of the sensor in the laboratory. After the sensor was installed on the strand, silicon sealant was used to fill the gap between the strand and the sensor.

Sensor Specifications

The sensors were designed at the University of Illinois at Chicago in the Civil Eng. laboratory and permeability function for each sensor was calibrated. Following are the specifications for the sensors used in the field test:

Cross-sectional area of 0.5" strand , A_f=0.153 in^2 = 98.71 mm^2

Effective area for 0.5" sensor , A_o = 0.332 in^2 =214.98 mm^2

Capacitor voltage Vcap =150 V , ΔV=0.272 V

Primary coil , 1700 turns, 18 gauge (0.01" in diameter) magnetic wire

Secondary coil , 700 turns, 38 gauge (0.004" diameter) magnetic wire.

According to the laboratory test results, optimal working point is calibrated at I_{avg} equal to 1.29 A, ΔI as 0.544 A and the corresponding permeability function is listed below.

$$\mu(\sigma,T) = 5.7113 - 2.4531\times10^{-5}\sigma^2 + 3.3558\times10^{-2}\sigma - 1.390\times10^{-2}T \qquad (1)$$

To solve the stress from above equation, we rewrite the equation as

$$\mu(\sigma,T) = k\sigma(\sigma-\sigma_0) + \alpha_1 T + \mu(0,0) \qquad (2)$$

thus stress can be expressed as

$$\sigma = \frac{1}{2}[\sigma_0 - \sqrt{\sigma_0^2 + 4(\mu - \mu_0 - \alpha_1 T)/k}] \qquad (3)$$

where σ_0 =-m1/m2=1367.98 ksi

k=m2=-2.4531$\times10^{-5}$

α_1 =-1.39 $\times10^{-2}$

$\mu(0,0)$ =5.7113

Here we have focused on the linear elastic region. The permeability equation (Eqn. 1) gives 2 roots for stress. The root out of elastic region is excluded because the yield stress for FW 0.5" strand is less than 500 ksi. Table I list some parameters obtained in the laboratory. Detailed description and analysis of the method is given in Appendix I.

TABLE I

PARAMETERS FOR THE SENSORS USED IN FIELD TEST

Sensor number	Resistant of primary coil (Ω)	Resistant of secondary coil (Ω)	U_{high}(V) optimal working point	U_{low}(V) Optimal working point	U_{int}(V) Electromotie force at T=23°C
1	18.3	73.7	0.802	0.530	1.3513
2	17.9	72.6	0.802	0.530	1.3562
3	18.0	73.7	0.802	0.530	1.3513
4	18.6	74.9	0.802	0.530	1.3583

Discussion :

The test was conducted at Gage Brothers Inc. in Sioux Falls, SD from May 16 to May 23. Three beams of length 54', 61' and 54' respectively, were fabricated in a 200' long prestressing 'bed' simultaneously. Four sensors were installed on the strand before the strand was tensioned up to 31,000 Lb. Figure 3 to Figure 5 show the sensors on the strand. As shown in Figure 6, a lab-top, a pulsed measuring device and a voltage controlled current source were used to measure the permeability of strand. Stress is calculated by inserting the permeability value into Equation 3. Table II is the measured results of forces along the strand at various stages of loading history.

Loading history includes the pouring of concrete in the test bed as shown in Fig. 7, after cutting the strand while resting in the concrete yard as shown in Fig. 8 and before pouring the concrete while resting at the bridge site as shown in Fig. 9. Fig. 10 shows the plot of Force vs Time for the sensors 1-4 during the complete test.

Conclusions :

1. The first measurement was taken after the strand was tensioned up to 31,000 lbs. From the results, it is seen that the stress is almost homogeneous along the four measured locations. As listed in Table II, the measured force is approximately 4% less than that of applied force (31,000 lbs). Considering the force applied at the end i.e. 160' away from measuring location, the measured value of stress is reasonable.
2. The second measurement taken 2 hours after the strand was tensioned showed no significant loss in stress.
3. The beam was cast on May 18, 2000. Third measurement was taken 6 days after the strand was tensioned. Stress loss of 1 % to 2% was measured during this period.

4. Concrete cylinders were cast using the same concrete as the I-beams and at the same time when the beams were fabricated. Strands were not released until the compressive strength of the concrete cylinder sample reached 8.75 ksi. On June 15, another measurement was taken after the strand was released. The value obtained from the first sensor showed stress loss to 97.7 ksi (14946 lbs in tension) that is half of the original stress value. This was because the measured location was 1' ¾" away from the end of beam where the released stress of the strand was zero. It is also seen from the results that there is an increase of about 0.5% to 1% in stress at other three locations even though the strand was released. This is due to the reason that the temperature went down to 12 C and a tensile force was applied to the strand by the concrete due to difference in their coefficient of expansion.
5. As seen from step 4 to step 5 there is an increase in force by 400 lbs when the beam was under its self weight at its final position at the construction site. However, the sensor that is 1'3/4" from the anchorage is further relaxed in tension of about 2100 lbs. This is attributed to the continuation of slippage between the strand and concrete. Several strain gages were also installed near the anchorage. These strain were covered by a thick layer of teflon for protection of strain gages against moisture. However, this cover prohibits the development of bond strength between the strand and the concrete.
6. There was an increase in force by 400 lbs after concrete was poured in the deck. Unfortunately, the wire of sensor 1 was damaged by the vibrator after pour of concrete.

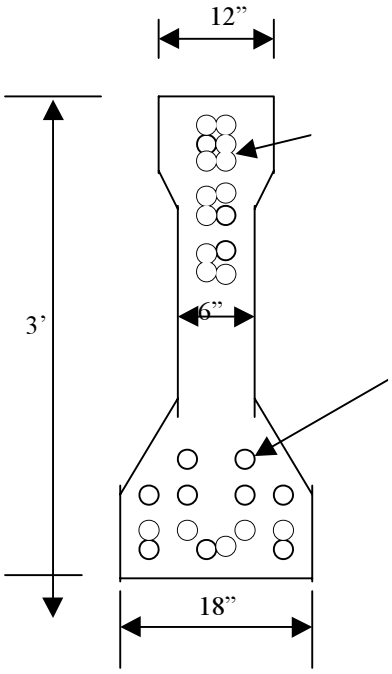

Figure 1. Cross section of the I-beam fabricated by Gage Brothers, Inc, SD

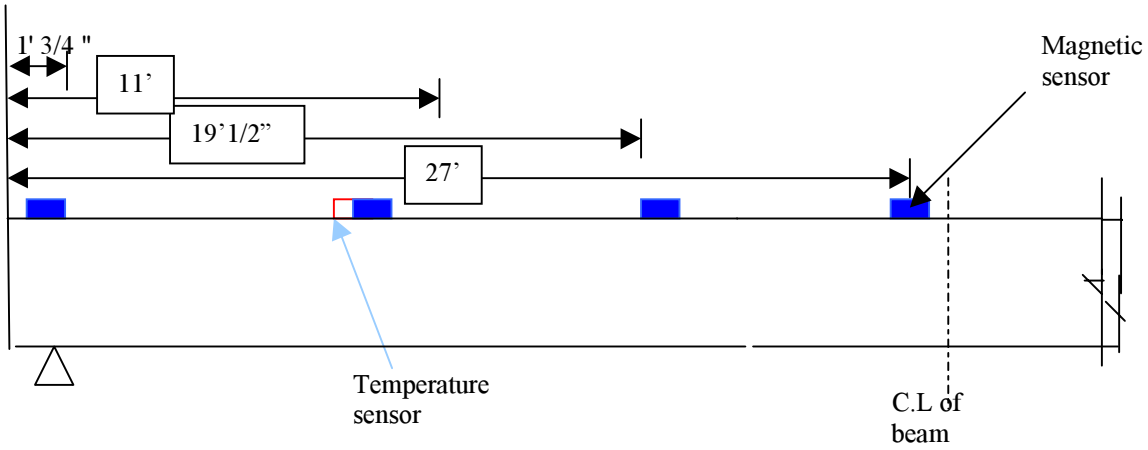

Figure 2. Sensor locations on the strand of a 54’ long simple supported I-beam

TABLE II: TEST RESULTS (Force Only)

Event	Schedule / Force	Sensor 1	Sensor 2	Sensor 3	Sensor 4
1	Tested after the strand was tensioned Strand un-released Concrete un-cast T=22 ° C (05/16/00)	29,300	29,391	29619	29656
2	2 hours after the strand was tensioned Strand un-released Concrete un-cast T=22 ° C (05/16/00)	29,272	28,700	28,714	28,760
3	6 days after the strand was tensioned , Strand unreleased 4 days after concrete was cast T=27.3 ° C (05/22/00)	28,934	28,554	28,639	28,825
4	30 days after the strand was tensioned Strand released 25 days after concrete was cast T=15.2 ° C at rest position (06/16/00)	14,946	28,714	28,760	29,085
5	Beam under it's self weight at final construction site Before pouring concrete on deck T = 15.4 C (6 p.m, 7/19/00)	12,820	29,121	29,180	29,463
6	Before pour of concrete on deck T= 15.0 C (10:30 a.m ,7/20/00)	13,089	29,133	29,189	29,464
7	After pour , deck formed T= 18.2 C (5 p.m , 07/20/00)	Wire damaged by vibrator	29,534	29,786	30,113
8	16 months from the casting, 11/27/01	Wire damaged by vibrator	Unable to take reading due to frozen connector	28,447	28,754

Figure 3. Magnetoelastic sensors installed on a strand

Figure 4. Magnetic sensor (colored in yellow) installed on a strand

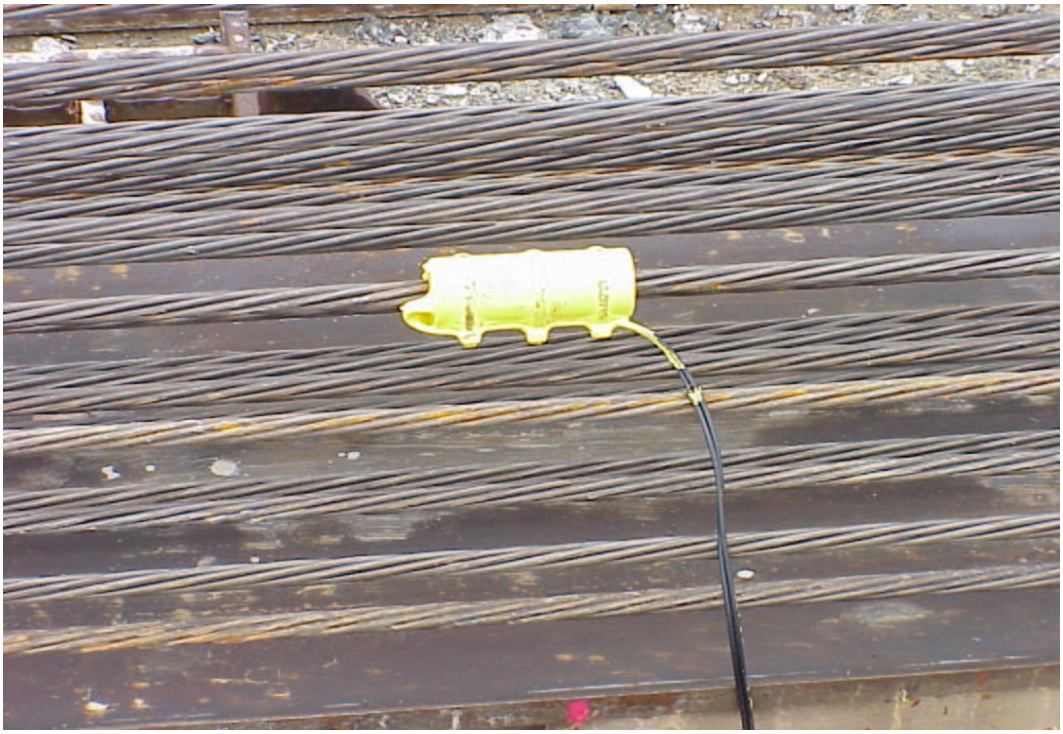

Figure . Magnetoelastic sensor on a tensioned strand

Figure 6. Field test facilities

Figure 7. Magnetoelastic sensors installed in a fabricated beam

Figure 8. Fabricated pre-tensioned I-beams

Figure 9. Final position of the beam at the site.

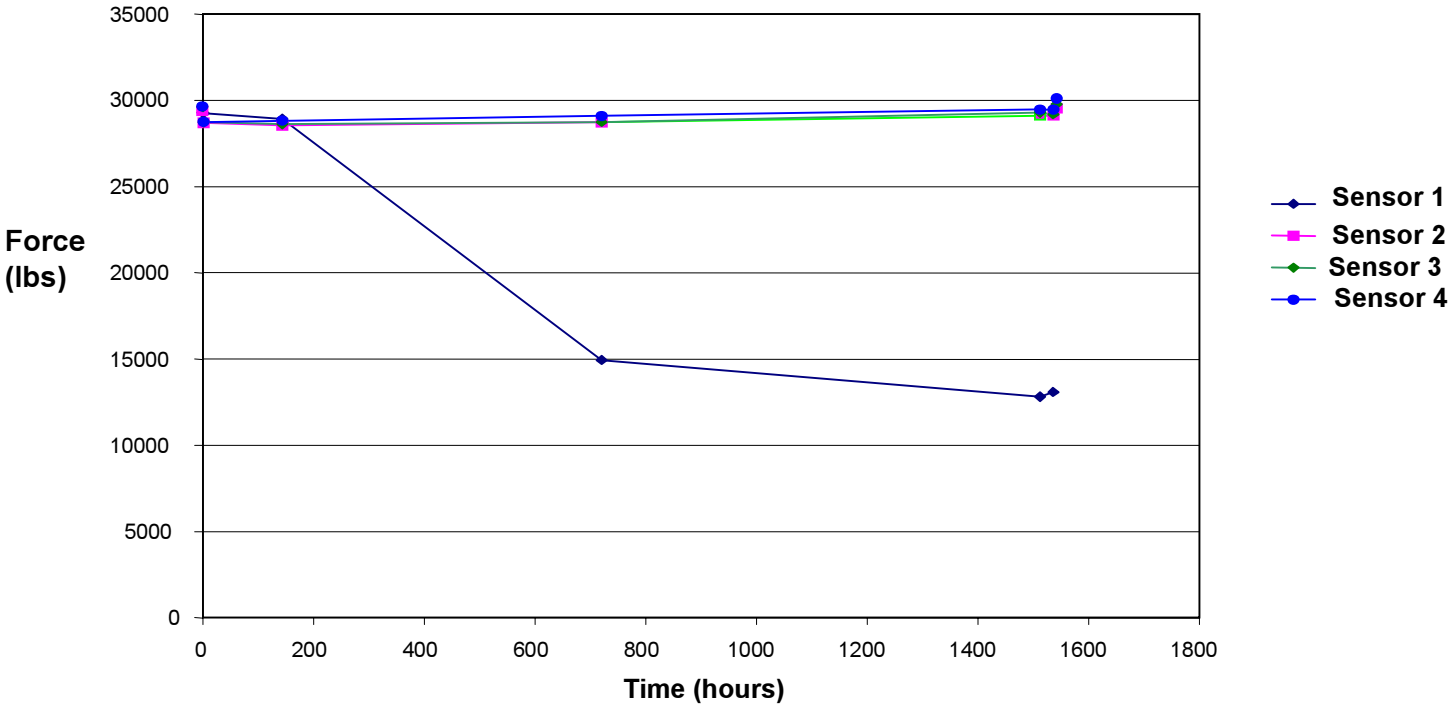

Fig. . i e vs Force for the sensors 1 - 4